

**CHARACTERIZATION OF SURFACE SOIL HYDRAULIC PROPERTIES IN
SLOPING LANDSCAPES**

A Thesis Submitted to the College of
Graduate Studies and Research
in Partial Fulfillment of the Requirements
for the Degree of Master of Science
in the Department of Soil Science
University of Saskatchewan
Saskatoon

By

Bodhinayake Waduawatte Lekamalage

PERMISSION TO USE

In presenting this thesis in partial fulfilment of the requirements for a Postgraduate degree from the University of Saskatchewan, I agree that the Libraries of this University may make it freely available for inspection. I further agree that permission for copying of this thesis in any manner, in whole or in part, for scholarly purposes may be granted by the professor or professors who supervised my thesis work or, in their absence, by the Head of the Department or the Dean of the College in which my thesis work was done. It is understood that any copying or publication or use of this thesis or parts thereof for financial gain shall not be allowed without my written permission. It is also understood that due recognition shall be given to me and to the University of Saskatchewan in any scholarly use which may be made of any material in my thesis.

Requests for permission to copy or to make other use of material in this thesis in whole or part should be addressed to:

Head of the Department of Soil Science

University of Saskatchewan

51 Campus Drive

Saskatoon, Saskatchewan, Canada

S7N 5A8

ABSTRACT

Saturated and near-saturated surface soil hydraulic properties influence the partition of rainfall and snowmelt into infiltration and runoff. The goal of this study was to characterize near-saturated surface soil hydraulic properties and water-conducting porosity in sloping landscapes. The specific objectives included exploration of tension and double-ring infiltrometers for estimation of soil hydraulic properties in sloping landscapes, development of an improved method for determining water-conducting porosity, and the application of these methods in characterizing soil hydraulic properties and water-conducting porosity under three land use.

Water infiltration from a double-ring infiltrometer and a tension infiltrometer at water pressures between -2.2 and -0.3 kPa were measured in a cultivated field with 0, 7, 15, and 20% slopes at Laura and under three land use (native grass, brome grass and cultivated) at St. Denis in Saskatchewan, Canada. Three-dimensional computer simulation studies were also performed for tension infiltrometer with various disc diameters, water pressures, and surface slopes. Steady infiltration rates and estimated field-saturated hydraulic conductivity (Kfs), hydraulic conductivity-water pressure relationship ($K(h)$), and inverse capillary length parameter (α) were compared for different slopes and land use. These parameters were not significantly different ($p < 0.05$) among slopes. For specific $K(h)$ functions, a new analytical solution was developed and compared with existing methods for calculating water-conducting porosity. The new method reliably determined water-conducting porosity of surface soils and gave

consistent results, regardless of the width of water pressure ranges. At the -0.3 kPa water pressure, hydraulic conductivity of grasslands was two to three times greater than the cultivated lands. Values of α were about two times and values of Kfs about four times greater in grasslands than in cultivated fields. Water-conducting macroporosity of grasslands and cultivated fields were 0.04% and 0.01% of the total soil volume, respectively. Over 40% and 50% of the total water flux at -0.06 kPa water pressure was transmitted through macropores (pores $> 1 \times 10^{-3}$ m in diameter) of the cultivated land and the grasslands, respectively.

Experimental and simulation results of this study indicated that both tension and double-ring infiltrometers are suitable for characterization of saturated and near-saturated surface soil hydraulic properties in landscapes up to 20% slope. The new method can be used to characterize water-conducting porosity from *in situ* tension and double-ring infiltrometers measurements more adequately and efficiently than the existing methods. Application of these methods for three land use indicated that land use modified surface soil hydraulic properties and consequently may alter the water balance of an area by affecting the partition between, and relative amount of infiltration and surface runoff.

ACKNOWLEDGEMENTS

I offer sincere thanks to my supervisor Dr. Bing Cheng Si for his invaluable guidance and encouragement throughout the course of this study. Thanks are due to the members of my committee, Dr. Dan J. Pennock and Dr. Fran L. Walley, and my external examiner Dr. Garth van der Kamp for their valuable comments.

I am thankful to Drs. K. Noborio (Japan), C. Xiao (Department of Physics, University of Saskatchewan), and E. de Jong (Department of Soil Science, University of Saskatchewan) for their support and useful discussions. My thanks also go to my fellow graduate students, the staff and faculty of Department of Soil Science and Saskatchewan Centre for Soil Research, University of Saskatchewan for their support.

Special thanks go to my friends Chandima, Sumith, Saman, Lasantha, Takele, Lindsay, Carol, Amanda, Angela, and Shaun Campbell for their constant support and encouragement.

Financial assistance by NSERC of Canada and the University of Saskatchewan through a graduate student scholarship is gratefully acknowledged.

DEDICATION

I dedicate this thesis to my wife Sujatha and my loving parents.

TABLE OF CONTENTS

PERMISSION TO USE	i
ABSTRACT	ii
ACKNOWLEDGEMENTS	iv
DEDICATION	v
TABLE OF CONTENTS	vi
LIST OF TABLES	x
LIST OF FIGURES	xi
1. GENERAL INTRODUCTION AND OBJECTIVES	1
1.1 References	5
2. LITERATURE REVIEW	7
2.1 Soil Hydraulic Properties	7
2.2 Saturated and Unsaturated Hydraulic Conductivity	8
2.3 Theory and <i>In Situ</i> Measurement Techniques Pertaining to Surface Soil Hydraulic Properties	8
2.3.1 One-dimensional ponded infiltration measurement techniques – the double-ring infiltrometer	9
2.3.1.1 Constant head model for double-ring infiltrometer	10
2.3.2 One- and three-dimensional tension infiltrometers	13
2.3.2.1 Three-dimensional (unconfined) tension infiltrometer	14
2.3.3 Analysis of water flow from 3-D tension infiltrometer	14
2.3.3.1 Steady-state flow procedure	16
2.3.3.2 Multiple-head approach	17
2.3.3.3 Multiple-disc approach	19
2.3.3.4 Transient flow procedure (Single-head – single-disc approach)	19
2.3.3.5 Inverse procedure	23

2.3.4 Advantages of using tension infiltrometers	26
2.3.5 Limitations and sources of error using tension infiltrometers	27
2.4 Factors Affecting Surface Soil Hydraulic Properties	28
2.4.1 Effect of topography or slope gradient on soil hydraulic properties	29
2.4.1.1 Soil hydraulic properties in sloping landscapes	29
2.4.1.2 Measurement of soil hydraulic properties in sloping landscapes	29
2.4.1.3 Use of tension and double-ring infiltrometers for estimation of surface soil hydraulic properties	30
2.4.1.4 Limitations of tension and double-ring infiltrometers in determining hydraulic properties in sloping landscapes	31
2.4.2 Effect of porosity and pore-size distribution on soil hydraulic properties	33
2.4.2.1 Porosity and pore-size distribution	33
2.4.2.2 Classification of soil pores	34
2.4.2.3 Relative contribution to flow by macro- and mesopores.....	35
2.4.2.4 Consequences of macro- and mesopore flow	36
2.4.2.5 Characterization of water-conducting macro- and mesoporosity.....	36
2.4.2.6 Overview of methods used to characterize water-conducting porosity and their limitations.....	37
2.4.3 Effect of land use on soil hydraulic properties	40
2.4.3.1 Management practices and hydraulic properties	40
2.4.3.2 Type of vegetation and soil hydraulic properties	41
2.4.3.3 Land use and water level of wetlands.....	42
2.5 Summary	43
2.6 References	45
3. DETERMINATION OF SOIL HYDRAULIC PROPERTIES IN SLOPING SURFACES USING TENSION AND DOUBLE-RING INFILTRMETERS.....	50
3.1 Abstract	50
3.2 Introduction	51
3.3 Materials and Methods	54
3.3.1 Treatments and experimental design	54
3.3.2 Estimation of field-saturated hydraulic conductivity from double-ring infiltrometer measurements	59

3.3.3 Estimation of soil hydraulic properties from tension infiltrometer measurements	60
3.3.4 Determination of water-conducting porosity.....	61
3.3.5 Computer simulation	64
3.3.6 Statistical analysis.....	65
3.4 Results and Discussion	66
3.5 Conclusions	74
3.6 References	75
4. NEW METHOD FOR DETERMINING WATER-CONDUCTING MACRO- AND MESOPOROSITY FROM TENSION INFILTROMETER	79
4.1 Abstract	79
4.2 Introduction	80
4.3 Theory	82
4.3.1 Watson and Luxmoore (1986) approach	84
4.3.2 Dunn and Phillips (1991a) approach	84
4.3.3 A New approach	85
4.3.3.1 Gardner (1958) exponential model.....	88
4.3.3.2 Brooks and Corey (1966) model	88
4.3.3.3 Gardner rational (1965) power model	89
4.3.3.4 van Genuchten-Mualem (1980) model.....	90
4.4 Demonstrations.....	92
4.5 Conclusions	102
4.6 Appendix	102
4.8 References	108
5. NEAR-SATURATED SURFACE SOIL HYDRAULIC PROPERTIES UNDER DIFFERENT LAND USE IN THE ST. DENIS NATIONAL WILDLIFE AREA, SASKATCHEWAN, CANADA	111
5.1 Abstract	111
5.2 Introduction	112
5.3 Materials and Methods	115
5.3.1 Study site	115
5.3.2 Treatments and experimental design	116
5.3.3 Measurements of bulk density, total porosity, organic carbon, and texture	116

5.3.4 Measurement of steady-state infiltration rate using double-ring infiltrometer	117
5.3.5 Measurement of infiltration rates using tension infiltrometer	119
5.3.6 Calculation of macroporosity	120
5.3.7 Estimation of unsaturated hydraulic properties from tension infiltrometer measurements	121
5.3.8 Determination of water-conducting porosity.....	122
5.3.9 Statistical analysis.....	125
5.4 Results and Discussion.....	125
5.5 Conclusions	140
5.6 References	141
6. SUMMARY AND CONCLUSIONS.....	146

LIST OF TABLES

Table 3. 1 Some selected soil physical properties of the experimental site.	66
Table 3. 2 Estimated water-conducting porosity (% of total soil volume) in each pore diameter interval for the different slopes.....	73
Table 4. 1 Estimated parameters (field-saturated hydraulic conductivity K_s , and the empirical curve fitting parameters) for the investigated soil.....	97
Table 4. 2 Estimated water-conducting porosity in each water pressure range for the models used	98
Table 5. 1 Grasslands had smaller bulk density and higher organic carbon content than cultivated land while soil separates contents in the surface 0.05 m of soil were not affected by land use.....	126
Table 5. 2 Average and standard deviations of estimated surface soil hydraulic properties for the three land use	131
Table 5. 3 Estimated water-conducting porosity \pm standard deviation (% of soil volume) in each pore diameter interval for the three land use.....	135

LIST OF FIGURES

Figure 3. 1 Double-ring infiltrometer.....	55
Figure 3. 2 Tension infiltrometer.....	55
Figure 3. 3 An experimental block showing the arrangement of the treatments.....	56
Figure 4. 1 Measured and fitted unsaturated hydraulic conductivity, $K(h)$ of the surface soil for the models used.....	96
Figure 5. 1 Effect of land use on macro-, meso + micro-, and total porosity (% of soil volume). The vertical bars on the graph represent least significant difference at $p < 0.1$	127
Figure 5. 2 Measured and fitted steady-state infiltration rates (mean) at different water pressures for the Wooding's (1968) function (Eq. [5.4]); a) Native grassland, b) Brome grassland, and c) Cultivated field.	129
Figure 5. 3 Mean hydraulic conductivity ($K(h)$) of surface soils under three land use ($K(0)$ is from double-ring infiltrometer).....	130
Figure 5. 4 Correlations between macroporosity and field-saturated hydraulic conductivity (K_{fs}) (solid line represents linear regression: $R^2=0.56$) and macroporosity and inverse capillary length scale, α (broken line represents linear regression: $R^2=0.70$). Each point was an average of six measurements.....	133
Figure 5. 5 Contribution to total flow at -0.06 kPa water pressure from the following pore diameter intervals: a: $<1.4 \times 10^{-4}$ m; b: 1.4×10^{-4} - 2.0×10^{-4} m; c: 2.0×10^{-4} - 4.3×10^{-4} m; d: 4.3×10^{-4} - 1.0×10^{-3} m; e: $>1.0 \times 10^{-3}$ m.....	136
Figure 5. 6 Field-saturated hydraulic conductivities (K_{fs}) for the three land use (0 indicates values below and above 10 th and 90 th percentiles, respectively).....	139

1. GENERAL INTRODUCTION AND OBJECTIVES

Soil hydraulic properties include hydraulic conductivity as a function of both soil water pressure and soil water content, and the soil moisture retention relationship (Hillel, 1998). These soil hydraulic properties are needed for understanding water balance, irrigation and transport processes. Furthermore, saturated and near-saturated hydraulic properties of surface soils influence the partition of irrigation water, rainfall and snowmelt into runoff and soil water storage. Topography or slope gradient, pore-size distribution and pore continuity, and land use are among the main soil and management factors that affect hydraulic properties of surface soils (Zebarth and de Jong, 1989; Rawls *et al.*, 1993). Thus, knowledge of surface soil hydraulic properties with respect to these soil and management factors is essential for efficient land and water management.

The majority of the landscapes under cultivation in many parts of the world are non-level (slope > 0.5%). For instance, only about 2.4% of agricultural lands in Saskatchewan (SK), Canada are nearly level (0-0.5% slope) (Eilers, W., University of Saskatchewan, personal communication, 2003). Several researchers have reported that topography or slope gradient influences soil properties such as moisture content, infiltration rate, and saturated and unsaturated hydraulic conductivity (Sinai *et al.*, 1981; Zebarth and de Jong, 1989; Zebarth *et al.*, 1989). Consequently, surface soil hydraulic properties may vary between level and sloping landscapes. Moreover, the significance

of considering land-surface morphology, which includes slope gradient in designing landscape-scale research projects in SK, Canada has been emphasized (e.g., Pennock *et al.*, 1987). Measurement techniques and instruments available for sloping lands include the use of excavated trenches (Dunne and Black, 1970), tensiometers, piezometers and lysimeters (Harr, 1977), and hillslope infiltrometer (Mendoza and Steenhuis, 2002). These methods, however, are time consuming, destructive and tedious to perform under field conditions. Tension infiltrometer (Perroux and White, 1988) and single-ring or double-ring infiltrometer (Bower, 1986) provide simple, cost-effective, non-destructive or less-destructive and convenient means of *in situ* measurements of surface soil hydraulic properties. These are primarily designed and tested in horizontal surfaces. However, this equipment has been extensively used in the past to obtain saturated and near-saturated soil hydraulic properties on sloping lands (Watson and Luxmoore, 1986; Wilson and Luxmoore, 1988; Elliott and Efetha, 1999). Despite the extensive use of tension and double-ring infiltrometers in determining surface soil hydraulic properties in sloping lands, no systematic studies were conducted on the suitability of this equipment for the estimation of these properties in sloping lands to the best of my knowledge. Hence exploration of such standard tools is urgently needed.

The importance of continuous macro- and mesopores to water flow in soils, especially to infiltration and fast movement of water and potential pollutants through soils is well documented (Thomas and Phillips, 1979; Beven and Germann, 1982; Luxmoore *et al.*, 1990). Methods available for quantification of water-conducting macro- and mesopores include dye staining (Bouma *et al.*, 1979), computer assisted tomography with x-ray scanners (Anderson *et al.*, 1990), tracers and breakthrough curves (Yeh *et al.*, 2000),

and infiltration redistribution (Timlin *et al.*, 1994). These techniques, however, are destructive, costly or laborious and not suitable for routine field use. Using simple, rapid and *in situ* ponded- and tension-infiltration measurements, Watson and Luxmoore (1986) and Dunn and Phillips (1991) developed a method to characterize water-conducting macro- and mesoporosity of surface soils. However, their calculation procedures, which are based on Poiseuille's law and capillary theory, assume a single pore size (minimum pore radius for Watson and Luxmoore and mean pore radius for Dunn and Phillips). This is an unrealistic assumption and may lead to erroneous results. Therefore, development of a reliable and accurate method for the estimation of water-conducting macro- and mesoporosity in soil is greatly needed.

Type of land use is generally known to affect surface soil hydraulic properties and pore-size distribution. Lands under undisturbed grass cover tend to increase infiltration and decrease runoff due to improved organic matter content, soil aggregation and faunal activities (Lepilin, 1989; Naeth *et al.*, 1990; Schwartz *et al.*, 2000). Relative to well-managed grasslands, conventional crop-fallow rotation decrease macroporosity and saturated and unsaturated hydraulic conductivity (Spewak, 1997) resulting in a decrease in water infiltration and increased surface runoff. Despite this, information on surface soil hydraulic properties and pore-size distribution in sloping lands with undisturbed grass cover and traditional crop-fallow rotation, particularly under Saskatchewan conditions, is lacking.

In light of the above, the goal of the research described in this thesis is to determine surface soil hydraulic properties and water-conducting porosity in sloping landscapes.

The specific objectives of the study are:

1. To evaluate the suitability of tension and double-ring infiltrometers for the estimation of surface soil hydraulic properties in sloping lands;
2. To develop an improved method for determining water-conducting porosity from tension infiltrometer measurements;
3. To apply these methods in characterizing surface soil hydraulic properties and water-conducting porosity in sloping lands under different land use systems in the St. Denis National Wildlife area, SK, Canada.

This thesis consists of six chapters. Chapter one deals with the general rationale and objectives of the study. Chapter two reviews the literature relevant to soil hydraulic properties, theory and measurement techniques of tension and double-ring infiltrometers, and major factors that influence surface soil hydraulic properties. Detailed materials and methods and results pertinent to the experiments conducted to achieve the three research objectives are presented in chapters three, four and five. Summary and major conclusions are listed in chapter six. The format of the chapters is in the form of intact papers for submission to journals. As a result this format leads to some duplication of introductory material in each chapter.

1.1 References

- Anderson, S.H., R.L. Peyton, and C.J. Gantzer. 1990. Evaluation of constructed and natural soil macropores using X-ray computed tomography. *Geoderma*. 46:13-29.
- Beven, K., and P. Germann. 1982. Macropores and water flow in soils. *Water Resour. Res.* 18:1311-1325.
- Bouma, J.A., A. Jongerius, and D. Schoonderbeek. 1979. Calculation of saturated hydraulic conductivity of some pedal clay soils using micromorphometric data. *Soil Sci. Soc. Am. J.* 43:261-264.
- Bower, H. 1986. Intake rate. Cylinder infiltrometer. p. 825-843. *In* A. Klute (ed.) *Methods of soil analysis. Part 1. Physical and mineralogical properties.* 2nd ed. ASA, Madison, WI.
- Dunn, G.H., and R.E. Phillips. 1991. Macroporosity of a well-drained soil under no-till and conventional tillage. *Soil Sci. Soc. Am. J.* 55:817-823.
- Dunne, T., and R.D. Black. 1970. An experimental investigation of runoff production in permeable soils. *Water Resour. Res.* 6:478-490.
- Elliott, J.A., and A.A. Efetha. 1999. Influence of tillage and cropping system on soil organic matter, structure and infiltration in a rolling landscape. *Can. J. Soil Sci.* 79:457-463.
- Harr, R.D. 1977. Water flux in soil and subsoil on a steep forested slope. *J. Hydrology.* 33:37-58.
- Hillel, D. 1998. *Environmental soil physics.* Academic Press. New York. Iowa State University Press. USA.
- Lepilin, A. 1989. Effect of the age of perennial grasses on the physical properties of Meadow-Chernozem soil. *Soviet Soil Sci.* 21:121-126.
- Luxmoore, R.J., P.M. Jardine, G.V. Wilson, J.R. Jones, and L.W. Zelazny. 1990. Physical and chemical controls of preferred path flow through a forested hillslope. *Geoderma*. 46:139-154.
- Mendoza, G., and S.T. Steenhuis. 2002. Determination of hydraulic behavior of hillsides with a hill slope infiltrometer. *Soil Sci. Soc. Am. J.* 66:1501-1504.
- Naeth, M.A., R.L. Rothwell, D.S. Chanasyk, and A.W. Bailey. 1990. Grazing impacts on infiltration in mixed prairie and fescue grassland ecosystems of Alberta. *Can. J. Soil Sci.* 70:593-605.
- Pennock, D.J., B.J. Zebarth, and E. de Jong. 1987. Landform classification and soil distribution in hummocky terrain, Saskatchewan, Canada. *Geoderma*. 40:297-315.

- Perroux, K.M., and I. White. 1988. Design for disc permeameters. *Soil Sci. Soc. Am. J.* 52:1205-1215.
- Rawls, W.J., L.R. Ahuja, D.L. Brakensiek, and A. Shirmohammadi. 1993. Infiltration and soil water movement. p. 5.1-5.51. *In* D. R. Maidment. (ed.) *Handbook of hydrology*. McGraw Hill, Inc. NY.
- Schwartz, R.C., P.W. Unger, and S.R. Evett. 2000. Land use effects on soil hydraulic properties. http://www.cprl.ars.usda.gov/programs/land_use.pdf.
- Sinai, G., D. Zaslavsky, and P. Golany. 1981. The effect of soil surface curvature on moisture and yield-Beer Sheva Observation. *Soil Sci.* 132:367-375.
- Spewak, R.P. 1997. The effect of land use on the soil macropores characteristics of prairie soils. MSc Thesis. University of Saskatchewan.
- Thomas, G.W., and R.E. Phillips. 1979. Consequences of water movement in macropores. *J. Environ. Qual.* 8:149-152.
- Timlin, D.J., L.R. Ahuja, and M.D. Ankeny. 1994. Comparison of three field methods to characterize apparent macropore conductivity. *Soil Sci. Soc. Am. J.* 58:278-284.
- Watson, K.W., and R.J. Luxmoore. 1986. Estimating macroporosity in a forest watershed by use of a tension infiltrometer. *Soil Sci. Soc. Am. J.* 50:578-582.
- Wilson, G.V., and R.J. Luxmoore. 1988. Infiltration, macroporosity and mesoporosity distributions on two forested watersheds. *Soil Sci. Soc. Am. J.* 52:329-335.
- Yeh, Y.J., C.H. Lee, and S.T. Chen. 2000. A tracer method to determine hydraulic conductivity and effective porosity of saturated clays under low gradients. *Ground Water.* 38:522-529.
- Zebarth, B.J., and E. de Jong. 1989. Water flow in a hummocky landscape in central Saskatchewan, Canada. III. Unsaturated flow in relation to topography and land use. *J. Hydrol.* 110:199-218.
- Zebarth, B.J., E. de Jong, and J.L. Henry. 1989. Water flow in a hummocky landscape in central Saskatchewan, Canada. II. Saturated flow and ground water recharge. *J. Hydrol.* 110:181-198.

2. LITERATURE REVIEW

In the following a review of the literature relevant to soil hydraulic properties, methods for determining surface soil hydraulic properties based on one-dimensional and three-dimensional infiltration and some factors affecting surface soil hydraulic properties are presented.

2.1 Soil Hydraulic Properties

The rate of movement of water in soils is an important aspect of agriculture. The entry of water into the soil, movement of water in the soil profile, flow of water to drains, and evaporation from soil surface are some of the examples in which the rate of water movement plays a major role. The soil properties that govern the behavior of such soil water movements are hydraulic conductivity and water retention relationship. These are collectively referred to as soil hydraulic properties (Klute and Dirksen, 1986). These properties are needed to address problems of water balance, irrigation, drainage and solute movement.

The surface soil (0- to 5-cm) is the interface between the external environment and the soil. Hydraulic properties of surface soils influence the partition of rainfall, snowmelt and irrigation water into runoff and soil water storage, and thus knowledge of surface soil hydraulic properties is essential for efficient land and water management. Of the

surface soil hydraulic properties, this thesis concentrates only on the saturated hydraulic conductivity and hydraulic conductivity as a function of water pressure.

2.2 Saturated and Unsaturated Hydraulic Conductivity

Hydraulic conductivity is the proportionality factor in Darcy's law as applied to the viscous flow of water in soil (SSSA, 2003), i.e., the flux of water per unit gradient of hydraulic potential. Simply it is the ability of the soil to transmit water (under standard temperature condition) in response to an energy gradient. Hydraulic conductivity could be expressed under saturated and unsaturated conditions. For a saturated soil, the proportionally factor (saturated hydraulic conductivity) is a single-valued parameter which is determined at maximum water content (saturation) and unit water pressure head gradient. Unsaturated hydraulic conductivity, on the other hand, is the conductivity at a given water pressure (less than zero) ($K(h)$) or water content (less than saturation) ($K(\theta)$), and thus is a function of soil water content (θ) or water pressure (h).

2.3 Theory and *In Situ* Measurement Techniques Pertaining to Surface Soil Hydraulic Properties

Hydraulic properties may be measured or estimated either by measurements on undisturbed samples in the laboratory or *in situ* (field) measurements. While laboratory measurements are more controlled and generally more convenient than field methods, a large area of measurements and preservation of field structure are the inherent advantages of field methods over laboratory methods. Therefore, development of *in situ* techniques to determine both the saturated and unsaturated hydraulic properties of the surface soil has received much attention of soil scientists and engineers dealing with water and solute flow in the soil.

Measurement of soil hydraulic properties *in situ* is quite difficult. However, infiltration-based methods are recognized as promising tools to investigate hydraulic and transport properties of soil. In particular, three complimentary methods have become popular in the study of saturated and near-saturated soil behavior. They are the confined one-dimensional pressure double-ring infiltrometer, the unconfined three-dimensional single-ring pressure infiltrometer, and the unconfined three-dimensional tension disc infiltrometer methods (Angulo-Jaramillo *et al.*, 2000). For the experiments described in this thesis, the infiltration data measured with a double-ring infiltrometer and a tension disc infiltrometer were used to estimate surface soil hydraulic properties.

2.3.1 One-dimensional ponded infiltration measurement techniques – the double-ring infiltrometer

Ring infiltrometers are usually thin-walled, open-ended metal cylinders of about 5- to 20-cm long and 10- to 50-cm in diameter. The cylinders are generally pushed or driven to a short distance into the soil. The area inside the cylinders is filled with water and the rate of water loss from the ring is taken as an estimate of the one-dimensional infiltration rate of which water is assumed to flow vertically into the soil. Various cylinder arrangements are possible. In the double-ring infiltrometer, a smaller ring is placed concentrically inside the larger one. For a more meaningful data, the minimum recommended diameters of the rings are 20 cm for the inner ring and 30 cm for the outer ring (Bower, 1986). Equal water depth is maintained in both cylinders and the infiltration rate is measured only from the inner ring. The rationale for the use of outer ring (buffer cylinder) is that the water in the space between the two rings takes care of flow divergence so that an approximate vertical flow can be simulated under the inner measuring ring. The double-ring infiltrometers are used primarily for measuring

cumulative infiltration, infiltration rate and field-saturated hydraulic conductivity based on the infiltration at the soil surface.

In the unsaturated or vadose zone (above the water table), measurements of field-saturated water flow parameters (e.g., field-saturated hydraulic conductivity, matrix flux potential, inverse macroscopic capillary length parameter, sorptivity) can be easily obtained by using a double-ring infiltrometer. Depending on the desired flow parameters, several flow analyses such as one-dimensional (1-D) or three-dimensional (3-D), transient or steady-state, constant head or falling head, are possible for double-ring infiltrometers. Steady-state flow under constant head conditions have traditionally been used because constant head devices are easy to maintain experimentally and the analysis is relatively simple. Therefore, steady-state flow under constant head (pressure) conditions was used for the estimation of field-saturated hydraulic conductivity (K_{fs}) from double-ring infiltration measurements in the field experiments discussed in this thesis.

2.3.1.1 Constant head model for double-ring infiltrometer

In the constant head method, a constant water depth is maintained in the infiltrometer either by a Mariotte reservoir system or manually by frequently adding a small amount of water (Bower, 1986). Depth of water ponding is usually on the order of 3- to 20-cm. The rate of water loss from the inner ring is taken as an estimate of the 1-D infiltration rate of the soil. The quasi-steady-state infiltration rate is generally used for the estimation of K_{fs} . Quasi-steady flow in the near-surface soil under the measuring cylinder is assumed when the amount of water entered into soil did not change with time usually for three consecutive measurements taken at 10 or more min intervals. The

time required to reach quasi-steady-state flow tends to increase with finer soil texture and decreasing soil structure, and as the depth of water ponding, depth of cylinder insertion, and cylinder radius increases.

For a deep soil profile, a unit hydraulic gradient is commonly assumed and the steady-state infiltration rate (q_{∞}) is considered as K_{fs} ,

$$q_{\infty} = K_{fs} \quad [2.1]$$

Although the estimation is very simple, the Eq. [2.1] neglects the effects of hydrostatic pressure and capillarity on the infiltration rate. Therefore, this tends to overestimate K_{fs} by varying degrees depending on the magnitudes of steady depth of ponded water in the ring, H (L), depth of ring insertion into the soil, d (L), radius of the inner ring, a (L), and soil parameter, α (L⁻¹).

An analysis of steady, vertical ponded infiltration from a double-ring, which takes into account the soil hydraulic parameters, ring radius, depth of ring insertion, and depth of ponding was given by Reynolds *et al.* (2002). The K_{fs} (LT⁻¹) can be obtained from quasi-steady-state infiltration rate through a double-ring as,

$$K_{fs} = \frac{q_s}{\left(\frac{H}{(C_1 d + C_2 a)} \right) + \left(\frac{1}{(\alpha (C_1 d + C_2 a))} \right) + 1} \quad [2.2]$$

where q_s (L T⁻¹) is the quasi-steady-state infiltration rate, $C_1 = 0.316\pi$ and $C_2 = 0.184\pi$ are dimensionless quasi-empirical constants. A difficulty with this approach is that insufficient information is obtained from the measurement of steady-state flow under one constant head to evaluate K_{fs} or α . The parameter α must be either selected

from the soil texture and structure categories from the table given by Elrick *et al.* (1989 as cited by Reynolds *et al.*, 2002), estimated independently or steady-state flow measurements need to be taken for two or more consecutive ponded heads (Reynolds *et al.*, 2002).

The parameter α represents the relative importance of the gravity and capillarity forces during infiltration (Reynolds *et al.*, 2002). Large α corresponds to infiltration dominated by gravity over capillarity, which occurs primarily in coarse-textured and/or highly structured porous soils. On the other hand, small α indicates dominance of capillarity over gravity, which occurs in fine-textured and/or unstructured porous soils. As a consequence, infiltration is often gravity-driven in coarse-textured and structured porous soils, and capillarity-driven in fine-textured and structure less soils. The relationship between the magnitude of α and porous medium texture and structure makes it possible to estimate α from soil texture and structure categories.

As shown in Eq. [2.2] there are three main components that influence flow from ring infiltrometers. The first term in the denominator on the right-hand side of Eq. [2.2] represents the flow due to hydrostatic pressure of the ponded water on the cylinder, the second term corresponds to the flow due to capillarity (capillary suction) of the unsaturated soil under and adjacent to the cylinder and the third term represents the flow due to gravity. For special case of $H = d = 0$, Eq. [2.2] reduces to the Wooding's (1968) expression for steady infiltration from a shallow circular pond (Eq. [2.4]).

The advantages of the ring infiltrometers are that only a small area is needed for measurements, and flow analysis is relatively simple. It is also inexpensive to construct and simple to run.

2.3.2 One- and three-dimensional tension infiltrometers

The initial efforts to predict the important features of rainfall infiltration in the field up to the time of ponding were unsuccessful when *in situ* ponded techniques were used to estimate soil hydraulic properties. This is partly because ponded measurements are heavily influenced by preferential pathways, which do not participate in rainfall infiltration until the soil water potential at the soil surface approaches zero (Clothier and White, 1982). This suggested that the relevant soil parameters should be determined at pressures less than zero.

As the importance of preferential flow paths in the rapid redistribution of surface water became understood, techniques to distinguish preferential flow from soil matrix flow were developed. Among the prominent achievements in this direction during the last three decades was the development of the 1-D and 3-D tension infiltrometers with varying design and water pressure ranges. Some of these were negative head permeameter, one-dimensional infiltrometer through gypsum crusts, closed top single ring infiltrometer, the sorptivity tube, and the tension infiltrometer (White *et al.*, 1992). The tension infiltrometer, which is very popular for measuring surface soil hydraulic properties, was used in this study for unconfined 3-D infiltration measurements and will be discussed in the following sections.

2.3.2.1 Three-dimensional (unconfined) tension infiltrometer

The tension infiltrometer (Perroux and White, 1988) consists of three major components, namely a bubble tower, water reservoir, and a circular disc. The bubble tower contains a moveable air-entry tube. This air-entry tube is used to impose the desired negative water pressure at the base of the disc by varying the distance between the air-entry point and the water level. The other large tube besides the bubble tower is a water reservoir, which contains a scale for measuring the drop in water level. For each imposed negative water pressure, the volume of water infiltrating into the soil is measured either by recording the height change of water in the reservoir manually or automated reservoir level reading (Ankeny *et al.*, 1988). The disc is to establish hydraulic continuity with the soil. This is plexiglass plate that was grooved and drilled with circular holes, approximately 1.5 mm in diameter, allowing water to freely pass through. The base of the disc is covered with a nylon membrane (400 meshes).

2.3.3 Analysis of water flow from 3-D tension infiltrometer

Infiltration under the tension infiltrometer may be considered as axisymmetric 3-D water flow in a variably saturated porous medium. The governing water flow equation for a non-swelling, homogeneous, isotropic soil with uniform initial soil water content can be described with the following form of Richards' equation (Warrick, 1992):

$$\frac{\partial \theta}{\partial t} = \frac{1}{r} \frac{\partial}{\partial r} \left[r K(h) \frac{\partial h}{\partial r} \right] + \frac{\partial}{\partial z} \left[K(h) \left(\frac{\partial h}{\partial z} - 1 \right) \right] \quad [2.3]$$

where θ is the volumetric water content ($L^3 L^{-3}$), t is time (T), h is the pressure head (L), $K(h)$ is the hydraulic conductivity function ($L T^{-1}$), and r and z are radial and vertical coordinates (L), respectively.

For the tension infiltrometer, appropriate initial and boundary conditions are described by (Warrick, 1992)

$$h(r, z, 0) = h_i \quad [2.3a]$$

$$h(r, 0, t) = h_0 \quad 0 < r < r_0 \quad [2.3b]$$

$$\frac{\partial h}{\partial z} = 0 \quad z=0 \quad r > r_0 \quad [2.3c]$$

$$\frac{\partial h}{\partial r} = 0 \quad r \rightarrow \infty \quad [2.3d]$$

$$\frac{\partial h}{\partial z} = 0 \quad z \rightarrow \infty \quad [2.3e]$$

where h_i is the initial uniform pressure head in the soil, h_0 is the pressure head of the infiltrometer, and r_0 is the disc radius. Subsurface boundary conditions are assumed to be located far enough from the supply source so that they do not affect the infiltration process (Zhang, 1997; Angulo-Jaramillo *et al.*, 2000).

Although unconfined 3-D water flow below the infiltrometer disc complicates the analysis of infiltration measurements, several methods have been devised to infer soil hydraulic properties such as sorptivity, hydraulic conductivity, soil diffusivity, macroscopic capillary length, and representative pore size from cumulative infiltration data obtained from tension infiltrometer measurements. These techniques are based on steady-state flow for homogeneous soils (Ankeny *et al.*, 1991), quasi-analytical solutions of transient (time dependent) flow at early times (Smettem *et al.*, 1994), or

numerical solutions of Eq. [2.3] through inverse parameter optimization methods for homogeneous or heterogeneous soils (Simunek and van Genuchten, 1996).

2.3.3.1 Steady-state flow procedure

Most methods for inferring water transmission properties from steady-state models for analyses of 3-D flux out of a tension infiltrometer into the soil depend on Wooding's (1968) solution. The Wooding's equation approximates the steady-state infiltration rate, q_{∞} ($L T^{-1}$) from shallow circular source of radius r (L) at the soil surface:

$$q_{\infty} = K_0 + \frac{4\phi_0}{\pi} \frac{1}{r} \quad [2.4]$$

where ϕ_0 is the matrix flux potential ($L^2 T^{-1}$) defined by

$$\phi_0 = \int_{h_i}^{h_0} K(h) dh \quad h_i \leq h_0 \quad [2.5]$$

and K_0 ($L T^{-1}$) is the hydraulic conductivity at the imposed pressure h_0 , ($K_0 = K(h_0)$).

The subscripts i and 0 refer respectively, to the initial and surface boundary conditions.

It is assumed in Eq. [2.4] that the initial soils pressure head h_i is sufficiently small for the condition $K(h_i) \ll K(h_0)$ to be fulfilled.

As shown in Eq. [2.4], the flow from tension infiltrometer is 3-D and is the result of gravity acting downward, capillary forces acting in all directions, and the geometry of the water supply source.

Wooding assumed that the $K(h)$ of soil varies with water pressure as proposed by Gardner (1958).

$$K(h) = K_{fs} \exp(\alpha h) \quad [2.6]$$

where K_{fs} is the field-saturated hydraulic conductivity [$L T^{-1}$], and α is a fitting parameter and is called inverse macroscopic capillary length scale [L^{-1}]. Substituting Eq. [2.6] into Eq. [2.5] and integrating gives,

$$\phi_0 = \frac{K_0}{\alpha} \quad [2.7]$$

Substitution of Eq. [2.7] into Eq. [2.4] yields

$$q_\infty(h) = K(h) \left(1 + \frac{4}{\pi r \alpha} \right) \quad [2.8a]$$

Substitution of Eq. [2.6] into Eq. [2.8a] gives

$$q_\infty(h) = K_{fs} \exp(\alpha h) \left(1 + \frac{4}{\pi r \alpha} \right) \quad [2.8b]$$

Part of the success of the tension infiltrometer is a result of relative simplicity of the associated methods of analysis. There are only two unknowns to be determined: K_0 and ϕ_0 in Eq. [2.4] or K_{fs} and α in Eq. [2.8b]. This can be achieved by imposing two (or more) negative water pressures (multiple-head) at the soil surface (Ankeny *et al.*, 1991) or by using two (or more) disc radii (multiple-disc) (Smettem and Clothier, 1989).

2.3.3.2 Multiple-head approach

Measured steady-state flow for n water pressures at the same site, results in n equations, each with two unknowns of $K(h)$ and α . For two supply water pressures, h_1 and h_2 , division of two equations from Eq. [2.8a] with two pressures and solving for α yields,

$$\alpha = \frac{|\ln(q_\infty(h_2) - q_\infty(h_1))|}{|h_2 - h_1|} \quad [2.9]$$

provided that α is constant over the range h_1 and h_2 . Because $q_\infty(h_1)$ and $q_\infty(h_2)$ are measured, and h_1 and h_2 , are known, α can be computed directly from Eq. [2.9]. Applying this procedure to sequential pairs of measurements produces a piece wise $K(h)$ curve. A pair of infiltration measurements yields estimates of α . The hydraulic conductivity is determined for each supply water pressure using Eq. [2.8a] by taking the arithmetic average of $K(h)$ determined using left and right side estimates of α when available. The K_{fs} can be estimated from Eq. [2.8a] using $K(h)$ and α obtained from infiltration pairs at zero and the next lowest supply pressure. This piecewise approach is recommended, particularly for structured soils of which α do not remain constant as water pressure decreases (Ankeny *et al.*, 1991).

Instead of fitting infiltration measurements by a piecewise relationship made at sequential water pressures, Logsdon and Jaynes (1993) introduced a non-linear regression technique for fitting simultaneously all data into Eq. [2.8b] for the determination of K_{fs} and a single α value. Comparing different methods, Hussien and Warrick (1993) found that the single-disc method with multiple (more than three) pressures, and with a large disc radius, gave the most stable and accurate results.

An advantage of this multiple-head method is that measurements at different water pressures can be made at the same location, which avoids possible spatial variation differences between the water pressures.

2.3.3.3 Multiple-disc approach

Smettem and Clothier (1989) proposed a method to determine K_0 and ϕ_0 using two or more contrasting disc radii. For two discs with radii, r_1 and r_2 , and respective steady-state flow rates q_1 and q_2 , the simultaneous solution of Eq. [2.4] results,

$$K_0 = \frac{q_1 r_1 - q_2 r_2}{r_1 - r_2} \quad [2.10a]$$

and

$$\phi_0 = \frac{\pi}{4} \frac{q_1 - q_2}{\frac{1}{r_1} - \frac{1}{r_2}} \quad [2.10b]$$

In order to obtain reasonable sensitivity in the solution it is recommended that $r_1 > 2r_2$.

Alternatively, if more than two disc sizes are employed, K_0 and ϕ_0 can be found through linear regression between q_i and $1/r_i$ (Eq. [2.4]). The intercept and slope provide K_0 and $4\phi_0/\pi$, respectively. Again, the $(1/r)$ ratio should be greater than two for reasonable sensitivity (Smettem and Clothier, 1989).

This multi disc approach avoids the difficulties of taking measurements during the initial phase of infiltration. However, this method requires measurements at different locations, and thus is very sensitive to spatial variability of soil hydraulic properties.

2.3.3.4 Transient flow procedure (Single-head – single-disc approach)

This method is based on the transient flow models at early time infiltration. The majority of the transient flow models for the tension infiltrometers are the 3-D extensions of the Phillip's (1957) 1-D horizontal infiltration equation. For a homogeneous, infinitely deep soil profile at uniform initial moisture content, Phillip

(1957) derived an exact solution, which describes the time dependence of cumulative infiltration in terms of a power series. For vertical infiltration, the cumulative infiltration, $I(L)$ is expressed by

$$I(t) = S_0 t^{1/2} + A_2 t + A_3 t^{3/2} + \dots + A_n t^{n/2} \quad [2.11]$$

where t is time elapsed and A_2 and A_3 are constants representing the characteristics of the soil. The S_0 ($L T^{-1/2}$) ($S_0 = S(h_0)$) is an integral soil characteristic and is known as sorptivity. Sorptivity is the dominant parameter governing the early stages of infiltration and is the capacity to absorb or release water during early times of infiltration.

During early stages, when the effect of gravity is negligible, Eq. [2.11] reduces to

$$I(t) = S_0 \sqrt{t} \quad [2.12]$$

The S_0 can be determined from the slope of a graph of I vs. \sqrt{t} (White *et al.*, 1992),

$$S_0 = \lim_{t \rightarrow 0} \left[\frac{dI}{d\sqrt{t}} \right] \quad [2.13]$$

Once the S_0 is known, ϕ_0 can be estimated from the following relationship (White *et al.*, 1992),

$$\phi_0 = \frac{b s_0^2}{\theta_0 - \theta_n} \quad [2.14]$$

where θ_n and θ_0 are the initial and final water contents under the disc. The shape factor b is a constant dependent on the slope of the soil water diffusivity function. Factor b generally lies in the range of $1/2$ and $\pi/4$, and is assumed to be 0.55 for field soils. From

the soil moisture content, steady-state flow, and S_0 the hydraulic conductivity can be calculated corresponding to the supply water pressure.

The standard analysis of tension infiltration measurements uses Wooding's solution for the 3-D steady-state infiltration which is valid for infinite time and uniform initial conditions. Unfortunately, neither of these conditions is often met in the field (Smettem *et al.*, 1994). In order to overcome these limitations, various models have been developed by various researchers for the analysis of 3-D transient flow (Zhang, 1997; Warrick, 1992), as an extension for the Phillip (1957) 1-D infiltration equation. The recent expressions have in common two-term form of the cumulative infiltration equation although they differ by the expression of coefficients,

$$I(t) = C_1 \sqrt{t} + C_2 t \quad [2.15]$$

Among the recent models available, the Haverkamp *et al.* (1994) model, which is developed using previous findings of other researchers, is simple and is based on parameters with sound physical meanings. For short to medium times, the Haverkamp model can be expressed as,

$$C_1 = S_0 \quad [2.16]$$

$$C_2 = \frac{2-\beta}{3} K_0 + \frac{\gamma S_0^2}{r(\theta_0 - \theta_n)} \quad [2.17]$$

where γ is the proportionality coefficient with bounds $0.6 < \gamma < 0.8$ and β is a shape factor lying between 0 and 1. The second term of the right hand side of the Eq. [2.17] takes care of the edge effects of the disc (lateral capillary flow), and thus provides accurate estimates of S_0 .

The coefficients C_1 and C_2 can be estimated through linear fitting technique for the following differential equation,

$$\frac{dI}{d\sqrt{t}} = C_1 + 2C_2 \sqrt{t} \quad [2.18]$$

For the linear graph between $dI/d\sqrt{t}$ vs. \sqrt{t} , C_1 and C_2 equal to the intercept and half of the slope, respectively (Vandervaere *et al.*, 2000). Hydraulic conductivity is then calculated using either steady-state flow through Eqs. [2.4] and [2.14],

$$K_0 = q_\infty - \frac{4bS_0^2}{\pi r(\theta_0 - \theta_n)} \quad [2.19]$$

or transient flow by combining Eqs. [2.14], [2.16] and [2.17]:

$$K_0 = \frac{3}{2-\beta} \left(C_2 - \frac{\gamma S_0^2}{r(\theta_0 - \theta_n)} \right) \quad [2.20]$$

In Eq. [2.19], it is assumed that the capillary forces acting to draw water into the soil when steady-state flow is attained are similar as those at early time. The early-time capillary forces cause the initial 1-D flow to occur and allow S_0 to be measured. However, if there is a change in either the water content or the structure of the soil with depth, then the capillary forces acting when capillary forces are measured may be different from those at steady-state. The S_0 can then probably be invalid, and subsequently, the values of K_0 calculated from this method will be less accurate.

This transient flow approach is attractive because it requires only a single disc and a single supply pressure to obtain S_0 and K_0 at any supply potential (provided θ_n and θ_0 are measured) (Smettem *et al.*, 1994). The analysis of disc infiltration observations with this transient solution allows better point estimation of the hydraulic conductivity and

sorptivity for a set of chosen initial and boundary conditions. Further, transient flow approach requires shorter experiments and smaller sampled volumes of soil (shallow soil depth), which is certainly in better agreement with assumptions of homogeneity, and uniform initial soil water content. This method therefore, is suited to layered soils, shallow surface soils, and soil tillage studies (White *et al.*, 1992). It also utilizes information at early part of infiltration and removes the uncertainties about the time at which quasi-steady infiltration is attained.

2.3.3.5 Inverse procedure

Inverse method is an alternative to direct estimates of hydraulic properties from *in situ* measurements of infiltration. With this approach, the parameters describing the soil hydraulic properties are estimated by an optimization procedure that minimizes discrepancies between the measured (observed) values of one or more flow variables, and the corresponding values estimated (calculated) by solving numerically the Richards' equation (Eq. [2.3]). Initial estimates of the parameters are usually iteratively improved during the minimization process until a desired degree of precision is obtained.

The objective function (OF) to be minimized during the parameter estimation process may be defined as (Simunek and van Genuchten, 1996)

$$OF [b, \dots, q_m] = \sum_{j=1}^m \left[\frac{1}{n_j \sigma_j^2} \sum_{i=1}^{n_j} w_{ij} (q_j^*(t_i) - q_j^*(t_i, b))^2 \right] \quad [2.21]$$

where m represents the different sets of measurements (e.g., the cumulative infiltration, or additional information), n_j the number of measurements in a particular set, σ_j the

standard deviation associated with measurement errors, $q_j^*(t_i)$ are the specific measurements at time t_i for the j th measurement set, b is the vector of optimized parameters, $q_j(t_i, b)$ are the corresponding model predictions for the parameter vector b , and w_{ij} the weight associated with a particular measurement point.

The inverse parameter optimization procedure is especially suitable for heterogeneous soils. This method offers an economical means to infer soil hydraulic properties from *in situ* measurement of infiltration as the information on not only hydraulic conductivity but also water retention curve can be obtained from cumulative infiltration data from a single experiment of a tension infiltrometer at several consecutive water pressures. The identifiability of parameters can be improved when information such as initial and final water contents of the soil profile and water retention data points (Schwartz and Evett, 2002), included in the objective function, in addition to the cumulative infiltration data.

For vertical flow, Eq. [2.12] is only valid within a very short infiltration time. In reality, it is difficult to measure enough data points of cumulative infiltration in the very short time span within which Eq. [2.12] is valid. This problem is exacerbated in a 3-D field, where the time is even less. In addition, tension infiltrometers are usually placed on a layer of sand to ensure hydraulic contact between the infiltrometer and the soil. The effect of this layer on the first stages of infiltration may be sufficient to mask the portion of infiltration curve desired for analysis (Vandervaere *et al.*, 2000) and error may occur if the thickness of the sand layer is not taken into account. Furthermore, short-term measurements may be influenced by many factors including water repellency, mesopore changes, and excessive 3-D influence for small diameter infiltrometers (Smettem *et al.*,

1994; Vandervaere *et al.*, 2000). As a consequence, estimation of sorptivity and hydraulic conductivity from transient flow is less reliable.

Unlike the transient flow analysis, only steady-state measurements are needed for the steady-state flow analysis. Analysis based on steady-state flow requires neither measurements of changes in volumetric moisture content (initial and final moisture content) on the infiltration surface, nor estimation of sorptivity from the early square-root-of-time infiltration behavior. As indicated by Smettem and Clothier (1989), both of these parameters can be difficult to obtain in wet or highly permeable soils. For steady-state flow analysis, measurements are taken on the same soil surface. Measurements taken by using different disc radii are more dependent on the assumptions of soil homogeneity (Ankeny *et al.*, 1991). The contact sand layer would not affect steady-state measurements of infiltration rate (Vandervaere *et al.*, 2000) and the sand layer need only have a $K(h)$ value and air-entry value that are not limiting for the soil or range of applied water pressures. Therefore, use of steady infiltration rate for the estimation of hydraulic properties of surface soils seems to be more appropriate than transient flow analysis.

The soils in the cultivated fields appears to be reasonably homogeneous for at least 10- to 15-cm depth and the initial water content gradients close to the surface are not too steep (Vandervaere *et al.*, 2000). In comparison with uncertainty due to spatial and temporal variability of hydraulic conductivity and sorptivity, errors due to assumptions of the theory not being met are probably insignificant in many situations. Furthermore, the single exponential relationship between hydraulic conductivity and applied water pressures was sufficient to represent the entire pressure range tested in the field

experiments. For these reasons, single-disc multiple-head procedure with Logsdon and Jaynes (1993) non-linear regression technique was used for the estimation of K_{fs} and α for all the experiments described in this thesis.

2.3.4 Advantages of using tension infiltrometers

The use of tension infiltrometers has advantages which make it attractive to researchers interested in surface soil hydraulic properties and macroporosity. Due to sensitivity of hydraulic and transport properties to soil structure, *in situ* methods which do not greatly disturb the soil surface being measured such as tension infiltrometers are potentially more accurate than laboratory methods. The device is relatively inexpensive, easy to use, portable, simple, and small amount of water are generally needed. Generally two liter of water is sufficient to perform infiltration measurements at four different negative water pressures. Further, the 3-D geometry of infiltration allows steady-state to be reached much faster than in the case of 1-D experiments. Therefore, measurements can be made quickly. Generally, only 20- to 30-min are required to achieve steady-state flow rates at a given pressure (White *et al.*, 1992). These qualities of the tension infiltrometer make it particularly suitable for spatial variability studies (Sauer *et al.*, 1990; Shouse and Mohanty, 1993). The initial and boundary conditions are well controlled, and therefore, tension infiltrometer experiments are particularly appropriate for data analysis through inverse procedures. The most important advantage of the tension infiltrometer is that by varying the negative water pressure pores of a certain size can be eliminated from the flow process, and thus the effect of pore-size distribution on infiltration can be determined.

2.3.5 Limitations and sources of error using tension infiltrometers

The principal limitations of the tension infiltrometers are those associated with the simplifying assumptions of the analysis (White *et al.*, 1992). Gradients in water content, soil layering, and changes in soil texture and bulk density can all occur near the soil surface. Therefore, assumptions that the soil is uniform, homogeneous, and non-swelling may not be true. Water-conducting porosity calculations assume macropore flow to follow Poiseuille's law (laminar flow) and capillary theory. These assumptions are not strictly valid, but the calculations for field measurements are helpful in relative sense (Logsdon *et al.*, 1993). Nevertheless, the uppermost layer of tilled soil to about 10- to 15-cm depth may well approximate to homogeneous, isotropic conditions. In this context, the depth of wetting attained at the end of a complete sequence of infiltration runs at the soil surface will be confined to this tilled layer (Vandervaere *et al.*, 2000). This enables us to use tension infiltrometer for the estimation of soil hydraulic properties in cultivated fields.

Difficulties can arise when applying supply potentials close to zero in freshly cultivated soils (White *et al.*, 1992). The strength of the soil after a recent tillage event may not be adequate to support the weight of the tension infiltrometer, causing a collapse of soil macropores. Use of a tension infiltrometer with a disc separated from the water tower and attached to it via a flexible tube may reduce the weight of the disc, and thus the effect of weight on surface soil structure.

Ensuring intimate contact between the soil and the source of water is crucial (Perroux and White, 1988). This involves use of a contact material, generally fine sand. Problems may arise in uneven soil surfaces, as more contact sand is needed. In this case, the

contact material itself may dominate measurements in the early part of flow. Furthermore, the hydraulic conductivity of the sand must be higher than that of the soil being tested, or else the sand layer will impede the movement of water into the soil. However, steady-state flow is not affected by contact sand layer if the hydraulic conductivity of it is greater than that of soil (Vandervaere *et al.*, 2000). Further, contact sand layer effect can be minimized by taking its thickness and the volume of water stored in the sand layer into account in calculations (Reynolds and Zebchuck, 1996; Vandervaere *et al.*, 2000).

Finally, there may be problems associated with the interception of solar radiation by the water reservoir on hot sunny days (White *et al.*, 1992). This can result in heating of the water and consequently lower viscosity. This effect is generally negligible, and can be prevented by either insulating the reservoir or inserting a temperature probe and correcting for viscosity changes.

2.4 Factors Affecting Surface Soil Hydraulic Properties

Factors affecting infiltration and hydraulic properties can be grouped into soil, soil surface and agricultural management categories. Soil factors include texture, structure (bulk density, porosity, pore-size distribution and pore continuity), structural stability and soil layering. Surface factors are mainly topography or slope gradient, the presence or absence of cover materials and soil crust. Agricultural management systems involve type of land use or vegetation, tillage, residue management and type of grazing practices in grasslands (Rawls *et al.*, 1993). Topography or slope gradient and type of land use are among the main soil and management factors that greatly influence surface soil hydraulic properties and will be discussed in the following sections.

2.4.1 Effect of topography or slope gradient on soil hydraulic properties

In this section, the necessity of characterizing surface soil hydraulic properties in sloping lands, methods available for measuring hydraulic properties in sloping lands together with their limitations, and the importance of the evaluation of tension and double-ring infiltrometers for the estimation of surface soil hydraulic properties are discussed.

2.4.1.1 Soil hydraulic properties in sloping landscapes

Most of the landscapes under cultivation and watersheds, in many parts of the world, are non-level. For instance, of the agricultural lands in Saskatchewan, approximately 2.4% is nearly level (0-0.5% slope), and 64.9% and 25.1% of lands lie between 0.5-5% and 5-15% slopes, respectively (Eilers W.D., University of Saskatchewan, personal communication, 2003). It has also been reported by various researchers that the topography or slope gradient influence soil properties such as soil moisture, infiltration rate, saturated and unsaturated hydraulic conductivity (Sinai *et al.*, 1981; Zebarth and de Jong, 1989a; Zebarth and de Jong, 1989b). Furthermore, experiments carried out by Pennock *et al.* (1987) in Saskatchewan, Canada highlighted the importance of considering land-surface morphology, which include slope gradient, profile (downslope) curvature, and plan (across-slope) curvature for designing landscape-scale research projects. In this context, estimation of surface soil hydraulic properties in sloping landscapes is of utmost importance.

2.4.1.2 Measurement of soil hydraulic properties in sloping landscapes

Only a few measurement techniques exist for determining hydraulic characteristics *in situ* on hillslopes. Dunne and Black (1970) carried out an experiment in a hillslope by

measuring subsurface flow in a trench in Vermont, U.S.A. Similarly, Mosley (1982) measured hydraulic characteristics in a hillslope by excavating a trench along the contour to the bedrock and applying water with a line source uphill in South Island, New Zealand. Later, Torres *et al.* (1998) conducted tracer studies in a steep watershed in Oregon using tensiometers, piezometers and suction lysimeters. The main interest of these hillslope experiments was to identify subsurface flow pathways. These techniques, however, are time consuming and tedious to perform under field conditions. Therefore, they are usually not suitable for routine application at a great number of measurement points over the field. Recently, an apparatus called hillslope infiltrometer was developed by Mendoza and Steenhuis (2002) for determining vertical and horizontal saturated hydraulic conductivity of soils where the conductivity is decreasing with depth. The hillslope infiltrometer is a metal box that slides around and isolates a soil column. It has open ends at the bottom, top, and downhill sides. The installation of this device requires the carving of a soil block that is slightly smaller than the infiltrometer (36 cm in length, 30.5 cm in width and 41 cm in height) and excavation of a trench around the block for ease of installation of the device and water collectors. This particular method is destructive, time consuming and somewhat cumbersome, for routine field use.

2.4.1.3 Use of tension and double-ring infiltrometers for estimation of surface soil hydraulic properties

No specifically designed instruments are commercially available for the estimation of surface soil hydraulic properties in sloping lands. As a result, the tension and single-ring or double-ring infiltrometers, which are primarily designed and tested in horizontal surfaces, have been widely used in the past for the determination of saturated and near-

saturated soil hydraulic properties at and near the soil surface. Tension and double-ring infiltrometers have been employed by Watson and Luxmoore (1986) and Wilson and Luxmoore (1988) to measure infiltration rates (hydraulic conductivity), macropore flow and water-conducting macroporosity and mesoporosity in forest watersheds with slopes up to 20%. Using tension infiltrometers, Joel and Messing (2000) compared two procedures (split-location method and one-location method) for determining near-saturated hydraulic conductivity on sloping lands. In the split-location method, the tension infiltrometer was moved to an adjacent spot after infiltration measurement at each applied water pressure. In the one-location method, the tension infiltrometer was not moved during the measurements of infiltration at each sequence of applied water pressure. They recommended the one-location method for studies in which disturbance of the soil surface must be kept to a minimum (e.g., experimental plots). The influence of aspect and slope on hydraulic conductivity in two hillsides was studied by Casanova *et al.* (2000). They observed a tendency to increase in $K(h)$ with increasing slope gradient. Conversely, both Joel and Messing (2000) and Casanova *et al.* (2000), did not test the suitability of tension infiltrometers for the characterization of hydraulic properties in sloping lands, and recommended further studies on the influence of slope on tension infiltrometer measurements.

2.4.1.4 Limitations of tension and double-ring infiltrometers in determining hydraulic properties in sloping landscapes

When tension infiltrometer tests are carried out on steep sloping surfaces, the applied negative water pressure varies from the upslope to the downslope side of the interface between disc and soil (White *et al.*, 1992). From upslope to downslope it increases linearly over the interface with the maximum value at the lower edge. The

predetermined pressure may valid only for the midpoint of the disc. A slightly negative pressure applied at the centre of the disc may impose a positive pressure at the lower edge. As indicated by Reynolds and Zebchuck (1996), the variation of pressure across the sloping surface will have a substantial impact on the validity of the tension infiltrometer results because the infiltrometer operates in the 'macropore range' where water transmission properties can change drastically with even small changes in water pressure. Sullivan *et al.* (1996) avoided this problem on gently sloping fields by placing the contact sand layer on the soil surface and building it up level. On steep slopes, they created a 'bench', which requires some disturbance and removal of some of the surface soil on the upslope side of a test location. Furthermore, several researchers (Zaslavsky and Sinai, 1981; McCord *et al.*, 1991) have shown that downslope flow is greatly influenced by slope gradient and can occur even under unsaturated condition in the presence of soil layering close to the surface and/or anisotropy favoring downslope flow. However, small constant anisotropy causes too little lateral downslope flow relative to vertical flow (Jackson, 1992). As a consequence, the infiltration rate, and the estimated hydraulic properties from infiltration measurements would not vary much between level and sloping lands.

In the case of double-ring infiltrometer, the infiltration measurements are carried out with a constant head at the center of the inner ring. Like that of tension infiltrometer, the pressure varies across the sloping surface with the maximum value at the downslope side and lowest value in upslope side. Therefore, infiltration rate would be lower at the upslope side than that of the downslope side. The decrease in infiltration rate at the upslope side may be compensated by the increase in infiltration rate at the downslope

side. Furthermore, Phillip (1991) reported that downslope flow occur as a result of downslope component of gravity in sloping lands. Magnitude of slope effects on downslope flow increases with the increase of slope. However, for homogeneous and isotropic soils under constant flux boundary condition, Phillip theoretically showed that the infiltration normal to the slope differed relatively little from infiltration from a horizontal surface for slope gradients less than 30° (slope = 58%).

Despite the extensive use of tension and double-ring infiltrometers in determining surface soil hydraulic properties in sloping lands with certain limitations, no systematic studies were conducted on the suitability of this equipment for the estimation of those properties in sloping lands to the best of our knowledge. Hence, exploration of these versatile tools (tension and double-ring infiltrometers) for determination of soil hydraulic properties is urgently required.

2.4.2 Effect of porosity and pore-size distribution on soil hydraulic properties

The early part in this section deals with definition and classification of soil pores. Then the role of water-conducting pores (macro- and mesopores) in the infiltration process is discussed. The last section reviews the techniques use for quantifying water-conducting porosity characteristics.

2.4.2.1 Porosity and pore-size distribution

Soil porosity is the part of the bulk volume of soil not occupied by soil particles (SSSA, 2003). Soil pores are not only important because of their role in moisture retention, root growth and aeration, but also for their hydrological importance (Ankeny *et al.*, 1990; Luxmoore *et al.*, 1990). When considering water movement in soil, pore-size distribution is more important than the total porosity.

Some of the pores in soils may be dead-ended and others may be continuous. The continuous macropores will contribute to fast water flow and we call these pores water-conducting (macro) pores and the ratio of the volume of these pores to the total soil volume the water-conducting (macro) porosity. Examination of water-conducting macropores allows characterization of pore connectivity and tortuosity and provides insight into effects of soil management on hydrological processes.

2.4.2.2 Classification of soil pores

Soil pores can be classified into different groups based on their size or capillary potential. Of the classifications available (Beven and Germann, 1981; Reeves, 1980; Marshall, 1959; Brever, 1964; Mc Donald, 1967 as quoted by Beven and Germann, 1982), one suggested by Luxmoore (1981) seem to be more appropriate than that of others for characterization of pores in the field. He designated three main pore classes: micropores ($< 10 \mu\text{m}$ diameter or $< -30 \text{ kPa}$ pressure), mesopores (10 to 1000 μm diameter or -30 to -0.3 kPa pressure), and macropores ($> 1000 \mu\text{m}$ diameter or $> -0.3 \text{ kPa}$ pressure).

When macropores are considered, a constant definition of macropores has not been produced on the basis of capillary potential, as sizes range from 30- (Marshall, 1959 in Beven and Germann, 1982) to 3000- μm diameter (Beven and Germann, 1981). It has been suggested that the function and continuity of macropores in terms of water movement are often more important than their size (Bouma, 1981). In this context, the definition given by Skopp (1981), which is “the pore space which provides preferential paths of flow so that mixing and transfer between such pores and remaining pores is limited” seem to be more appropriate. On the basis of morphology, Beven and Germann

(1982) developed four categories of macropores, namely pores formed by the soil fauna and plant roots, and cracks, fissures and natural pipes. However, it has been suggested that the classification of macropores size classes is rather arbitrary and is often related more to the details of experimental technique than to considerations of flow processes (Beven and Germann, 1982). Based on the simplicity and field applicability, the classification system proposed by Luxmoore (1981) for macro-, meso- and micropores was used in the three experiments discussed in this thesis.

2.4.2.3 Relative contribution to flow by macro- and mesopores

The significance of macropores and mesopores to water flow in soils, particularly to infiltration and rapid movement of water, solutes and pollutants through soils are well recognized (Beven and Germann, 1982; Luxmoore *et al.*, 1990; Ankeny *et al.*, 1990). The Hagen-Poiseuille's law predicts that flow rate increases with the fourth power of the pore (tube) radius. Therefore, macro- and mesopores can substantially increase water flux through a soil. Watson and Luxmoore (1986) reported that 73% of the ponded flow was conducted through the pores with a diameter greater than 1×10^{-3} m in a forest watershed; 96% of the water flux was transmitted through only 0.32% of the total soil volume. Dunn and Phillips (1991a) observed that 43% of the total flow was conducted through macropores while 77% of the total flow at -0.06 kPa water pressure was transmitted through the pores $> 2 \times 10^{-2}$ m in diameter in conventional tillage plots. It is clear that although macro- and mesopores comprise of small fraction of the total soil volume, they are capable of rapidly transmitting large quantities of water through soil.

2.4.2.4 Consequences of macro- and mesopore flow

Due to the significant amount of water that can move through macro- and mesopores, their effect on water and solute movement during infiltration process is of great importance. The presence of macro- and mesopores continuous with depth allows infiltrating water to bypass portions of the soil matrix to greater depths than predicted by Darcian theory and such behavior is known as channeling, short circuiting, by passing or preferential flow (Beven and Germann, 1982). Due to bypassing the soil matrix by macro- and mesopore flow, plants may not benefit from a rainfall or irrigation as much as anticipated since some of the water may move directly below the root zone, and begin recharging ground water long before the soil matrix reaches field capacity (Thomas and Phillips, 1979). Probably the most important consequence of macropore flow is the fact that the rapid leaching of fertilizers, soluble and particulate waste materials, and other potential pollutants below the rooting depth may occur. A major concern is that of intensive agricultural systems which are dependent upon use of large amount of fertilizers, pesticides and/or herbicides where the presence of water-conducting continuous macropores in conjunction with appropriate hydrological conditions leads to rapid transport of these chemicals to the ground water system, which may be a source of drinking water.

2.4.2.5 Characterization of water-conducting macro- and mesoporosity

Macroporosity and mesoporosity (the fractions of soil volume comprise of pores with diameters $> 1 \times 10^{-3}$ m and between 1×10^{-5} and 1×10^{-3} m, respectively) of soil core samples or soil columns can be easily determined in the laboratory (Flint and Flint, 2002). Macro- and mesopores include dead-ended and non-continuous pores, as well as

continuous pores with cylindrical or irregular geometry, but only the continuous or interconnected pores (water-conducting pores) contribute to fast water flow in soil. Furthermore, the equivalent diameter of the water-conducting continuous pores is controlled primarily by the part with the smallest diameter (bottle neck) along its pathway although the bottle-neck may only be a small fraction of the total length of the pore (Dunn and Phillips, 1991b). The function of water-conducting pores is also influenced by pore tortuosity, surface roughness etc. (Skopp, 1981). Therefore, higher soil macro- and mesoporosity does not necessarily imply higher hydraulic conductivity and faster chemical transport, and static measurements of pore characteristics such as total macro- and mesoporosity measurements in the laboratory will not adequately describe the actual contribution of pores to flow of water and solutes in soil (Messing and Jarvis, 1993). Hence, *in-situ* measurement of actual water-conducting porosity is of utmost importance in understanding movement of water and solutes into and through soils.

2.4.2.6 Overview of methods used to characterize water-conducting porosity and their limitations

Characterization of water-conducting macro- and mesoporosity has been accomplished by various methods. The characterization may be either qualitative or quantitative and can be achieved by direct or indirect methods. Quantitative analysis of water-conducting macro- and mesoporosity is usually acquired with direct methods. One of the popular direct methods is a dye staining or dye tracing (Bouma *et al.*, 1979; Weiler and Naef, 2003). Dye tracers and breakthrough curves have also been widely employed to evaluate preferential flow paths and parameters for preferential flow models (Yeh *et al.*, 2000). A relatively new method to identify pore structures without soil sectioning,

as in staining studies, involves the use of computer assisted tomography with X-ray scanners (Anderson *et al.*, 1990). Timlin *et al.*, (1994) used an infiltration-redistribution pattern to determine contribution of water-conducting macro- and mesoporosity during infiltration. The infiltration-redistribution method has advantages such that it does not require the soil to be homogeneous with depth, and the apparent macropore conductivity can be determined for subsurface layers without much soil disturbance. This gives a measure of macropore continuity as well. These methods, however, require either undisturbed soil cores/columns, are costly or are laborious and tedious to perform under field conditions. Rapid, simple, and *in situ* ponded- and tension-infiltration measurements, on the other hand, have become popular recently in characterizing water-conducting macro- and mesoporosity in the surface soils.

Using the tension infiltrometer measurements in conjunction with ponded infiltration in double-ring infiltrometer, Watson and Luxmoore (1986) and Wilson and Luxmoore (1988) characterized hydraulically active macro- and mesopores. Based on the capillary theory and Poiseuille's law, Watson and Luxmoore (1986) calculated the number of pores per unit area $N(a,b)$, between two pore radii a and b ($a < b$). Assuming pore radius equals to the minimum pore radius, the number of pores resulting in a difference in total soil water flux or hydraulic conductivity between two water pressures, $\Delta I(a,b)$, corresponding to the two pore radii, is

$$N(a,b) = \frac{8 \mu \Delta I(a,b)}{\pi \rho g} \frac{1}{a^4} \quad [2.22]$$

where μ is the dynamic viscosity of water ($M L^{-1} T^{-1}$), ρ is the density of water ($M L^{-3}$), and g is the acceleration due to gravity ($L T^{-2}$). The total water-conducting porosity ($L^3 L^{-3}$) due to pores in this range, $\varepsilon(a,b)$ is then given by

$$\varepsilon(a,b) = N(a,b) \pi a^2 = \frac{8\mu I(a,b)}{\rho g} \frac{1}{a} \quad [2.23]$$

Watson and Luxmoore (1986) estimated the number of pores per unit area of soil surface using the minimum equivalent pore radius in each pressure range. However, their calculation results in the maximum number of pores hence maximum water-conducting porosity, since pore radius (a) appear in the denominator of Eq. [2.22] and [2.23]. Consequently, their approach results in an overestimation of the number of pores per unit area and the total water-conducting porosity in the pressure range.

Dunn and Phillips (1991a) modified the approach of Watson and Luxmoore (1986) by assuming a uniform (Box-car) distribution of pore number. Their calculation results in the mean number of pores per unit area $\overline{N(a,b)}$, as if all the pores have the same radius.

The $\overline{N(a,b)}$ is given by

$$\overline{N(a,b)} = \frac{8\mu \Delta I(a,b)}{\pi \rho g} \frac{\int_a^b r^{-4} dr}{\int_a^b dr} \quad [2.24]$$

where a and b are pore radii of the lower and upper limits of the integrals of each sequential water pressure range.

Neglecting the dependence between $N(a,b)$ and pore cross-sectional area, and assuming constant slope of infiltration rate I as a function of pore radius ($\Delta I(a,b) / \int_a^b dr = \Delta I(a,b) / (b-a)$),

which means a linear dependence of $I(a,b)$ on r , Dunn and Phillips (1991a) also calculate the mean water-conducting porosity $\overline{\varepsilon(a,b)}$, for pore size between a and b ,

$$\overline{\varepsilon(a,b)} = \overline{N(a,b)} \pi \frac{\int_a^b r^2 dr}{\int_a^b dr} \quad [2.25]$$

The common place of the approaches of Watson and Luxmoore (1986) and Dunn and Phillips (1991a) is that they both assumed a single pore size (minimum pore radius for Watson and Luxmoore and mean pore radius for Dunn and Phillips). The assumption is unrealistic and may lead to incorrect water-conducting porosity, an unrealistic parameterization of soil properties, and poor performance of hydrological models. Therefore, there is a need for development of a reliable and convenient method for the estimation of water-conducting macro- and mesoporosity.

2.4.3 Effect of land use on soil hydraulic properties

In this section the influence of management practices such as tillage and vegetation on surface hydraulic properties is discussed. Then the relationship among land use, wetland water level and surface hydraulic properties with special reference to Canadian prairies are reviewed.

2.4.3.1 Management practices and hydraulic properties

Soil hydraulic properties at saturated and near-saturated conditions are strongly affected by soil structure. One important parameter in soil structure is the size distribution and stability of aggregates which in turn influence pore-size distribution. Therefore, any management factor that affect structure or pores geometry of soil may affect hydraulic properties, especially at saturated and near-saturated conditions.

Management practices such as tillage influence pore-size distribution and pores continuity and thereby soil hydraulic properties. Several studies have been conducted on soil hydraulic properties in relation to tillage and the results were contradictory. Depending on cultivation history, climate zone, and the soil management, saturated and unsaturated hydraulic conductivity under no-till or minimum tillage can be either greater (Benjamin, 1993), or lower (Miller *et al.*, 1998) than that under continuously tilled treatments, or not significantly different from that under continuously tilled treatments (Obi and Nnabude, 1988).

2.4.3.2 Type of vegetation and soil hydraulic properties

Hydraulic properties near saturation are highly correlated with structural stability and macroporosity. Soil organic matter is mainly responsible for stability of soil aggregates (Chaney and Swift, 1984). Generally, soil organic matter content is greater in lands under pasture or forest cover than continuous cultivated lands. Hence large and stable aggregates and more macropores are expected under grass and forest cover than in cultivated fields.

A few studies have been concentrated on macroporosity and hydraulic properties of forest soils and pasture lands. Watson and Luxmoore (1986) and Wilson and Luxmoore (1988) quantified water flow in forested watersheds with the use of a tension infiltrometer and a double-ring infiltrometer. Watson and Luxmoore (1986) observed that 73% of the ponded flux was conducted through macropores with diameter $> 1 \times 10^{-3}$ m while Wilson and Luxmoore (1988) found 85% of the ponded flux moved through macropores. Change in land use from natural forest to crop cultivation modified the hydraulic properties of the surface soil resulting in an increased runoff/infiltration ratio

(Leduc *et al.*, 2001). Generally, permanent or well-managed pasture plots had higher infiltration rates and saturated and unsaturated hydraulic conductivity than conventionally cultivated plots (Chan and Mead, 1989; Spewak, 1997). Since the hydraulic properties are highly correlated with structural stability and macroporosity, more stable soil structure and increased biological activity may be the reasons for improved hydraulic properties in forests, permanent pasture lands and no-till or minimum tillage systems.

2.4.3.3 Land use and water level of wetlands

Soil management or land use affects soil hydraulic properties, and thus the water balance and hydrology of the land. Nevertheless, only a few investigations have concentrated on the effect of land use on soil water content and hydrology in the prairie soils. Studies carried out by Euliss and Mushet (1996) revealed that surface runoff due to precipitation is larger from cultivated catchments than that from grasslands. De Jong and Kachanoski (1987) documented that over-winter soil water recharge is about 0.05 to 0.1 m under tall stubble, buck-brush and native grass whereas it is virtually zero for fallow land. These findings suggest that infiltration of summer precipitation and snowmelt is likely to be greater and runoff is smaller in undisturbed grasslands than that in cultivated fields.

Van der Kamp *et al.* (1999) studied water levels of wetlands in St. Denis National Wildlife Area (SDNWA), Saskatchewan, Canada, and concluded that conversion of croplands into permanent brome grass resulted in drying out of wetlands within the grassland area. Van der Kamp *et al.* (2003) showed that water level in the wetlands decreased drastically in the mid 1980s since the cultivated lands converted to permanent

brome grasslands. They also studied the infiltration rate of soils using single-ring infiltrometers under ponded condition during summer and winter and concluded that infiltrability beneath brome grass was much higher than that of land under cultivation. They attribute the drying out of wetlands in the SDNWA to the better snow trapping and well-developed macropore network in brome grasslands. However, no measurement is available on macropore network (van der Kamp *et al.*, 2003). Further, previous studies on hydraulic properties under different land use were mainly focused on saturated hydraulic properties. However, soils in cold and semi-arid climate in the northern plains of North America remain mostly under unsaturated conditions. Effects of land use on unsaturated hydraulic properties, particularly in the near-saturated region, have not been documented in the Canadian prairies to the best of our knowledge. This information is needed for improving our understanding of the effects of soil management/land use on runoff and infiltration, and thus wetland hydrology.

2.5 Summary

The preceding review briefly describes the importance of characterization of saturated and near-saturated surface soil hydraulic properties and water-conducting porosity in sloping landscapes under different land use systems, and some of the existing measurement and analytical techniques, and their limitations.

Slope of the surface soil and type of land use are among the main soil and management factors that influence surface soil hydraulic properties and water-conducting porosity. Characterization of surface soil hydraulic properties under these conditions requires reliable instruments, and measurement and analytical techniques. Knowledge of surface soil hydraulic properties is needed for efficient land and water management. However,

information on soil hydraulic properties such as K_{fs} and $K(h)$ near saturation and water-conducting porosity in sloping lands with different land use systems in the Canadian prairies is lacking. Furthermore, no specifically designed instruments are available for the estimation of surface soil hydraulic properties in sloping lands.

The equipment (tension and double-ring infiltrometers) along with the measurement and analytical procedures reviewed in this chapter has been used to evaluate the suitability of these two techniques for the characterization of surface soil hydraulic properties in sloping lands (Chapter 3), to develop and compare a new method with existing methods for determining water-conducting porosity using these two techniques (Chapter 4), and to evaluate the surface soil hydraulic properties and water-conducting porosity under different land use systems using these two techniques (Chapter 5).

2.6 References

- Anderson, S.H., R.L. Peyton, and C.J. Gantzer. 1990. Evaluation of constructed and natural soil macropores using X-ray computed tomography. *Geoderma*. 46:13-29.
- Angulo-Jaramillo R, J.P., Vandervaere, S. Roulier, J.L Thony, J.P. Gaudet, and M. Vaucelin. 2000. Field measurement of soil surface hydraulic properties by disc and ring infiltrometers: A review and recent developments. *Soil Tillage Res.* 55:1-29.
- Ankeny, M.D., T.C. Kaspar, and R. Horton. 1988. Design for an automated tension infiltrometer. *Soil Sci. Soc. Am. J.* 52:893-896.
- Ankeny, M.D., M. Ahmed, T.C. Kaspar, and R. Horton. 1991. Simple field method for determining unsaturated hydraulic conductivity. *Soil Sci. Soc. Am. J.* 55:467-470.
- Ankeny, M.D., T.C. Kaspar, and R. Horton. 1990. Characterization of tillage and traffic effects on unconfined infiltration measurements. *Soil Sci. Soc. Am. J.* 54:837-840.
- Benjamin, J.G. 1993. Tillage effects on near surface soil hydraulic properties. *Soil Tillage Res.* 26:277-288.
- Beven, K. and P. Germann. 1982. Macropores and water flow in soils. *Water Resour. Res.* 18:1311-1325.
- Bouma, J. 1981. Comment on Micro-, meso- and macroporosity of soil. *Soil Sci. Soc. Am. J.* 45:1244-1245.
- Bouma, J.A., A. Jongerius, and D. Schoonderbeek. 1979. Calculation of saturated hydraulic conductivity of some pedal clay soils using micromorphometric data. *Soil Sci. Soc. Am. J.* 43:261-264.
- Bower H. 1986. Intake rate. Cylinder infiltrometer. p. 825-843. *In* A. Klute (ed.) *Methods of soil analysis. Part 1. Physical and mineralogical properties.* 2nd ed. ASA, Madison, WI.
- Chaney, K, and R.S. Swift. 1984. The influence of organic matter on aggregate stability in some British soils. *J. Soil Sci.* 35:223-230.
- Clothier, B.E., and I. White. 1982. Water diffusivity of a field soil. *Soil Sci. Soc. Am. J.* 46:636-640.
- de Jong E., and R.G. Kachanoski. 1987. The role of grasslands in hydrology. p. 213-215. *In* M. C. Healy and R. R. Wallace (ed.) *Canadian Aquatic Resources.* Can. Bull. of Fisheries and Aquatic Resources. No. 215. Can. Govt. Publishing Centre, Ottawa, Canada.

- Dunn, G.H., and R.E. Phillips. 1991a. Macroporosity of a well-drained soil under no-till and conventional tillage. *Soil Sci. Soc. Am. J.* 55:817-823.
- Dunn, G.H., and R.E. Phillips. 1991b. Equivalent diameter of simulated macropore systems during saturated flow. *Soil Sci. Soc. Am. J.* 55:1244-1248.
- Dunne, T., and R.D. Black. 1970. An experimental investigation of runoff production in permeable soils. *Water Resour. Res.* 6:478-490.
- Euliss, N.H., and D.M. Mushet. 1996. Water level fluctuations in wetlands as a function of landscape condition in the prairie pothole region. *Wetlands.* 16:587-593.
- Flint, L.E., and A.L. Flint. 2002. The soil solution phase. Porosity. p. 241-254. *In* J. H. Dane and G. C. Topp (ed.) *Methods of soil analysis: Part 4. Physical methods*, SSSA, Madison, WI.
- Gardner, W.R. 1958. Some steady-state solutions of unsaturated moisture flow equations with application to evaporation from a water table. *Soil Sci.* 85:228-232.
- Haverkamp, R., P.J. Ross, K.R.J. Smettem, and J.Y. Parlange. 1994. Three dimensional analysis of infiltration from the disc infiltrometer. Part 2. Physically based infiltration equation. *Water Resour. Res.* 30:2931-2935.
- Hussen, A.A., and A.W. Warrick. 1993. Alternative analysis of hydraulic data from disc tension infiltrometers. *Water Resour. Res.* 29:4103-4108.
- Jackson, C.R. 1992. Hillslope infiltration and lateral downslope unsaturated flow. *Water Resour. Res.* 28:2533-2539.
- Joel, A., and I. Messing. 2000. Application of two methods to determine hydraulic conductivity with disc permeameters on sloping land. *European J. Soil Sci.* 51:93-98.
- Klute, A., and C. Dirksen. 1986. Hydraulic conductivity and diffusivity. Laboratory methods. p. 687-734. *In* A. Klute (ed.) *Methods of soil analysis. Part 1: Physical and mineralogical properties*. 2nd ed. ASA, Madison, WI.
- Leduc, C., G. Favreau, and P. Schroeter. 2001. Long-term rise in a shahelian water-table: the continental terminal in south-west Niger. *J. Hydrol.* 243:43-54.
- Logsdon, S.D., and D.B. Jaynes. 1993. Methodology for determining hydraulic conductivity with tension infiltrometers. *Soil Sci. Soc. Am. J.* 57:1426-1431.
- Logsdon, S.D., E.L. McCoy, R.R. Allmaras, and D.R. Linde. 1993. Macropore characterization by indirect methods. *Soil Sci.* 155:316-324.

- Luxmoore, R.J. 1981. Micro-, meso- and macroporosity of soil. *Soil Sci. Soc. Am. J.* 45:671-672.
- Luxmoore, R.J., P.M. Jardine, G.V. Wilson, J.R. Jones, and L.W. Zelazny. 1990. Physical and chemical controls of preferred path flow through a forested hillslope. *Geoderma*. 46:139-154.
- McCord, J.T., D.B. Stephens, and J.L. Wilson. 1994. Hysteresis and state-dependent anisotropy in modeling unsaturated hillslope hydrologic processes. *Water Resour. Res.* 27:1501-1518.
- Mendoza, G., and S.T. Steenhuis. 2002. Determination of hydraulic behavior of hillsides with a hill slope infiltrometer. *Soil Sci. Soc. Am. J.* 66:1501-1504.
- Messing, I., and N.J. Jarvis. 1993. Temporal variation in the hydraulic conductivity of a tilled clay soil as measured by tension infiltrometers. *J. Soil Sci.* 44:11-24.
- Miller, J.J., N.J. Sweetland, F.J. Larney, and K.M. Volkmar. 1998. Unsaturated hydraulic conductivity of conventional and conservation tillage soils in southern Alberta. *Can. J. Soil Sci.* 78:643-648.
- Mosley, M.P. 1982. Subsurface flow velocities through selected forest soils, South Island, New Zealand. *J. Hydrology.* 55:65-92.
- Obi, M.E., and P.C. Nnabude. 1988. The effect of different management practices on the physical properties of a sandy loam soil in southern Nigeria. *Soil Tillage Res.* 12:81-90.
- Pennock, D.J., B.J. Zebarth, and E. de Jong. 1987. Landform classification and soil distribution in hummocky terrain, Saskatchewan, Canada. *Geoderma*. 40:297-315.
- Perroux, K.M., and I. White. 1988. Design for disc permeameters. *Soil Sci. Soc. Am. J.* 52:1205-1215.
- Phillip, J.R. 1957. The theory of infiltration. 1: The infiltration equation and its solution. *Soil Sci.* 83:345-357.
- Phillip, J.R. 1991. Hill slope infiltration: Planar slopes. *Water Resour. Res.* 27:109-117.
- Rawls, W.J., L.R. Ahuja, D.L. Brakensiek, and A. Shirmohammadi. 1993. Infiltration and soil water movement. p. 5.1-5.51. *In* D. R. Maidment. (ed.) *Handbook of hydrology*. McGraw Hill, Inc. NY.
- Reynolds, W.D., and W.D. Zebchuck. 1996. Use of contact material in tension infiltrometer measurements. *Soil Technology.* 9:141-159.)
- Reynolds, W.D., D.E. Elrick, and E.G. Youngs. 2002. The soil solution phase. Single-ring and double- or concentric-ring infiltrometers. p. 821-826. *In* J.H. Jane and

- G.C. Topp (ed.) Methods of soil analysis: Part 4. Physical methods, SSSA, Madison, WI.
- Sauer, T.J., B.E. Clothier, and T.C. Daniel. 1990. Surface measurements of the hydraulic properties of a tilled and untilled soil. *Soil Tillage Res.* 15:359-369.
- Schwartz, R.C., and S.R. Evett. 2002. Estimating hydraulic properties of a fine-textured soil using a disc infiltrometer. *Soc. Am. J.* 66:1409-1423.
- Shouse, P.J., and B.P. Mohanty. 1993. Scaling of near-saturated hydraulic conductivity measured using disc infiltrometers. *Water Resour. Res.* 34:1195-1205.
- Simunek, J., and M. Th. van Genuchten. 1996. Estimating unsaturated soil hydraulic properties from tension disc infiltrometer data by numerical inversion. *Water Resour. Res.* 32:2683-2696.
- Sinai, G., D. Zaslavsky, and P. Golany. 1981. The effect of soil surface curvature on moisture and yield-Beer Sheba Observations. *Soil Sci.* 132:367-375.
- Skopp, J. 1981. Comment on 'Micro- meso- and macroporosity of soil'. *Soil Sci. Soc. Am. J.* 45:1246.
- Smettem, K.R., and B.E. Clothier. 1989. Measuring unsaturated sorptivity and hydraulic conductivity using multiple disc permeameters. *J. Soil Sci.* 40:563-568.
- Smettem, K.R.J., J.Y. Parlange, P.J. Ross, and R. Haverkamp. 1994. Three-dimensional analysis of infiltration from the disc infiltrometer. Part 1. A capillary-based theory. *Water Resour. Res.* 30:2925-2929.
- Soil Science society of America. 2003. Glossary of Soil Science Terms. *Soil Sci. Soc. Am.* <http://www.soils.org/sssagloss/>
- Spewak, R.P. 1997. The effect of land use on the soil macropores characteristics of prairie soils. MSc Thesis. University of Saskatchewan.
- Sullivan, M., J.J. Warwick, and S.W. Tyler. 1996. Quantifying and delineating spatial variations of surface infiltration in a small watershed. *J. Hydrol.* 181:149-168.
- Thomas, G.W., and R.E. Phillips. 1979. Consequences of water movement in macropores. *J. Environ. Qual.* 8: 149-15.
- Timlin, D.J., L.R. Ahuja, and M.D. Ankney. 1994. Comparison of three field methods to characterize apparent macropore conductivity. *Soil Sci. Soc. Am. J.* 58:278-284.
- Torres, R., W.E. Dietrich, D.R. Montgomery, S.P. Anderson, and K. Loague. 1998. Unsaturated zone processes and the hydrologic response of a steep, unchanneled catchment. *Water Resour. Res.* 34:1865-1879.

- van der Kamp, G., M. Hayashi, and D. Gallen. 2003. Comparing the hydrology of grassland and cultivated catchments in the semi-arid Canadian Prairies. *Hydrological Processes*. 17:559-575.
- van der Kamp, G., W.J. Stolte, and R.G. Clark. 1999. Drying out of small prairie wetlands after conversion of their catchments from cultivation to permanent brome grass. *Hydrological Sciences J.* 44:387-397.
- Vandervaere, J.P., M. Vauclin, and D.E. Elrick. 2000. Transient flow from tension infiltrometers. I. The two-parameter equation. *Soil Sci. Soc. Am. J.* 64:1263-1272.
- Warrick, A.W. 1992. Models for disc infiltrometers. *Water Resour. Res.* 28:1319-1327.
- Watson, K.W., and R.J. Luxmoore. 1986. Estimating macroporosity in a forest watershed by use of a tension infiltrometer. *Soil Sci. Soc. Am. J.* 50:578-582.
- Weiler, M., and F. Naef. 2003. An experimental tracer study of the role of macropores in infiltration in grassland soils. *Hydrol. Process.* 17:477-493.
- White, I., M.J. Sully, and K.M. Perroux. 1992. Measurement of surface-soil hydraulic properties: Disc permeameters, tension infiltrometers, and other techniques. p. 69-103. *In* G.C. Topp *et al.* (ed.) *Advances in measurement of soil physical properties: Bringing theory into practice*. SSSA Spec. Publ. 30. SSSA, Madison, WI.
- Wilson, G.V., and R.J. Luxmoore. 1988. Infiltration, macroporosity and mesoporosity distributions on two forested watersheds. *Soil Sci. Soc. Am. J.* 52:329-335.
- Wooding, R.A. 1968. Steady infiltration from a shallow circular pond. *Water Resour. Res.* 4:1259-1273.
- Yeh, Y.J., C.H. Lee, and S.T. Chen. 2000. A tracer method to determine hydraulic conductivity and effective porosity of saturated clays under low gradients. *Ground Water*. 38:522-529.
- Zaslavsky, D., and G. Sinai. 1981. Surface hydrology: I-Explanation of phenomena. *J. Hydrol. Div. Am. Soc. Civ. Eng.*, 107:1-16.
- Zebarth, B.J., and E. de Jong. 1989a. Water flow in a hummocky landscape in central Saskatchewan, Canada. I. Distribution of water and soils. *J. Hydrol.* 107:309-327.
- Zebarth, B.J., and E. de Jong. 1989b. Water flow in a hummocky landscape in central Saskatchewan, Canada. III. Unsaturated flow in relation to topography and land use. *J. Hydrol.* 110:199-218.
- Zhang, R. 1997. Determination of soil sorptivity and hydraulic conductivity from disk infiltrometer. *Soil Sci. Soc. Am. J.* 61:1024-1030.

3. DETERMINATION OF SOIL HYDRAULIC PROPERTIES IN SLOPING SURFACES USING TENSION AND DOUBLE-RING INFILTROMETERS

3.1 Abstract

The majority of the landscapes, natural or cultivated, are non-level. However, specifically designed instruments are not available for estimation of soil hydraulic properties in sloping landscapes. A field experiment was conducted in a cultivated silt loam soil (Dark Brown Chernozems) in Saskatchewan, Canada to explore the tension and double-ring infiltrometers for the determination of soil hydraulic properties in sloping landscapes. Soil surface was prepared to represent four treatments, 0% (level), 7%, 15% and 20% slopes. Treatments were arranged in a randomized complete block design with five replicates. For each treatment, water infiltration rates were measured using double-ring and tension infiltrometers at -0.3, -0.6, -1.0, -1.3, -1.7 and -2.2 kPa water pressures. Hydraulic properties and water-conducting porosity of the surface soil were estimated. Three-dimensional computer simulation studies were also performed for tension infiltrometer with various disc diameters and water pressures on soil surface of different slopes. Level and sloping lands were not significantly different ($p < 0.05$) for steady-state infiltration rates and estimated field-saturated hydraulic conductivity, unsaturated hydraulic conductivity as a function of water pressure, macroscopic capillary length parameter and water-conducting macro- and mesoporosity. Experimental and numerical results of this study suggest that both tension and double-

ring infiltrometers are suitable for characterization of surface soil hydraulic properties in landscapes with slopes up to 20%.

3.2 Introduction

Tension infiltrometers (Perroux and White, 1988) and double-ring infiltrometers (Bower, 1986) are useful instruments that offer a simple, fast and convenient means of determining soil hydraulic properties based on *in situ* infiltration measurements at the soil surface. Tension infiltrometers have proven useful for characterizing soil's hydraulic conductivity near saturation (Ankeny *et al.*, 1991; Messing and Jarvis, 1993), sorptivity (Phillip, 1969; Zhang, 1997), mobile-immobile water content (Angulo-Jaramillo *et al.*, 2000) and water-conducting porosity (Watson and Luxmoore, 1986; Dunn and Phillips, 1991; Cameira *et al.*, 2003). Double-ring infiltrometers have also been widely used for the estimation of field-saturated hydraulic conductivity under ponded condition without much disturbance to the soil at the measurement site (Bower, 1986).

Most of the landscapes under crop cultivation and watersheds, in many parts of the world, are non-level (slopes > 1%). Very few measurement techniques are available for determining hydraulic characteristics *in situ* on hillslopes. Dunne and Black (1970) and Mosley (1982) estimated hillslope hydraulic characteristics by measuring subsurface flow in excavated trenches in Vermont, U.S.A. and South Island, New Zealand, respectively. In the mean time, Harr (1977) measured water flux in soil and subsoil on a steep forested slope in Oregon using field installed tensiometers, lysimeters and piezometers. Later, Anderson *et al.* (1997) and Torres *et al.* (1998) carried out tracer studies in a steep watershed in Oregon using tensiometers, piezometers and suction

lysimeters to identify subsurface flow pathways. These methods, however, are time consuming, tedious to perform under field conditions and sometimes required laboratory derived hydraulic parameters for the determination of hydraulic conductivity. The hillslope infiltrometer, which is open at the bottom, top, and downhill sides, was introduced by Mendoza and Steenhuis (2002) for the determination of vertical and horizontal saturated hydraulic conductivity of soil horizons in steep lands. The installation of this device requires the carving of a soil block that is slightly smaller than the infiltrometer (36 cm in length, 30.5 cm in width and 41 cm in height) and excavation of a trench around the block for ease of installation of the device and water collectors. This particular method is destructive, time consuming and somewhat cumbersome, for routine field use.

Tension and single-ring or double-ring infiltrometers are primarily designed and tested in horizontal surfaces. However, this equipment has been extensively used in the past to obtain saturated and near-saturated soil hydraulic properties on sloping lands. Watson and Luxmoore (1986) and Wilson and Luxmoore (1988) used tension infiltrometers in conjunction with double-ring infiltrometers for measuring infiltration rates (hydraulic conductivity), macropore flow and water-conducting macro- and mesoporosity (the fractions of soil volume comprised of pores with diameters $> 1 \times 10^{-3}$ m and between 1×10^{-5} and 1×10^{-3} m, respectively; Luxmoore, 1981) in forest watersheds with slopes up to 20%. Using single-ring infiltrometers, Elliott and Efetha (1999) measured infiltration rates in conventionally tilled and zero-tilled fields with slopes ranging from 6 to 30% in a rolling landscape in Canada. Using tension infiltrometers, Joel and Messing (2000) compared two procedures for estimating the hydraulic conductivity near-saturation on

sloping lands. In the first method, the split-location method, the tension infiltrometer was moved to an adjacent location after infiltration measurement at each applied water pressure. In the second, one-location method, the tension infiltrometer was not moved during the measurements of infiltration at each sequence of applied pressure. Based on the simplicity of operation and the amount of soil disturbance, Joel and Messing (2000) recommended the one-location method over the split-location method. Casanova *et al.* (2000) studied the influence of aspect and slope on hydraulic conductivity, which were different in soil properties such as soil texture. Both Joel and Messing (2000) and Casanova *et al.* (2000), however, did not evaluate the appropriateness of tension infiltrometers for the determination of hydraulic properties in lands with different slopes, and recommended further studies on the influence of slope on tension infiltrometer measurements. Despite the extensive use of tension and double-ring infiltrometers in determining surface soil hydraulic properties in sloping lands, no systematic studies were conducted on the suitability of these equipments for the estimation of these properties in sloping lands to the best of our knowledge. Hence, exploration of these versatile tools (tension and double-ring infiltrometers) for determination of soil hydraulic properties is of utmost importance.

The objective of this study was to evaluate the suitability of tension and double-ring infiltrometers for the estimation of surface soil hydraulic properties at saturated and near-saturated conditions.

z3.3 Materials and Methods

3.3.1 Treatments and experimental design

Field experiments using a double-ring infiltrometer and a tension infiltrometer (Figures 3.1 and 3.2, respectively) were carried out at Laura (approximately 50 km west of Saskatoon), Saskatchewan, Canada ($51^{\circ} 52' N$ lat., $107^{\circ} 18' W$ long.). The soil in that area is described as an Elstow association: Dark Brown Chernozems (Typic Haplustolls) developed on loamy glacio-lacustrine parent material with a silt loam texture in both Ap (0- to 0.14-m) and Bm (0.14- to 0.25-m) soil horizons. The lacustrine sediments are underlain by glacial till that is drained by the Tessier aquifer. The water table occurs at approximately 15 m below the surface within a sand layer (Dyck *et al.*, 2003). The site has been under a crop-fallow rotation dominated by wheat (*Triticum aestivum* L.) with some barley (*Hordeum vulgare* L.) since 1966. During the study period (2002 growing season), the site was chemical fallow in which herbicides were applied to control weeds over the fallow season.

Four slopes, 0 (level), 7, 15 and 20% were chosen as treatments. Generally, the maximum slope of the lands used for agricultural purposes in the Canadian prairies is 15%. The treatments were selected to represent level as well as one below and one above the maximum slope of the agricultural lands. Treatments were arranged in a randomized complete block design. There were five replications. For each replicate, a site of 9 m^2 ($3 \text{ m} \times 3 \text{ m}$) area was randomly selected from an area of about 10 m wide and 100 m long and then the site was prepared to represent 0, 7, 15 and 20% slopes (treatments) by removing all residues, any large clods and loose soil from the selected area (Figure 3.3). This site preparation was required to have a nearly uniform soil in the

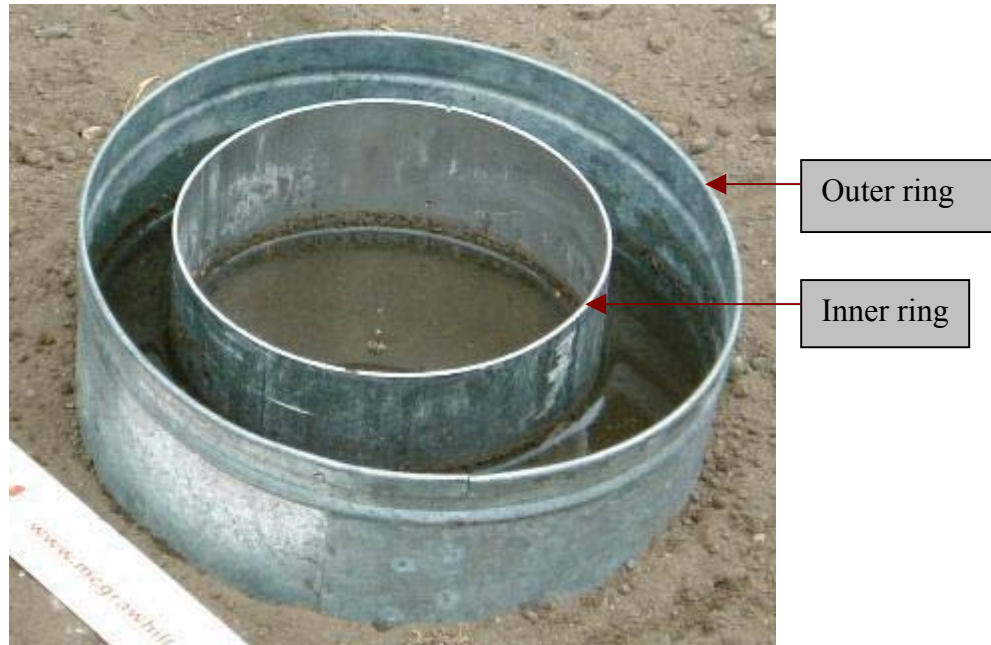


Figure 3. 1 Double-ring infiltrometer

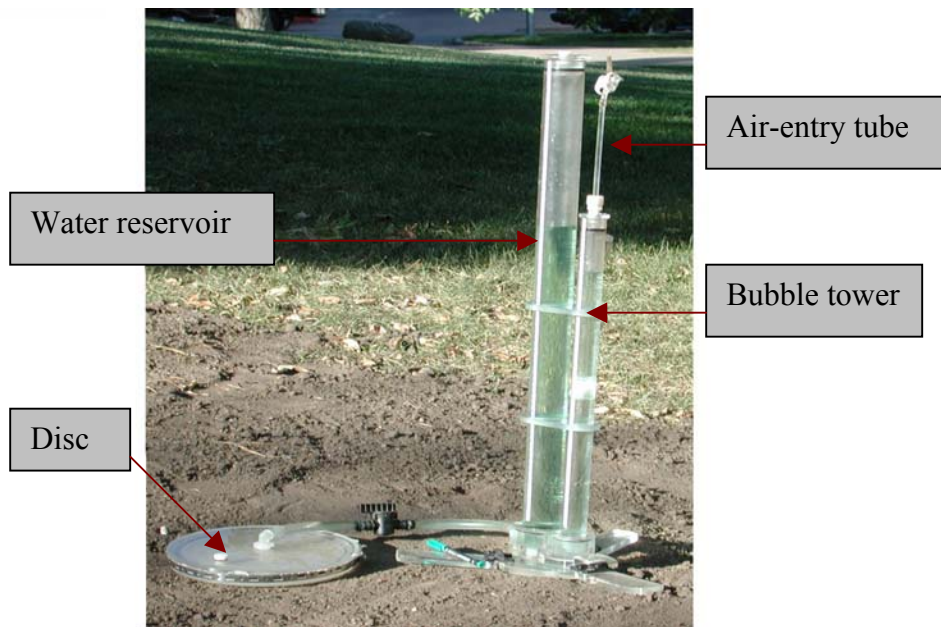


Figure 3. 2 Tension infiltrometer

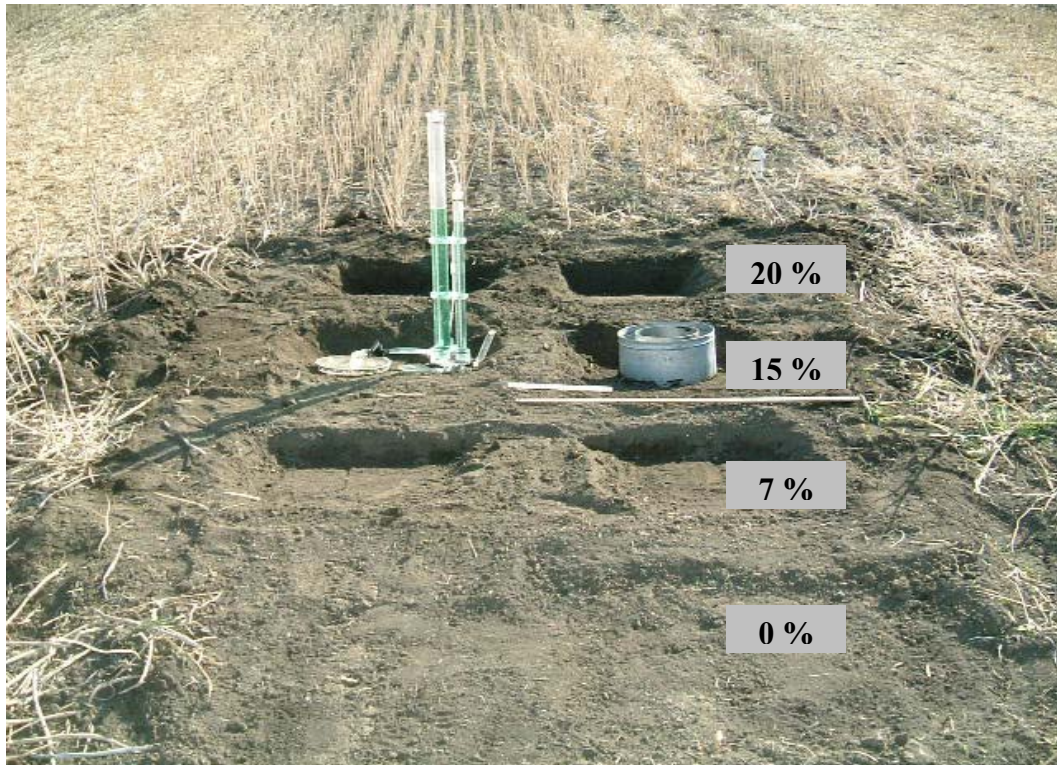


Figure 3. 3 An experimental block showing the arrangement of the treatments

experimental area, particularly with respect to bulk density. In each treatment, an undisturbed soil sample (0.075 m in diameter and 0.05 m in height) was taken from an area near the measurement location (20 cores in total). These cores were used for the determination of bulk density by oven drying at 105⁰C. Total porosity was estimated from soil bulk density and particle density (Flint and Flint, 2002). To measure soil moisture content, time domain reflectometry (TDR) probe was installed prior to the infiltration measurements. A TDR probe (consisting of two parallel, 15 cm long, 0.2 cm diameter stainless steel rods with a separation of 1 cm) was inserted horizontally at 2- to 2.5-cm depth in line with the center of the measurement area (infiltrometer disk) and in

a direction perpendicular to the slope. A small trench of about 2.5 cm in depth was excavated just outside of the disk and TDR probe was inserted 2.5 cm beneath the soil surface. The probe depth (2- to 2.5-cm) was chosen so that the electromagnetic fields associated with the TDR signal are contained within the soil while the wave guides are located within the saturated soil zone. The trench was backfilled to conditions similar to the original soil. TDR reading was recorded just before the commencement of infiltration measurement to get antecedent soil moisture content.

Infiltration measurements were carried out using a tension infiltrometer with a 0.2 m diameter disk (Soil Measurement Systems, Tuscon, AZ). A thin layer ($< 5 \times 10^{-3}$ m) of moist fine testing sand was applied over the prepared surface at each measurement location in a circular area with a diameter equal to that of the infiltrometer disk. This smoothed out any irregularities of the soil surface and ensured good contact between the soil surface and the infiltrometer membrane. The testing sand is reported to have saturated hydraulic conductivity of $5.3 \times 10^{-5} \text{ m s}^{-1}$ and an air-entry value slightly higher than -3 kPa water pressure. The testing sand was of sufficient porosity not to be a hydraulically limiting layer, yet had fine enough pores to remain saturated at the pressures used in this study. The nylon mesh attached to the infiltrometer disc had an air-entry value of about -3 kPa pressure. Although the testing sand layer may have an impact on early-time hydraulic conductivity (Vandervaere *et al.*, 2000), the thin layer of sand we used would not affect the steady-state infiltration rates, and thus the estimated hydraulic properties of the surface soil (Vandervaere *et al.*, 2000). The infiltration rates were measured at -0.3 , -0.6 , -1.0 , -1.3 , -1.7 and -2.2 kPa water pressures (corresponding to 1×10^{-3} , 5×10^{-4} , 3×10^{-4} , 2.31×10^{-4} , 1.76×10^{-4} and 1.36×10^{-4} m

equivalent pore diameters). Measurements were performed from low to high water pressures, i.e., beginning with the -2.2 kPa pressure. For the beginning of the infiltration measurements, the water pressure of the infiltrometer was adjusted to -2.2 kPa. The unit that consisted of reservoir tower and tension control tube was placed on a wooden bench kept aside the measurement location. Simultaneously the infiltrometer disc, which was attached to the reservoir tower and tension control tube via a flexible tube, inclined at an angle (to the horizontal) corresponding to that of the soil surface was placed on the contact sand, so that the negative water pressure in the middle of the disc was similar to the pressure of the bubbling outlet at the bottom of the water supply tube.

The amount of water infiltrating into the soil was measured by recording the water level drop in the graduated reservoir tower as a function of time. When the amount of water entered into the soil did not change with time for three consecutive measurements taken at five minute intervals, steady-state flow was assumed and steady-state infiltration rate was calculated based on the last three measurements. The water pressures were then set sequentially to -1.7 , -1.3 , -1.0 , -0.6 and -0.3 kPa and the corresponding steady-state infiltration rates were obtained. Generally, steady-state was achieved within 20- to 30-min. Once the steady-state infiltration rate was attained at -0.3 kPa pressure, TDR reading was taken to determine soil moisture content. Macroporosity was determined as the difference between total porosity and volumetric moisture content held at the -0.3 kPa pressure.

Immediately adjacent to the tension infiltrometer, a double-ring infiltrometer with inner and outer rings of 0.2 and 0.3 m in diameter, respectively, was used to determine steady

infiltration rate at a constant head (Reynolds *et al.*, 2002). Steel rings were pushed into the soil concentrically and parallel to the measurement surface to a depth of 0.05 m with minimum soil disturbance. After the insertion of the rings the contact between the inside surface of the ring and the soil was tamped lightly using the blunt edge of a pencil to minimize the short-circuit flow along the inside wall of the ring. A steel pointer was positioned at the center of the inner cylinder with 0.03 m height above the soil surface. The inner cylinder was then filled with water equivalent to a 0.04 m water head initially. The time taken to drop the water level in the inner cylinder to the pointer was recorded. Thereafter, a measured volume of water that is equivalent to 0.01 m in depth in the ring was filled successively and the time taken to infiltrate this amount was recorded. When the amount of water entered into the soil did not change with time for three consecutive measurements taken at 5-minute intervals, steady-state flow was assumed and steady-state infiltration rate was calculated based on the last three measurements. Generally, steady-state flow was achieved within 30- to 60-min. Water level in the outer ring was maintained exactly the same height as that in the inner ring.

3.3.2 Estimation of field-saturated hydraulic conductivity from double-ring infiltrometer measurements

Field-saturated hydraulic conductivity, K_{fs} ($L T^{-1}$), was estimated for each location from the one-dimensional steady-state infiltration rates obtained from double-ring infiltrometer following the procedure outlined by Reynolds *et al.* (2002). The K_{fs} is given by,

$$K_{fs} = \frac{q_s}{\left(\frac{H}{(C_1 d + C_2 a)}\right) + \left(\frac{1}{(\alpha(C_1 d + C_2 a))}\right) + 1} \quad [3.1]$$

where q_s ($L T^{-1}$) is quasi-steady infiltration rate, H (L) is steady depth of ponded water in the ring, $C_1 = 0.316\pi$ and $C_2 = 0.184\pi$ are dimensionless quasi-empirical constants, d (L) is depth of ring insertion into the soil, a (L) is radius of the inner ring, and α (L^{-1}) is the soil macroscopic capillary length parameter. There were four measurements in each plot with a total of 20 double-ring infiltrometer measurements. A value of $12 m^{-1}$ was taken as the appropriate value for the α as it is the most common value for many agricultural soils (Elrick *et al.* 1989 in Reynolds *et al.*, 2002). Water pressure head at the center of the inner ring varied from 0.04 to 0.03 m during infiltration measurements. Therefore, the mid-way elevation between 0.03 and 0.04 m (3.5×10^{-2} m) was taken as the steady depth of ponded water in the inner ring (H).

3.3.3 Estimation of soil hydraulic properties from tension infiltrometer measurements

The 3-dimensional steady infiltration rates obtained at different water pressures were used to obtain unsaturated hydraulic properties. For Gardner's (1958) exponential hydraulic conductivity function,

$$K(h) = K_{fs} \exp(\alpha h) \quad [3.2]$$

where $K(h)$ is the unsaturated hydraulic conductivity ($L T^{-1}$) for a given water pressure head, h (L), Wooding (1968) derived the following approximate solution for steady-state infiltration rate under a shallow circular disc,

$$q_{\infty}(h) = \left(1 + \frac{4}{\alpha \pi r_d}\right) K_{fs} \exp(\alpha h) \quad [3.3]$$

where $q_{\infty}(h)$ is steady-state infiltration rate ($L T^{-1}$) corresponding to the applied water pressure head h , and r_d is radius of the disc (L). Equation [3.3] has two unknown parameters, K_{fs} and α . Following Logsdon and Jaynes (1993), these parameters were estimated through non-linear regression of q_{∞} as a function of h using MathCad 2000 (MathSoft, Cambridge). Values for $K(h)$ were then estimated by substituting the resulting values of K_{fs} and α into Eq. [3.2].

3.3.4 Determination of water-conducting porosity

The equivalent radius r (L) of the largest water-filled pore in the soil at a given water pressure can be calculated from the capillary rise equation as given by (Bear, 1972),

$$r = \frac{2 \gamma \cos \beta}{\rho g h} \quad [3.4]$$

where γ is the surface tension of water ($M T^{-2}$), β is the contact angle between water and the pore wall (assumed to be zero), ρ is the density of water ($M L^{-3}$), and g is the acceleration due to gravity ($L T^{-2}$).

This study assumes that the equivalent pores smaller than the r value estimated by Eq. [3.4] are full of water and are responsible for 100% of the flux of water for a given water pressure head. Also, it is assumed that the equivalent pores larger than the value of r calculated from Eq. [3.4] are air-filled and do not contribute to any of the water flux. With the combination of the Poiseuille's law and capillary theory, the flow rate through a single macropore can be given as,

$$Q(r) = \frac{\pi \rho g}{8 \mu} r^4 \quad [3.5]$$

where $Q(r)$ is the flow rate ($L^3 T^{-1}$) as a function of pore radius r and μ is the dynamic viscosity of water ($M L^{-1} T^{-1}$).

Bodhinayake *et al.* (2003) derived a new equation for determining macroporosity from tension infiltrometer measurements. Bodhinayake and Si (2003) applied the derived equation in comparing the effect of land use on macroporosity. Detailed description of the derivation of the new equation is given in Bodhinayake *et al.* (2003). Briefly, we considered the number of pores per unit area (L^2) as a function of pore radius r . The cumulative pore number distribution is then given by

$$n(r) = \int_0^r P(r) dr \quad [3.6]$$

where $n(r)$ is the total number of pores in a given pore size range and $P(r)$ is the number of pores per unit soil surface area per unit pore radius. The hydraulic conductivity, K ($L T^{-1}$) at a given pore size r , $K(r)$ can be expressed as

$$K(r) = \int_0^r P(r) Q(r) dr \quad [3.7]$$

where r is the upper limit of the integrals determined by the water pressure.

The water-conducting porosity in a given pore radii (a and b) range can be expressed as,

$$\varepsilon(a, b) = \int_a^b \pi r^2 P(r) dr \quad [3.8]$$

An expression for $P(r)$ can be obtained by taking the derivatives of both sides of Eq. [3.7]. Then the substitution of the $P(r)$ into Eq. [3.8] yields

$$\varepsilon(a, b) = \int_a^b \frac{dK(r)}{dr} \frac{1}{Q(r)} \pi r^2 dr \quad [3.9]$$

Normally, unsaturated hydraulic conductivity of soil is expressed in relation to soil water content or water pressure. In Eq. [3.9] hydraulic conductivity is expressed as a function of pore radius. Therefore, in the following Eq. [3.9] is revised and water-conducting porosity is expressed as a function of hydraulic conductivity in relation to water pressure, $K(h)$. Introducing a new variable

$$H(r) = \frac{2 \gamma}{\rho g r} \quad [3.10]$$

where $H(r)$ is the water pressure corresponding to the radius r , and substitution of Eq. [3.5] for $\varrho(r)$ and Eq. [3.10] for r into Eq. [3.9], results

$$\varepsilon(a, b) = \frac{2 \mu \rho g}{\gamma^2} \int_{H(a)}^{H(b)} \frac{dK(h)}{dh} h^2 dh \quad [3.11]$$

Integration of Eq. [3.11] by parts and substituting Eq. [3.2] for $K(h)$ leads to

$$\varepsilon(a, b) = \frac{2 \mu \rho g K_{fs}}{\gamma^2} \left(h^2 \exp(-\alpha h) \Big|_{H(a)}^{H(b)} - 2 \int_{H(a)}^{H(b)} h \exp(-\alpha h) dh \right) \quad [3.12]$$

Substitution of Eq. [3.10] into Eq. [3.12] and subsequent integration result (Gradshteyn and Ryzhik, 2000; Eq. 2.322, p.104),

$$\varepsilon(a, b) = \frac{2 \mu \rho g K_{fs}}{\gamma^2} \left\{ \exp\left(\frac{-2 \gamma \alpha}{\rho g b}\right) \left(\frac{4 \gamma^2}{(\rho g b)^2} + \frac{4 \gamma}{\rho g b \alpha} + \frac{2}{\alpha^2} \right) - \exp\left(\frac{-2 \gamma \alpha}{\rho g a}\right) \left(\frac{4 \gamma^2}{(\rho g a)^2} + \frac{4 \gamma}{\rho g a \alpha} + \frac{2}{\alpha^2} \right) \right\} \quad [3.13]$$

From Eq. [3.10], it can be seen that the value of 0 kPa water pressure can not be related to a pore size. Therefore, the upper limit of the integral of Eq. [3.12] can not be defined. However, a small pressure can be related to a pore size. We assumed that the maximum

pore diameter at the sites is 5×10^{-3} m. This is a reasonable assumption as no pores greater than 5×10^{-3} m in diameter existed at any of the infiltration measurement locations. Equation [3.13] (with K_{fs} and α from tension infiltrometer measurements) was then used for the estimation of water-conducting porosity with pore diameter ranges from 1 to 5×10^{-3} , 5×10^{-4} to 1×10^{-3} , 3 to 5×10^{-4} , 2.31 to 3×10^{-4} , 2.31 to 1.76×10^{-4} , 1.36 to 1.76×10^{-4} , and 1.36×10^{-4} to 5×10^{-3} m.

3.3.5 Computer simulation

Water infiltration from a tension infiltrometer placed at a sloping landscape was simulated with various disk diameters, water pressures applied at the soil surface, and sloping degrees. Numerical solution of Richards' equation and moisture retention relationship given by Russo *et al.* (1991) were employed for the simulation. The Richards' equation for three dimensional water flow in a homogenous and isotropic soil at a sloping landscape may be expressed as

$$C(h) \frac{\partial h}{\partial t} = \frac{\partial}{\partial x} \left[-K(h) \left(\frac{\partial h}{\partial x} - \sin \delta \right) \right] + \frac{\partial}{\partial y} \left[-K(h) \frac{\partial h}{\partial y} \right] + \frac{\partial}{\partial z} \left[K(h) \left(\frac{\partial h}{\partial z} + \cos \delta \right) \right] \quad [3.14]$$

where $C(h)$ is the soil water capacity ($L^3 L^{-4}$), h the pressure head (L), $K(h)$ the unsaturated hydraulic conductivity ($L T^{-1}$) as defined in Eq. [3.2], δ the angle of a slope (rad), t the time (T), and x, y, z axes of the Cartesian coordinate system (L) with z positive upward. The soil water characteristic curve is described (Russo *et al.*, 1991) as

$$\theta = \theta_r + (\theta_s - \theta_r) \left[\exp \left(-\frac{\alpha |h|}{2} \right) \left(1 + \frac{\alpha |h|}{2} \right) \right]^{\frac{2}{m+2}} \quad [3.15]$$

where θ , θ_s , and θ_r are volumetric water content ($L^3 L^{-3}$), saturated volumetric water content ($L^3 L^{-3}$), and residual volumetric water content ($L^3 L^{-3}$), respectively, α the soil

macroscopic capillary length parameter (L^{-1}), and m an empirical parameter ($= 0.5$). The soil water capacity, $C(h)$, is defined as the slope of the soil water retention curve as $d\theta/dh$.

To numerically solve Eq. [3.14] a general partial differential equation solver, FlexPDE (PDE Solutions Inc., 2000), which uses the finite element method as a solver, was deployed. Its reasonable performance to solve the problems on one- and two-dimensional water or solute transport in soil was found elsewhere (Noborio, 2001). The size of triangular elements and a time step increment were automatically changed to meet prescribed criteria. Equation [3.14] was solved with conditions as $h = -1.0$ m for the initial water pressure head, $h = -0.03$, -0.07 , -0.10 , or -0.22 m at the center of the disk at the soil surface for a boundary condition, the natural boundary for other boundaries. The disk diameters of a tension infiltrometer simulated were 0.04, 0.20, 0.60, and 1.00 m. Surface slope of 0, 5, 10, and 15% with respective α and K_{fs} values obtained from tension infiltrometer measurements in the field were also used for the simulation. A calculating domain varied with the disk diameter of the tension infiltrometer to have enough domain space for water flow.

3.3.6 Statistical analysis

Natural log-transformed K_{fs} , $K(h)$ and α values were used for statistical analysis because their distributions are reported to be log normal (Nielsen *et al*, 1973; Russo and Bouton, 1992). Analysis of variance was performed using SAS (SAS Institute, Inc., 1990) for randomized complete block design with five replications. Treatment means for 7, 15 and 20% slopes were compared separately with the mean value for control (level land = 0% slope) by Dunnett's test. Two treatment means were considered as significantly

different whenever the absolute difference between the corresponding estimated means exceeds the calculated Dunnett's critical t value at a 5% significance level.

3.4 Results and Discussion

The mean bulk density, macroporosity, and soil texture of the surface 0- to 5-cm soil did not show a significant difference among slopes suggesting that the experimental units were nearly uniform in soil texture and soil structure (Table 3.1). The steady infiltration rate is a function of boundary conditions (flat or sloping surfaces) and the morphology of the pore system, which is controlled by the texture and the structure of the soil, its continuity to the soil surface, and potential forces applied to the water (Hillel, 1998). Uniform pore morphology allows us to examine the effect of slope gradient (boundary conditions) on measurement of soil hydraulic properties.

Table 3. 1 Some selected soil physical properties of the experimental site.

Parameter	Slope			
	%			
	0	7	15	20
Sand (%)	24.21 (2.19) [†]	26.01 (3.42)	21.40 (2.12)	23.19 (2.58)
Silt (%)	62.10 (4.15)	56.22 (5.10)	51.04 (4.53)	59.04 (4.01)
Clay (%)	13.69 (4.45)	17.77 (5.55)	27.56 (3.18)	17.77 (5.31)
Bulk density (Mg m ⁻³)	1.26 (0.02)	1.25 (0.01)	1.26 (0.09)	1.27 (0.05)
Macro porosity (%)	14.5 (10.3)	13.9 (5.1)	15.0 (4.7)	15.8 (4.01)
K _{fs} [‡] (×10 ⁻⁶ m s ⁻¹)	2.23 (2.15)	2.55 (1.55)	2.10 (2.18)	2.15 (2.31)
(Tension infiltrometer)				
K _{fs} (×10 ⁻⁶ m s ⁻¹)	1.78 (2.11)	1.73 (1.59)	1.17 (2.56)	1.16 (1.20)
(Double-ring infiltrometer)				
α [§] (m ⁻¹)	10 (2.7)	7.9 (1.2)	7.1 (1.3)	7.2 (1.3)

[†]Number in parentheses is the standard deviation of five replicates

[‡]Field-saturated hydraulic conductivity

[§]Macroscopic capillary length parameter

No significant differences were found among slope gradients for the steady infiltration rates obtained from double-ring infiltrometer. Although the infiltration measurements

were carried out with a constant head at the center of the inner ring, the pressure head varied across the sloping surface with the highest value at the downslope side and lowest value in upslope side. Therefore, infiltration rate would be lower at the upslope side than that of the downslope side. The decrease in infiltration rate at the upslope side would have offset by the increase in infiltration rate at the downslope side resulting in no substantial differences among slopes. Furthermore, Phillip (1991) reported that downslope flow occur as a result of downslope component of gravity in sloping lands. Magnitude of slope effects on downslope flow increases with the increase of slope. However, for homogeneous and isotropic soils under constant flux boundary condition, Phillip theoretically showed that the infiltration normal to the slope differed relatively little from infiltration from a horizontal surface for slope gradients less than 30° (slope = 58%). Harr (1977) also studied the magnitude and direction of downslope flow under different rainfall intensities in steep forested watersheds (average slope 75%) using tensiometers. He observed that even a slight change in soil water pressure due to slope could change both magnitude and direction of water flux. Harr related the significant downslope flow during and between storms to soil layering with significant differences in pore-size distribution and saturated hydraulic conductivity between surface (0- to 30-cm) and subsurface soils. The surface soil of our experimental site would be more or less homogeneous due to mixing of soil during cultivation. Soil layers with abrupt changes in soil texture were not reported within 1.2 m of the soil profile (Dyck *et al.*, 2003). As a consequence, the downslope (lateral) flow under constant head boundary condition would also be small showing no significant difference in infiltration rates between horizontal surface and lands with relatively small gradients (20%).

The statistical test showed that there are no significant differences among slope treatments for the steady infiltration rates measured at different water pressures using tension infiltrometer with 20 cm diameter disc (Figure 3.4). These findings in the field were substantiated by the simulation studies. The 20-min cumulative infiltration under 20 cm diameter disc at -0.3 kPa pressure was not considerably different between level and sloping land surfaces (Figure 3.5a). The pressure head contours under the disc also did not show considerable differences among sloping surfaces (data not shown). Simulated cumulative infiltration for a 20-min period with 0.04, 0.2, 0.6, and 1 m diameter discs at -0.7, -0.1, and -2.2 kPa pressures also did not show marked differences

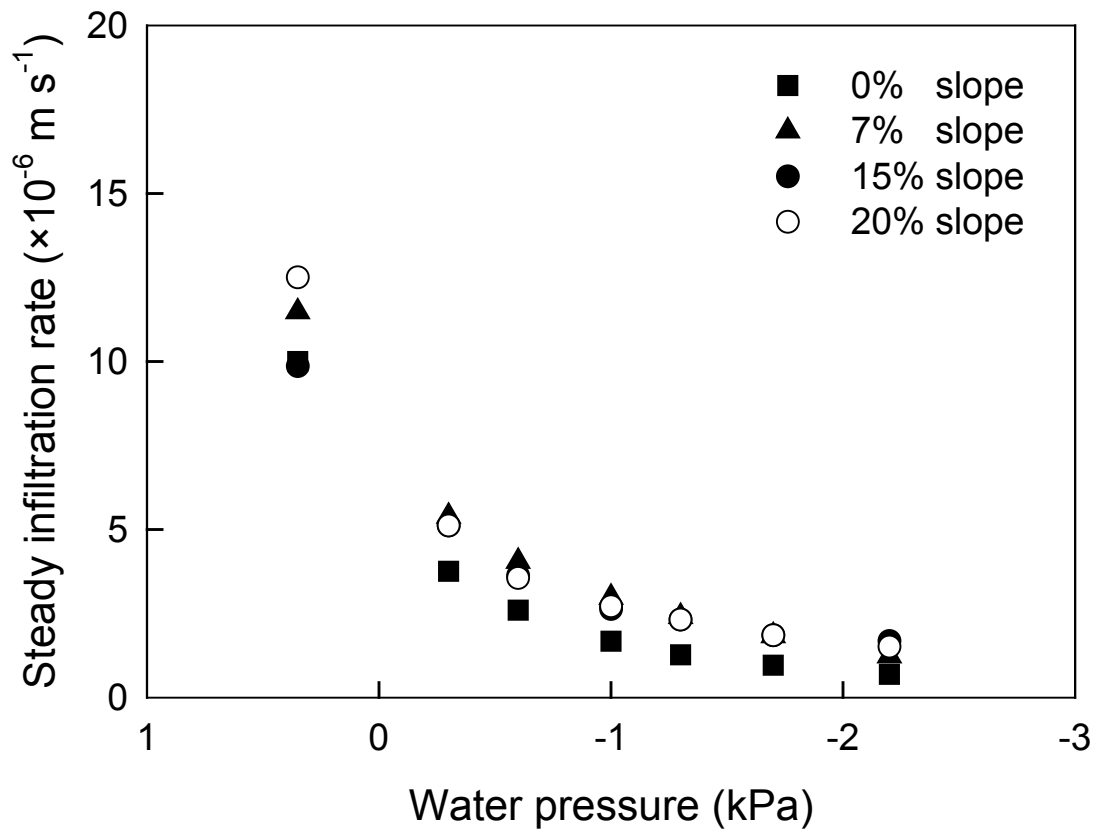


Figure 3. 4 Mean steady-state infiltration rates at different slopes

among slopes (data not shown). Only the cumulative infiltration simulated with a 1 m diameter disc at -0.3 kPa pressure showed small differences among slope gradients and the discrepancies increased with time elapsed (Figure 3.5b). In addition to reasons we stated for double-ring infiltrometer, gravity is less important under unsaturated conditions than at saturation. Like that of infiltration rate at different water pressures for flat soil surface, decreases in water pressure resulted in decreases in mean steady infiltration rates (Figure 3.4) and the rates of decrease are equivalent for all the slopes. A decrease in water pressure results in decreases in steady infiltration rates because a decrease in pressure reduces the size and number of pores that participate in conducting water. Similar slope gradient is likely a result of similar pore-size distribution among sloping surfaces.

Because the differences in infiltration rates measured using double-ring and tension infiltrometers are not statistically significant, in the following we use the method for flat surface to calculate hydraulic properties in sloping soil surfaces. The steady-state infiltration rates obtained from the tension infiltrometer fitted very closely ($R^2 > 0.9$) to Eq. [3.3] for all slope treatments. The fitting parameters (the saturated hydraulic conductivity (K_{fs}) and inverse capillary length scale (α)) were calculated. The K_{fs} estimated from tension infiltrometer measurements as well as the K_{fs} obtained from double-ring infiltrometer measurements were not significantly different between horizontal and sloping soil surfaces (Table 3.1). The K_{fs} values were estimated from steady infiltration rates which are mainly influenced by soil texture and structure. Uniform soil texture and bulk density in the experimental site will have contributed to nearly similar steady infiltration rates among slopes at different water pressures. As a

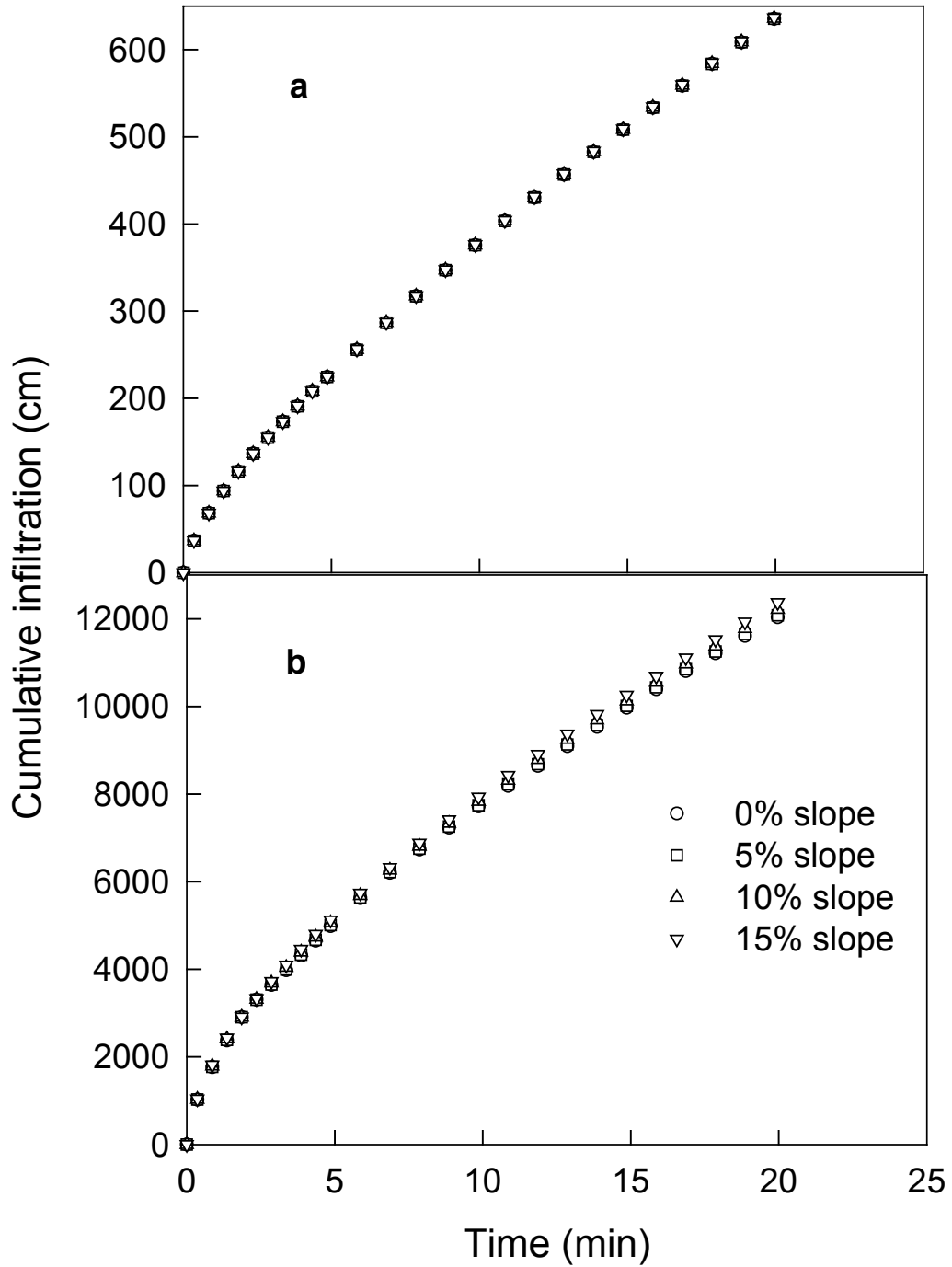


Figure 3. 5 Simulated cumulative infiltration as a function of elapsed time for different slopes at -0.3 kPa water pressure; a) 0.2-m diameter disc, and b) 1.0-m diameter disc.

consequence, K_{fs} would have become more or less uniform among the slopes tested.

The unconfined measurements of K_{fs} estimated from tension infiltrometers were slightly greater than those from confined infiltration in double-ring infiltrometers for all slope gradients (Table 3.1). This may be partly due to the effect of air entrapment, which acts to reduce infiltration rate when water enters a soil containing pockets of air. This is of a less problem with the unconfined measurements because of the radial shape and unconfined nature of the wetting front. The K_{fs} values are comparable with the values given by Rawls *et al.* (1993) for the USDA soil textural triangle for silt loam soils, i.e., $1.88 \times 10^{-6} \text{ m s}^{-1}$.

The macroscopic capillary length parameter (α) is a shape parameter of the relationship between hydraulic conductivity and applied water pressure and is a measure of the relative importance of the gravitational and capillary forces during water movement in unsaturated soils (Reynolds *et al.* (2002). The α values did not significantly vary among slopes (Table 3.1). The $K(h)$ functions estimated from infiltration measurements did not change considerably between level and sloping surfaces (Figure 3.6). Again, more or less uniform pore-size distribution among slope treatments likely explain such similar $K(h)$ relationships and thereby similar α values. Our α values are comparable with the values reported by Elrick *et al.* (1989) for cultivated soils as cited by Reynolds *et al.* (2002).

When considering macropores, the total volume occupied by them (macroporosity) as well as the amount of water they are capable of conducting is important. Macroporosity and water-conducting macro- and total porosity between -0.06 and -2.2 kPa pressure

ranges were not significantly different between level and sloping lands indicating that there will not be substantial differences in water transmission properties.

Macropores consisted of 13 to 16% of the total soil volume (Table 3.1). However, the real water-conducting macroporosity of the four slopes varies from 0.002 to 0.003% (Table 3.2). Macroporosity values in our study compare reasonably well with the values reported by Dunn and Phillips (1991) and Cameira *et al.* (2003) in silt loam soil for minimum tillage and conventional tillage plots.

The experimental and numerical results of this study clearly showed that, for the surface slopes ranging from zero to 20% in a cultivated field, there were no significant differences in hydraulic properties and water-conducting porosity estimated from both tension and double-ring infiltrometer measurements at the soil surface. As such, both tension infiltrometer and double ring infiltrometer are suitable for the measurement of soil hydraulic properties in level lands as well as non-level lands up to the slopes of 20%.

For steeper slopes, however, water supply pressure varies across the sloping surface (from the upslope to the downslope side). As indicated by Reynolds and Zebchuck (1996), this in turn will have a substantial impact on the validity of the tension infiltrometer results because the infiltrometer operates in the 'macropore range' where water transmission properties can change drastically with even small changes in water pressure. Our results did not indicate such effects. Furthermore, several researchers (Zaslavsky and Sinai, 1981; McCord *et al.*, 1991) have shown that downslope flow can occur even under unsaturated condition in the presence of soil layering close to the surface and/or anisotropy favoring downslope flow. However, small constant anisotropy

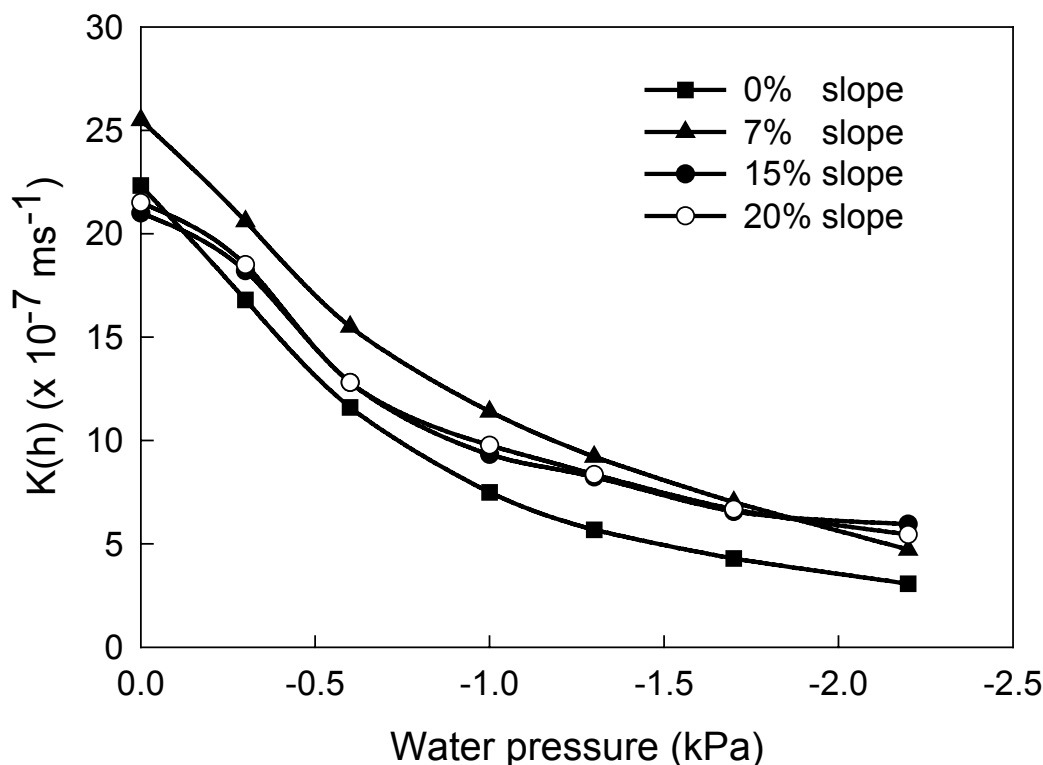


Figure 3. 6 Measured mean hydraulic conductivity, $K(h)$, of surface soils at different slopes

Table 3. 2 Estimated water-conducting porosity (% of total soil volume) in each pore diameter interval for the different slopes

Pore diameter ($\times 10^{-3}$ m)	Water-conducting porosity			
	Slope			
	%			
	0	7	15	20
1 to 5	0.003 (0.002) ^a	0.002 (0.001)	0.002 (0.001)	0.002 (0.001)
0.5 to 1	0.015 (0.002)	0.010 (0.001)	0.012 (0.001)	0.010 (0.001)
0.3 to 0.5	0.044 (0.004)	0.030 (0.003)	0.039 (0.003)	0.031 (0.003)
0.231 to 0.3	0.051 (0.005)	0.037 (0.004)	0.050 (0.004)	0.038 (0.004)
0.231 to 0.176	0.084 (0.007)	0.051 (0.005)	0.090 (0.007)	0.064 (0.006)
0.136 to 0.176	0.122 (0.009)	0.069 (0.007)	0.142 (0.010)	0.093 (0.010)
0.136 to 5	0.318 (0.027)	0.190 (0.019)	0.379 (0.026)	0.237 (0.024)

^aNumber in parentheses is the standard deviation of five replicates

causes too little lateral downslope flow relative to vertical flow (Jackson, 1992). Lack of soil layering and probably smaller anisotropy with more or less homogeneous conditions prevailing in soil close to the surface would have created small downslope flow. As a consequence, the infiltration rate, and the estimated hydraulic properties from infiltration rates would not vary much between level and sloping lands in our experimental site.

The results of this experiment may be different for heterogeneous soils that have soil layers close to the surface with contrasting hydraulic properties and/or broad range of pore sizes. Presence of soil layers may increase the downslope flow component. Due to water pressure variation across the slope, the number and size of pores that involve in conducting water will be different between downslope and upslope sides of the infiltrometer disc. Compared to the center of the disc, smaller pores would contribute to water conductivity at the upslope side due to lower pressure. On the other hand, at the downslope side, pores greater than the size corresponding to the imposed water pressure at the center of the disc will participate for water transmission due to higher pressure. Since the flow rate is proportional to the fourth power of pore radius, the flow rate at the downslope side would be much greater resulting in much higher overall infiltration rate in soils with wide range of pore sizes. Hence, further investigation is recommended on the slope effect on tension infiltration in soils with layers and broad pore-size ranges.

3.5 Conclusions

The suitability of tension and double-ring infiltrometers for the estimation of hydraulic properties in sloping lands *in situ* was evaluated using infiltration measurements at 0%, 7%, 15% and 20% slopes at a cereal crop cultivated field. Water infiltration from the

tension infiltrometer was also simulated with various disc diameters, water pressures at the soil surface, and sloping degrees. The measured steady-state infiltration rates and estimated field-saturated hydraulic conductivity, (K_{fs}), unsaturated hydraulic conductivity as a function of water pressure, ($K(h)$), macroscopic capillary length parameter, (α), and water-conducting macro- and mesoporosity were not significantly different among slopes. The steady infiltration rates obtained from double-ring infiltrometer varied from 9.0 to $12.5 \times 10^{-6} \text{ m s}^{-1}$. The K_{fs} values varied from 1.16 to $2.55 \times 10^{-6} \text{ m s}^{-1}$ while the α values ranged from 7 to 10 m^{-1} . The $K(h)$ decreased nearly by an order of magnitude across a small pressure range near saturation (zero to -2.2 kPa). Water-conducting macroporosity and water-conducting total porosity between 1×10^{-4} and $5 \times 10^{-3} \text{ m}$ pore diameter ranged from 0.002 to 0.003% and 0.19 to 0.38%, respectively. Experimental and numerical results of this study strongly suggest that both tension infiltrometer (0.2 m diameter disc) and double-ring infiltrometer are suitable for characterization of soil hydraulic properties in lands with slopes up to 20%.

3.6 References

- Anderson, S.P., W.E. Dietrich, D.R. Montgomery, R. Torres, M.E. Conrad, and K. Loague. 1997. Subsurface flow paths in a steep, unchanneled catchment. *Water Resour. Res.* 33:2637-2653.
- Angulo-Jaramillo R, J.P., Vandervaere, S. Roulier, J.L Thony, J.P. Gaudet, and M. Vauclin. 2000. Field measurement of soil surface hydraulic properties by disc and ring infiltrometers: A review and recent developments. *Soil Tillage Res.* 55:1-29.
- Ankeny, M.D., M. Ahmed, T.C. Kaspar, and R. Horton. 1991. Simple field method for determining unsaturated hydraulic conductivity. *Soil Sci. Soc. Am. J.* 55:467-470.
- Bear, J. 1972. *Dynamics of fluids in porous media*. Elsevier Pub. Co. Inc, New York, NY.

- Bodhinayake, W.L, B.C. Si, and C. Xiao. 2003. New method for determining water-conducting macro- and mesoporosity from tension infiltrometer. *Soil Sci. Soc. Am. J.* Accepted for publication.
- Bodhinayake, W.L, and B.C. Si. 2003. Near-saturated surface soil hydraulic properties under different land uses in the St. Denis National Wildlife Area, Saskatchewan, Canada. *J. Hydrol. Process.* In press.
- Bower, H. 1986. Intake rate. Cylinder infiltrometer. p. 825-843. *In* A. Klute (ed.) *Methods of soil analysis. Part 1. Physical and mineralogical properties.* 2nd ed. ASA, Madison, WI.
- Cameira, M.R., R.M. Fernando, and L.S. Pereira. 2003. Soil macropore dynamics affected by tillage and irrigation for a silt loam alluvial soil in southern Portugal. *Soil Tillage Res.* 70:131-140.
- Casanova, M., I. Messing, and A. Joel. 2000. Influence of aspect and slope gradient on hydraulic conductivity measured by tension infiltrometer. *Hydrol. Process.* 14:155-164.
- Dunn, G.H., and R.E. Phillips. 1991. Macroporosity of a well-drained soil under no-till and conventional tillage. *Soil Sci. Soc. Am. J.* 55:817-823.
- Dunne, T., and R.D. Black. 1970. An experimental investigation of runoff production in permeable soils. *Water Resour. Res.* 6:478-490.
- Dyck, M.F., R.G. Kachanoski, and E. de Jong. 2003. Long-term movement of a chloride tracer under transient, semi-arid conditions. *Soil Sci. Soc. Am. J.* 67:471-477.
- Elliott, J.A, and A.A. Efetha. 1999. Influence of tillage and cropping system on soil organic matter, structure and infiltration in a rolling landscape. *Can. J. Soil Sci.* 79:457-463.
- Gardner, W.R. 1958. Some steady-state solutions of unsaturated moisture flow equations with application to evaporation from a water table. *Soil Sci.* 85:228-232.
- Gradshteyn, I.S., and I.M. Ryzhik. 2000. *Table of integrals, series, and products.* 6th ed. Academic Press. San Diego, CA, USA.
- Harr, R.D. 1977. Water flux in soil and subsoil on a steep forested slope. *J. Hydrology.* 33:37-58.
- Hillel, D. 1998. *Environmental soil physics.* Academic Press. New York. Iowa State University Press. USA.

- Jackson, C.R. 1992. Hillslope infiltration and lateral downslope unsaturated flow. *Water Resour. Res.* 28:2533-2539.
- Joel, A., and I. Messing. 2000. Application of two methods to determine hydraulic conductivity with disc permeameters on sloping land. *European J. Soil Sci.* 51:93-98.
- Logsdon, S.D., and D.B. Jaynes. 1993. Methodology for determining hydraulic conductivity with tension infiltrometers. *Soil Sci. Soc. Am. J.* 57:1426-1431.
- Luxmoore, R.J. 1981. Micro-, meso- and macroporosity of soil. *Soil Sci. Soc. Am. J.* 45:671-672.
- Mendoza, G., and S.T. Steenhuis. 2002. Determination of hydraulic behavior of hillsides with a hill slope infiltrometer. *Soil Sci. Soc. Am. J.* 66:1501-1504.
- Messing, I., and N.J. Jarvis. 1993. Temporal variation in the hydraulic conductivity of a tilled clay soil as measured by tension infiltrometers. *J. Soil Sci.* 44:11-24.
- McCord, J.T., D.B. Stephens, and J.L. Wilson. 1991. Hysteresis and state-dependent anisotropy in modelling unsaturated hillslope hydrologic processes. *Water Resour. Res.* 27:1501-1518.
- Mosley, M.P. 1982. Subsurface flow velocities through selected forest soils, South Island, New Zealand. *J. Hydrology.* 55:65-92.
- Nielson, D.R., J.W. Biggar, and K.T. Ere. 1973. Spatial variability of field measured soil- water properties. *Hilgardia.* 42:215-260.
- Noborio, K. 2001. Application of a general PDE solver for analyzing water and solute transport in soil. *J. Jpn. Soc. Soil Phys.* 88:19-25. (in Japanese with English abstract).
- PDE Solutions Inc. 2000. FlexPDE User Guide, Version 2.19. PDE Solutions Inc., Antioch, CA.
- Perroux, K.M., and I. White. 1988. Design for disc permeameters. *Soil Sci. Soc. Am. J.* 52:1205-1215.
- Phillip, J.R. 1969. Theory of infiltration. *Adv. Hydrosci.*, 5:215-296.
- Phillip, J.R. 1991. Hill slope infiltration: Planar slopes. *Water Resour. Res.* 27:109-117.
- Rawls, W.J., L.R. Ahuja, D.L. Brakensiek, and A. Shirmohammadi. 1993. Infiltration and soil water movement. p. 5.1-5.51. *In* D. R. Maidment. (ed.) *Handbook of hydrology*. McGraw Hill, Inc. NY.

- Reynolds, W.D., and W.D. Zebchuck. 1996. Use of contact material in tension infiltrometer measurements. *Soil Technology*. 9:141-159.
- Reynolds, W.D., D.E. Elrick, and E.G. Youngs. 2002. The soil solution phase. Singlering and double- or concentric-ring infiltrometers. p. 821-826. *In* J. H. Dane and G. C. Topp (ed.) *Methods of soil analysis: Part 4. Physical methods*, SSSA, Madison, WI.
- Russo, D., and M. Bouton. 1992. Statistical analysis of spatial variability in unsaturated flow parameters. *Water Resour. Res.* 28:1911-1925.
- Russo, D., E. Bresler, U. Shani, and J.C. Parker. 1991. Analyses of infiltration events in relation to determining soil hydraulic properties by inverse problem methodology. *Water Resour. Res.* 27:1361-1373.
- SAS Institute Inc. 1990. *SAS/STAT user's guide*. Version 6. SAS Institute Inc., Cary, NC.
- Torres, R., W.E. Dietrich, D.R. Montgomery, S.P. Anderson, and K. Loague. 1998. Unsaturated zone processes and the hydrologic response of a steep, unchanneled catchment. *Water Resour. Res.* 34:1865-1879.
- Vandervaere, J.P., M. Vauclin and D.E. Elrick. 2000. Transient flow from tension infiltrometers. I. The two-parameter equation. *Soil Sci. Soc. Am. J.* 64:1263-1272.
- Watson, K.W., and R.J. Luxmoore. 1986. Estimating macroporosity in a forest watershed by use of a tension infiltrometer. *Soil Sci. Soc. Am. J.* 50:578-582.
- Wilson, G.V., and R.J. Luxmoore. 1988. Infiltration, macroporosity and mesoporosity distributions on two forested watersheds. *Soil Sci. Soc. Am. J.* 52:329-335.
- Wooding, R.A. 1968. Steady infiltration from a shallow circular pond. *Water Resour. Res.* 4:1259-1273.
- Zaslavsky, D, and G. Sinai. 1981. *Surface hydrology*. 1. Explanation of phenomena. *J. Hydrol. Div. Am. Soc. Civ. Eng.* 107:1-16.
- Zhang, R. 1997. Determination of soil sorptivity and hydraulic conductivity from disk infiltrometer. *Soil Sci. Soc. Am. J.* 61:1024-1030.

4. NEW METHOD FOR DETERMINING WATER-CONDUCTING MACRO- AND MESOPOROSITY FROM TENSION INFILTROMETER

4.1 Abstract

Characterization of water-conducting porosity at and near saturation is required in understanding rainfall and snowmelt infiltration and runoff as well as chemical transport in soil. There are methods available to quantify water-conducting porosity *in situ*, but with serious limitations. The objective of this paper was to present a general equation for water-conducting porosity based on ponded- and tension-infiltration measurements. Some analytical solutions are developed for specific unsaturated hydraulic conductivity functions such as the Gardner's exponential and rational power models, the Brooks and Corey model, and the van Genuchten-Mualem model. Tension infiltrometer measurements were taken at six different water pressures between -0.3 and -2.2 kPa and double-ring infiltrometer measurements at a pressure of 0.35 kPa. The analytical solutions were compared with numerical solutions and existing methods for calculation of water-conducting porosity. Both the analytical and numerical solutions can reliably determine the water-conducting porosity of surface soils *in situ* within the practical water pressure range of the tension infiltrometer. Our method gave consistent water-conducting porosity, regardless of the width of water pressure ranges. The existing methods over-estimated water-conducting macroporosity by a factor of greater

than two and over-estimated total water-conducting porosity by a factor of greater than ten for measurements taken at large water pressure intervals compared to that of our method. Combining with hydraulic parameter estimation from tension infiltrometer measurements, our method may reduce the number of tension infiltration measurements required to calculate water-conducting porosity.

4.2 Introduction

The significance of macropores and mesopores to water flow in soils, particularly to infiltration and rapid movement of water, solutes and pollutants through soils are well recognized (Beven and Germann, 1982; Wilson and Luxmoore, 1988; Luxmoore *et al.*, 1990; Ankeny *et al.*, 1990) and are the subject of considerable research interests. Macroporosity and mesoporosity (the fractions of soil volume comprise of pores with diameters $> 1 \times 10^{-3}$ m and between 1×10^{-5} and 1×10^{-3} m, respectively; Luxmoore, 1981) of soil core samples or soil columns can be easily determined in the laboratory (Flint and Flint, 2002). Macro- and mesopores include dead-ended and non-continuous pores, as well as continuous pores with cylindrical or irregular geometry, but only the continuous or interconnected pores contribute to fast water flow in soil. Furthermore, the equivalent diameter of the water-conducting continuous pores is controlled primarily by the part with the smallest diameter (bottle neck) along its pathway although the bottle-neck may only be a small fraction of the total length of the pore (Dunn and Phillips, 1991b). The function of water-conducting pores is also influenced by pore tortuosity, surface roughness etc. (Skopp, 1981; Bouma, 1982). Therefore, higher soil macro- and mesoporosity does not necessarily imply higher hydraulic conductivity and faster chemical transport. Static measurements of pore characteristics

such as total macro- and mesoporosity measurements in the laboratory will not adequately describe the actual contribution of pores to flow of water and solutes in soil (Messing and Jarvis, 1993). Hence, *in situ* measurement of actual water-conducting porosity is of utmost importance in understanding movement of water and solutes into and through soils.

In the past, several techniques have been employed to quantify the water-conducting macro- and mesoporosity in soil including: staining or dye tracing (Bouma *et al.*, 1979; Ghodrati and Jury, 1990; Weiler and Naef, 2003), tracers and breakthrough curves (Bouma and Wosten, 1979; Yeh *et al.*, 2000), X-ray computed tomography (Anderson *et al.*, 1990), gas diffusion (Bruckler *et al.*, 1989), and infiltration redistribution pattern (Timlin *et al.*, 1994). These methods, however, required either undisturbed soil cores/columns or are tedious to perform under field conditions. Rapid, simple, and *in situ* ponded- and tension-infiltration measurements, on the other hand, have become popular recently in characterizing water-conducting macro- and mesoporosity in the surface soils. Watson and Luxmoore (1986) and Wilson and Luxmoore (1988) calculated the water-conducting macro- and mesoporosity from the differences in infiltration rates between two water pressures by using the minimum equivalent pore radius. Several researchers (Azevedo *et al.*, 1998; Buttle and McDonald, 2000; Cameira *et al.* 2003) have followed the procedure used by Watson and Luxmoore (1986) as a means of estimating water conducting soil macro- and mesoporosity. Dunn and Phillips (1991a) modified the approach of Watson and Luxmoore (1986) by replacing the minimum pore radius with the mean pore radius in the pressure range. The approaches of Watson and Luxmoore (1986) and Dunn and Phillips (1991a) both assumed a single

pore size (minimum pore radius for Watson and Luxmoore and mean pore radius for Dunn and Phillips). The assumption is unrealistic and may lead to incorrect water-conducting porosity, an unrealistic parameterization of soil properties, and poor performance of hydrological models. Therefore, there is a need for development of a reliable and convenient method for the estimation of water-conducting macro- and mesoporosity.

The objectives of this study were to present a general equation for water-conducting porosity and to derive analytical solutions for the water-conducting porosity based on ponded- and tension–infiltration measurements in conjunction with four commonly-used hydraulic conductivity-water pressure functions: 1) Gardner exponential (1958); 2) Gardner rational (1965); 3) Brooks and Corey (1966); and 4) van Genuchten-Mualem (1980). The derived general equation and specific analytical solutions for water-conducting porosity are tested *in situ* using tension and double-ring infiltrometer measurements and compared with Watson and Luxmoore (1986) and Dunn and Philips (1991a) procedures.

4.3 Theory

The maximum water-filled equivalent pore size, r (L), at a specific water pressure head, h (L), can be calculated from the capillary rise equation (Bear, 1972)

$$r = \frac{2 \gamma \cos(\vartheta)}{\rho g h} \quad [4.1]$$

where γ is the surface tension of water ($M T^{-2}$), ϑ is the contact angle between water and the pore wall (assumed to be zero), ρ is the density of water ($M L^{-3}$), and g is the acceleration due to gravity ($L T^{-2}$).

We assume that the equivalent pores with radii smaller than r calculated from equation [4.1] are full of water and are responsible for all the flux of water under a given water pressure, and that the equivalent pores with radii larger than the value calculated from equation [4.1] are not contributing to the water flux. According to capillary theory and Poiseuille's law, the flow rate through a single macropore is given by

$$Q(r) = \frac{\pi \rho g}{8 \mu} r^4 \quad [4.2]$$

where $Q(r)$ is the flow rate ($L^3 T^{-1}$) as a function of pore radius r and μ is the dynamic viscosity of water ($M L^{-1} T^{-1}$). Considering the number of water-conducting pores per unit cross sectional area (L^2) for a given pore size r in soils $N(r)$, the water flux density, $I(r)$ ($L T^{-1}$), through pores of radius r is given by

$$I(r) = Q(r) N(r) \quad [4.3]$$

Substitution of Eq. [4.2] into Eq. [4.3] yields

$$I(r) = \frac{\pi \rho g}{8 \mu} r^4 N(r) \quad [4.4]$$

Therefore,

$$N(r) = \frac{8 \mu I(r)}{\pi \rho g} r^{-4} \quad [4.5]$$

The water-conducting porosity $\varepsilon_m(r)$ associated with each pore size equals the number of pores per unit area multiplied by the cross sectional area of the corresponding size pores:

$$\varepsilon_m(r) = N(r) \pi r^2 \quad [4.6]$$

4.3.1 Watson and Luxmoore (1986) approach

Watson and Luxmoore (WL) (1986) calculated the number of pores ($\Delta N(a, b)$), between two pore radii a and b ($a \leq b$). Assuming pore radius equals to the minimum pore radius, the number of pores resulting in a difference in total soil water flux or hydraulic conductivity between two water pressures corresponding to the two pore radii, is:

$$\Delta N(a, b) = \frac{8 \mu \Delta I(a, b)}{\pi \rho g a^4} \quad [4.7]$$

where $\Delta I(a, b)$ ($L T^{-1}$) is the soil water flux conducted by pores with radii between a and b . Then the water conducting porosity due to pores in this range $\varepsilon(a, b)$ can be calculated as

$$\varepsilon(a, b) = \Delta N(a, b) \pi a^2 = \frac{8 \mu \Delta I(a, b)}{\rho g a^2} \quad [4.8]$$

Watson and Luxmoore (1986) used Eqs. [4.7] and [4.8] for the estimation of $\Delta N(a, b)$ and $\varepsilon(a, b)$, respectively, using the minimum equivalent pore radius in each pressure range. However, their calculation results in the maximum number of pores and hence maximum water-conducting porosity, because pore radius (a) appears in the denominator of Eqs. [4.7] and [4.8]. Consequently, their approach results in an overestimation of the number of pores per unit area and the total water-conducting porosity in the pressure range considered.

4.3.2 Dunn and Phillips (1991a) approach

Dunn and Phillips (DP) (1991a) modified the approach of WL by assuming a uniform (Box-car) distribution of pore number. Their calculation results in the mean number of

pores per unit area $\overline{N(a,b)}$, as if all the pores have the same radius. The $\overline{N(a,b)}$ is given by

$$\overline{N(a,b)} = \frac{8 \mu \Delta I(a,b)}{\pi \rho g} \frac{\int_a^b r^{-4} dr}{\int_a^b dr} \quad [4.9]$$

where a and b are pore radii of the lower and upper limits of the integrals of each sequential water pressure range.

Neglecting the dependence between $N(a,b)$ and pore cross-sectional area, and assuming constant slope of infiltration rate I as a function of pore radius ($\Delta I(a,b) / \int_a^b dr = \Delta I(a,b) / (b-a)$), which means a linear dependence of $I(a,b)$ on r , DP also calculate the mean water-conducting porosity $\overline{\varepsilon(a,b)}$, for pore size between a and b ,

$$\overline{\varepsilon(a,b)} = \overline{N(a,b)} \pi \frac{\int_a^b r^2 dr}{\int_a^b dr} \quad [4.10]$$

Therefore, for calculation of water-conducting porosity, the DP approach as well as WL approach unrealistically assumed uniform pore size distribution within the pressure range, and linear dependence of hydraulic conductivity on pore radius.

4.3.3 A New approach

We considered the number of pores per unit area (L^2) as a function of r . The total number of pores in a given pore size range, $n(r)$, is the cumulative pore number distribution and is given by

$$n(r) = \int_0^r P(r) dr \quad [4.11]$$

where $P(r)$ is the number of pores per unit area per unit pore radius. For unit hydraulic gradient, steady infiltration rate at a water pressure equals the hydraulic conductivity K ($L T^{-1}$). The hydraulic conductivity at a given pressure h or pore size r , $K(r)$ can be expressed by

$$K(r) = \int_0^r P(r) Q(r) dr \quad [4.12]$$

where r is the upper limit of the integrals determined by the water pressure. The expression for $P(r)$ can be obtained by taking derivatives of both sides of Eq. [4.12]

$$P(r) = \frac{dK(r)}{dr} \frac{1}{Q(r)} \quad [4.13]$$

According to Eq. [4.6], the water-conducting porosity in a given pressure range can be expressed as,

$$\varepsilon(a, b) = \int_a^b \pi r^2 P(r) dr \quad [4.14]$$

Substitution of Eq. [4.13] for $P(r)$ in Eq. [4.14] leads to

$$\varepsilon(a, b) = \int_a^b \frac{dK(r)}{dr} \frac{1}{Q(r)} \pi r^2 dr \quad [4.15]$$

This is a general expression for water conducting porosity.

We can show that Eq. [4.15] reduces to WL equation. By assuming r constant and equal to minimum pore radius in the pressure range, Eq. [4.15] reduces to

$$\varepsilon(a,b) = \int_a^b \frac{dK(r)}{dr} \frac{1}{Q(r)} \pi r^2 dr = \frac{1}{Q(r)} \pi r^2 \int_a^b dK(r) = \Delta K \frac{\pi a^2}{Q(a)} \quad [4.15a]$$

For unit hydraulic gradient, infiltration rate is equal to hydraulic conductivity. Thus, Eq. [4.15a] is exactly the WL expression if unit gradient flow is assumed.

Generally, soil hydraulic conductivity is expressed as a function of soil water content or water pressure. Since Eq. [4.15] involves hydraulic conductivity as a function of pore radius, in the following we revise Eq. [4.15] and express water-conducting porosity in terms of hydraulic conductivity as a function of water pressure, $K(h)$. For convenience, we use the following variable substitution

$$H(r) = \frac{2 \gamma}{\rho g r} \quad [4.16]$$

Substituting Eq. [4.2] for $Q(r)$ and Eq. [4.1] for r into Eq. [4.15], leads to

$$\varepsilon(a,b) = \frac{2 \mu \rho g}{\gamma^2} \int_{H(a)}^{H(b)} \frac{dK(h)}{dh} h^2 dh \quad [4.17]$$

Integration of Eq. [4.17] by parts leads to

$$\varepsilon(a,b) = \frac{2 \mu \rho g}{\gamma^2} \left(h^2 K(h) \Big|_{H(a)}^{H(b)} - 2 \int_{H(a)}^{H(b)} K(h) h dh \right) \quad [4.18]$$

Equation [4.18] is an exact equation for calculation of soil water-conducting porosity for a given range of pore radii or water pressures. Integration in Eq. [4.18] may be carried out numerically by a software package such as MathCad 2000 (Math Soft, Cambridge). For known hydraulic property functions, like Gardner's exponential (1958) and rational (1965) functions, Brooks and Corey (1966), and van Genuchten-Mualem

(1980) function, exact analytical solution for Eq. [4.18] may be obtained by direct integration.

4.3.3.1 Gardner (1958) exponential model

Gardner's (1958) exponential hydraulic conductivity function has the following form,

$$K(h) = K_s \exp(-\alpha_{GE} h) \quad [4.19]$$

where, $K(h)$ is the hydraulic conductivity corresponding to the applied water pressure h , K_s is the saturated hydraulic conductivity ($L T^{-1}$), and α_{GE} is the inverse macroscopic capillary length scale (L^{-1}).

Substitution of Eq. [4.19] for $K(h)$ in Eq. [4.18] yields

$$\varepsilon(a,b) = \frac{2 \mu \rho g K_s}{\gamma^2} \left(h^2 \exp(-\alpha_{GE} h) \Big|_{H(a)}^{H(b)} - 2 \int_{H(a)}^{H(b)} h \exp(-\alpha_{GE} h) dh \right) \quad [4.20]$$

Substitution of Eq. [4.16] into Eq. [4.20] and subsequent integration give (Gradshteyn and Ryzhik, 2000, Eq. 2.322, p.104)

$$\varepsilon(a,b) = \frac{2 \mu \rho g K_s}{\gamma^2} \left\{ \exp\left(\frac{-2 \gamma \alpha_{GE}}{\rho g b}\right) \left(\frac{4 \gamma^2}{(\rho g b)^2} + \frac{4 \gamma}{\rho g b \alpha_{GE}} + \frac{2}{\alpha_{GE}^2} \right) - \exp\left(\frac{-2 \gamma \alpha_{GE}}{\rho g a}\right) \left(\frac{4 \gamma^2}{(\rho g a)^2} + \frac{4 \gamma}{\rho g a \alpha_{GE}} + \frac{2}{\alpha_{GE}^2} \right) \right\} \quad [4.21]$$

4.3.3.2 Brooks and Corey (1966) model

The Brooks and Corey (1966) model for the unsaturated hydraulic conductivity as a function of applied water pressure has the following form

$$K(h) = \begin{cases} K_s & h \leq h_e \\ K_s \left(\frac{h_e}{h} \right)^{\beta_{BC}} & \text{otherwise} \end{cases} \quad [4.22]$$

where h_e is the air entry potential (L) and β_{BC} is a fitting parameter. Note that $h_e \leq H(a)$ because h_e corresponds to the largest pore size in soil. Substitution of Eq. [4.22] for $K(h)$ in Eq. [4.18] yields

$$\varepsilon(a,b) = \frac{2\mu\rho g K_s h_e^{\beta_{BC}}}{\gamma^2} \left(h^{2-\beta_{BC}} \frac{H(b)}{H(a)} - 2 \int_{H(a)}^{H(b)} h^{1-\beta_{BC}} dh \right) \quad [4.23]$$

Substitution of Eq. [4.16] into Eq. [4.23] and subsequent integration yield

$$\varepsilon(a,b) = \frac{8\mu K_s h_e^{\beta_{BC}} (\rho g)^{\beta_{BC}-1}}{(2\gamma)^{\beta_{BC}}} \frac{\left(b^{\beta_{BC}-2} - a^{\beta_{BC}-2} \right) (-\beta_{BC})}{2-\beta_{BC}} \quad [4.24]$$

4.3.3.3 Gardner rational (1965) power model

Following Gardner (1965), we employ the following unsaturated hydraulic conductivity model to relate the capillary pressure to the reduction of hydraulic conductivity from its saturated value K_s :

$$K(h) = \frac{K_s}{1 + (\alpha_{GP} h)^{\beta_{GP}}} \quad [4.25]$$

where α_{GP} and β_{GP} are curve fitting parameters.

We can rewrite Eq. [4.18] as follows:

$$\varepsilon(a,b) = \frac{2\mu\rho g}{\gamma^2} (A - B) \quad [4.26]$$

where

$$A = h^2 K(h) \Big|_{H(a)}^{H(b)} \quad [4.27]$$

$$B = 2 \int_{H(a)}^{H(b)} h K(h) dh \quad [4.28]$$

Substituting Eq. [4.16] and Eq. [4.25] into Eq. [4.27], we get

$$A = K_s \left(\left(\frac{2\gamma}{\rho g b} \right)^2 \frac{1}{1 + \left(\frac{2\gamma \alpha_{GP}}{\rho g b} \right)^{\beta_{GP}}} - \left(\frac{2\gamma}{\rho g a} \right)^2 \frac{1}{1 + \left(\frac{2\gamma \alpha_{GP}}{\rho g a} \right)^{\beta_{GP}}} \right) \quad [4.29]$$

After introduction of a new variable $V(r) = (\alpha_{GP} h(r))^{\beta_{GP}}$, substitution of Eq. [4.25] into Eq. [4.28] and subsequent integration yields

$$B = \frac{K_s}{\alpha_{GP}^2} \left(V(b)^{\frac{2}{\beta_{GP}}} (V(b)+1)^{-1} \sum_{j=0}^{\infty} f\left(j, 1, 1 + \frac{2}{\beta_{GP}}; \frac{V(b)}{V(b)+1}\right) - V(a)^{\frac{2}{\beta_{GP}}} (V(a)+1)^{-1} \sum_{j=0}^{\infty} f\left(j, 1, 1 + \frac{2}{\beta_{GP}}; \frac{V(a)}{V(a)+1}\right) \right) \quad [4.30]$$

Complete derivation of the analytical solution for the Gardner rational (1965) power model is given in Appendix A1.

4.3.3.4 van Genuchten-Mualem (1980) model

Based on Mualem (1976) predictive hydraulic conductivity model, van Genuchten (1980) expressed hydraulic conductivity in terms of the water pressure as

$$K(h) = K_s \frac{\left(1 - (\alpha_{VG} h)^{n-1} \left(1 + (\alpha_{VG} h)^n\right)^{-m}\right)^2}{\left(1 + (\alpha_{VG} h)^n\right)^{\frac{m}{2}}} \quad [4.31]$$

where α_{VG} , n and m are curve fitting parameters. We can rewrite Eq. [4.18] as

$$\varepsilon(a, b) = \frac{2 \mu \rho g}{\gamma^2} (C - D) \quad [4.32]$$

where

$$C = h^2 K(h) \Big|_{H(a)}^{H(b)} \quad [4.33]$$

$$D = 2 \int_{H(a)}^{H(b)} h K(h) dh \quad [4.34]$$

Substituting Eq. [4.16] and Eq. [4.31] into Eq. [4.33], and substituting the limit we get

$$C = Ks \left(\left(\frac{2\gamma}{\rho g b} \right)^2 \frac{\left[1 - \left(\frac{2\gamma \alpha_{VG}}{\rho g b} \right)^m \left(1 + \frac{2\gamma \alpha_{VG}}{\rho g b} \right)^{-m} \right]^2}{1 + \left(\frac{2\gamma \alpha_{VG}}{\rho g b} \right)^{0.5m}} - \left(\frac{2\gamma}{\rho g a} \right)^2 \frac{\left[1 - \left(\frac{2\gamma \alpha_{VG}}{\rho g a} \right)^m \left(1 + \frac{2\gamma \alpha_{VG}}{\rho g a} \right)^{-m} \right]^2}{1 + \left(\frac{2\gamma \alpha_{VG}}{\rho g a} \right)^{0.5m}} \right) \quad [4.35]$$

where $m = 1 - \frac{1}{n}$. After introduction of a new variable $w(r) = (\alpha_{VG} h(r))^n$, substitution of Eq.

[4.16] and Eq. [4.31] into Eq. [4.34] leads to

$$D = \frac{2Ks}{n \alpha_{VG}^2} \int_{w(a)}^{w(b)} \left(\frac{V^{\frac{2}{n}-1}}{(1+V)^{0.5m}} - 2 \frac{V^{\frac{1}{n}}}{(1+V)^{1.5m}} + \frac{V}{(1+V)^{2.5m}} \right) dV \quad [4.36]$$

where V is a dummy integration variable. We can rewrite Eq. [4.36] as

$$D = \frac{2Ks}{n \alpha_{VG}^2} (E - F + G) \quad [4.37]$$

where

$$E = \left(\frac{w(b)^{\frac{2}{n}}}{\frac{2}{n}} (w(b)+1)^{-0.5m} \sum_{j=0}^{\infty} f\left(j, 0.5m, 1; 1 + \frac{2}{n}; \frac{w(b)}{w(b)+1}\right) - \frac{w(a)^{\frac{2}{n}}}{\frac{2}{n}} (w(a)+1)^{-0.5m} \sum_{j=0}^{\infty} f\left(j, 0.5m, 1; 1 + \frac{2}{n}; \frac{w(a)}{w(a)+1}\right) \right) \quad [4.38]$$

$$F = 2 \left(\frac{w(b)^{1+\frac{1}{n}}}{1+\frac{1}{n}} (w(b)+1)^{-1.5m} \sum_{j=0}^{\infty} f \left(j, 1.5m, 1; 2+\frac{1}{n}; \frac{w(b)}{w(b)+1} \right) - \frac{w(a)^{1+\frac{1}{n}}}{1+\frac{1}{n}} (w(a)+1)^{-1.5m} \sum_{j=0}^{\infty} f \left(j, 1.5m, 1; 2+\frac{1}{n}; \frac{w(a)}{w(a)+1} \right) \right) \quad [4.39]$$

$$G = \left(\frac{w(b)^2}{2} (w(b)+1)^{-2.5m} \sum_{j=0}^{\infty} f \left(j, 2.5m, 1; 3; \frac{w(b)}{w(b)+1} \right) - \frac{w(a)^2}{2} (w(a)+1)^{-2.5m} \sum_{j=0}^{\infty} f \left(j, 2.5m, 1; 3; \frac{w(a)}{w(a)+1} \right) \right) \quad [4.40]$$

Complete derivation of the analytical solution for the van Genuchten-Mualem (1980) model is given in Appendix A2.

4.4 Demonstrations

To test the above solutions, field experiments using a tension infiltrometer and a double-ring infiltrometer were carried out on a farm field in Laura, Saskatchewan, Canada (51° 52' N lat., 107° 18' W long.). The soil in that area is described as an Elstow association consisting of Dark Brown Chernozems (Typic Ustolls) developed on loamy glacio-lacustrine parent material with silt loam surface soil texture. The lacustrine sediments are underlain by glacial till that is drained by the Tessier aquifer. The water table occurs at approximately 15 m below the surface within a sand layer (Dyck *et al.*, 2003). The site has been under a crop-fallow rotation dominated by wheat (*Triticum aestivum* L.) with some barley (*Hordeum vulgare* L.) since 1966.

Before the infiltration measurements commenced, the straw residue was removed from the surface. Any vegetation present was carefully trimmed to the soil surface using a pair of scissors and then removed. A thin layer (5 mm or less) of testing sand was added to the soil surface to ensure a level base and good contact between the infiltrometer disk and the field soil. The testing sand is reported to have an air-entry value slightly higher

than -3 kPa water pressure and saturated hydraulic conductivity of $5.3 \times 10^{-5} \text{ m s}^{-1}$. The nylon mesh attached to the tension infiltrometer disc had an air-entry value of about -3 kPa water pressure. Infiltration measurements were carried out using a tension infiltrometer with a 0.2 m in diameter disc (Soil Moisture Measurement Systems, Tuscon, AZ). The tension infiltrometer, preset at -2.2 kPa pressure (corresponding equivalent pore diameter $1.36 \times 10^{-4} \text{ m}$), was gently placed on the sand and the amount of water infiltrating into soil, measured by the water level drop in the graduated reservoir tower, was recorded as a function of time. When the amount of water entered into the soil did not change with time for three consecutive measurements taken at 5-minute intervals, steady-state flow was assumed and steady-state infiltration was calculated based on the last three measurements. The water pressures were then set sequentially to -1.7, -1.3, -1.0, -0.6, and -0.3 kPa (corresponding to 1.76×10^{-4} , 2.3×10^{-4} , 3×10^{-4} , 5×10^{-4} and $1 \times 10^{-3} \text{ m}$ equivalent pore diameter) and the corresponding steady state infiltration rates were obtained. Generally, steady state was achieved within 20- to 30-minutes.

Immediately adjacent to the tension infiltrometer, a double-ring infiltrometer with inner and outer rings of 0.2 and 0.3 m in diameter, respectively, was used to determine steady infiltration rate at a constant head of $3.5 \times 10^{-2} \text{ m}$ (Reynolds *et al.*, 2002).

From Eq. [4.16], it is clear that the value of 0 kPa water pressure can not be related to a pore size and hence upper limit for the integral in Eq. [4.18] can not be defined. However, a small pressure can be related to a pore size. We assumed that the maximum pore diameter at the site is $5 \times 10^{-3} \text{ m}$. This is a reasonable assumption as no pores greater than $5 \times 10^{-3} \text{ m}$ in diameter exists at the infiltration measurement location. The water pressure corresponding to $5 \times 10^{-3} \text{ m}$ in diameter is -0.06 kPa. Combining the

measurements of tension infiltrometer and double-ring infiltrometer, a plot of steady infiltration rates (geometric means) at +0.35, -0.3, -0.6, -1.0, -1.3, -1.7, and -2.2 kPa pressures was created, and the infiltration rate at -0.06 kPa was estimated using a spline interpolation. Dunn and Phillips (1991a) also used similar procedure for the estimation of macroporosity in no-till and conventional tillage plots.

The 3-dimensional steady infiltration rates obtained at the above mentioned water pressures were used to obtain unsaturated hydraulic conductivity using the method proposed by Logsdon and Jaynes (1993). Their method is based on the Wooding's (1968) approximated solution for unconfined steady infiltration rate, $q_{\infty}(h)$ from a shallow circular water source and the Gardner's (1958) exponential hydraulic conductivity function as shown below,

$$q_{\infty}(h) = \left(1 + \frac{4}{\alpha\pi r_d}\right) K_s \exp(\alpha h) \quad [4.41]$$

where r_d is the radius (m) of the disc of tension infiltrometer. Following the Logsdon and Jaynes (1993) method, nonlinear regression of infiltration rates against water pressures was conducted to obtain the fitting parameter α . The fitted α value and measured $q_{\infty}(h)$ were then used to calculate $K(h)$ at each applied water pressure. We did not use the estimated α and K_s values to estimate $K(h)$ values based on Gardner (1958) exponential function of hydraulic conductivity, because the function may not best fit the measured data.

Once the hydraulic conductivity at different water pressures was known, Eqs. [4.8], [4.10], [4.21], [4.24], [4.26], and [4.32] were used for the estimation of water-

conducting macroporosity in -0.06 to -0.3, and mesoporosity in -0.3 to -0.6, -0.6 to -1.0, -1.0 to -1.3, -1.3 to -1.7, and -1.7 to -2.2, and total water-conducting macro- and mesoporosity in -0.06 to -2.2 kPa pressure ranges. The water-conducting porosity for the above pressure ranges were also estimated numerically for the four models based on Eq. [4.18], and following the WL and DP procedures. The mean differences of water-conducting porosity values obtained from WL, DP and new procedure for the four models were then compared using SAS PROC UNIVARIATE procedure (Delwiche and Slaughter, 1998).

The $K(h)$ function obtained from field measured steady state infiltration rate-water pressure data fitted very closely to the four models ($R^2 > 0.97$) over the range of water pressures studied (Figure 4.1). However, the Brooks and Corey (1966) model underestimated $K(h)$ at h between -0.06 to -1 kPa and overestimated from -1 to -2.2 kPa pressure. The fitted α values for the Gardner exponential (1958) and rational (1965) power models were within the range of typical values described by Elrick and Reynolds (1992) for different textural classes (Table 4.1). For the van Genuchten-Mualem (1980) model the curve fitting parameters were within the range of typical values of K_s , α and n described by Rawls and Brakensiek (1989) for silt loam soil. The estimated parameter β for the Brooks and Corey (1966) model, however, falls well below the theoretical minimum value reported by Brooks and Corey (1966). This is probably linked to the assumption that we made during curve fitting: the maximum continuous pore diameter at the site is 5×10^{-3} m. The water pressure corresponding to the pore size of 5×10^{-3} m in diameter is -0.06 kPa. In addition, presence of a wide range of pore sizes as indicated by the extremely low value of β and absence of discontinuity in the

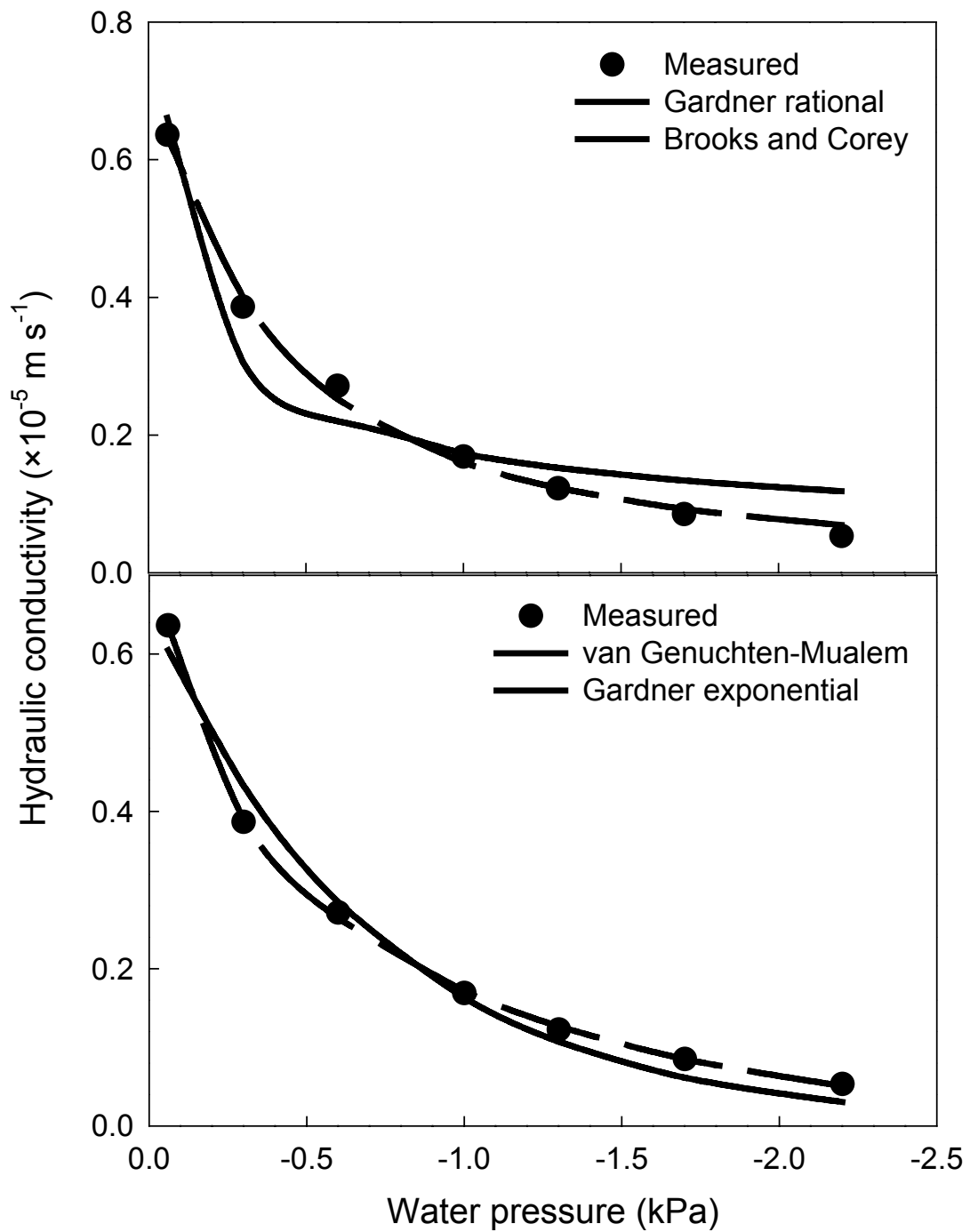


Figure 4. 1 Measured and fitted unsaturated hydraulic conductivity, $K(h)$ of the surface soil for the models used.

Table 4. 1 Estimated parameters (field-saturated hydraulic conductivity K_s , and the empirical curve fitting parameters) for the investigated soil.

Model	Parameter			
	K_s	α	n	β
	$\times 10^{-5} \text{ m s}^{-1}$	m^{-1}		
Gardner exponential	0.66	14	-	-
Gardner rational	0.69	26	-	1.26
Brooks and Corey	0.66	-	-	0.48
van Genuchten-Mualem	1.1	2	1.33	-

distribution of pore sizes may also be the reasons for the small β value (Brooks and Corey, 1966).

The analytical expressions were compared with the numerical solutions obtained using MathCad 2000. The water-conducting macro- and mesoporosity values obtained from the analytical solutions (Eqs. [4.21], [4.24], [4.26], and [4.32]) were exactly the same as the numerical solutions of Eq. [4.18] (data not shown). Therefore, one could use either analytical or numerical solution of the models for the estimation of water-conducting porosity. In the following, only the results from analytical solution will be presented and compared with that of WL and DP.

Soil water-conducting porosity was calculated at each water pressure interval (i.e. -0.06 to -0.3, -0.3 to -0.6, -0.6 to -1.0, -1.0 to -1.3, -1.3 to -1.7, -1.7 to -2.2 kPa) (Table 4.2). We compared WL and DP approaches to the new procedure. For all four hydraulic functions, the mean differences between the new approach and either WL or DP approaches were significantly different from zero at a 95% confidence level. The highest water-conducting porosity values for the small pressure ranges were given by WL approach followed by the DP and the new procedure. As well the sum of water-conducting porosity in the pressure range of -0.06 to -2.2 kPa follows the same trend.

This is not unexpected because Poiseuille's law states that soil water flux is proportional to the fourth power of pore radius. One large pore will conduct more water than a number of small pores with the same sum of cross-sectional area, because of the

Table 4. 2 Estimated water-conducting porosity in each water pressure range for the models used

Pressure Range	Method	Model			
		Gardner exponential	Gardner rational	Brooks and Corey	van Genuchten -Mualem
		Porosity			
kPa		$\times 10^{-5} \text{ m}^3 \text{ m}^{-3}$			
-0.06 to -0.3	WL†	0.56	0.75	1.16	0.78
	DP‡	0.48	0.64	0.99	0.67
	New§	0.22	0.28	0.29	0.25
-0.3 to -0.6	WL	1.93	1.95	1.13	1.54
	DP	1.31	1.33	0.77	1.05
	New	1.07	1.05	0.59	0.83
-0.6 to -1.0	WL	4.42	3.37	1.74	3.06
	DP	3.15	2.40	1.24	2.18
	New	2.76	2.07	1.07	1.91
-1.0 to -1.3	WL	3.50	2.34	1.28	2.50
	DP	2.81	1.88	1.03	2.01
	New	2.70	1.80	0.98	1.93
-1.3 to -1.7	WL	4.86	3.25	1.93	3.90
	DP	3.90	2.61	1.55	3.13
	New	3.72	2.49	1.49	3.00
-1.7 to -2.2	WL	5.43	4.05	2.70	5.39
	DP	4.40	3.28	2.19	4.36
	New	4.18	3.14	2.11	4.20
Sum¶	WL	20.7	15.7	9.95	17.20
	DP	16.0	12.1	7.76	13.40
	New	14.7	10.8	6.52	12.10
-0.06 to -2.2	WL	101	99.0	95.7	96.5
	DP	434	426	412	415
	New	14.7	10.8	6.52	12.1

† Watson and Luxmoore (1986)

‡ Dunn and Phillips (1991)

§ Method developed by the authors.

¶ The sum of porosity calculated by adding together the porosity from the water pressure ranges -0.06 to -0.3, -0.3 to -0.6, -0.6 to -1.0, -1.0 to -1.3, -1.3 to -1.7, and -1.7 to -2.2 kPa.

power dependence of flux on pore radius. By assuming smaller pore sizes in calculating porosity from a fixed soil water flux, one will end up with larger pore cross-sectional area, and thus with larger porosity than reality. In addition, hydraulic conductivity as a function of pore radius or water pressure is concave and linear approximation results in higher hydraulic conductivity, and thus more pores than reality.

Water-conducting macroporosity values given by the WL and DP procedures were more than twice those given by the new procedure (Table 4.2). This would suggest that both WL and DP approaches are unable to represent the initial rapid decrease in near-saturated hydraulic conductivity resulting from macropore drainage when water pressure decreases from -0.06 to -0.3 kPa. For large pressure ranges (i.e. -0.06 to -2.2 kPa), both the WL and DP approaches resulted in exceedingly greater soil water-conducting porosity than the new procedure. Therefore, the DP and the WL approaches are not reliable in estimating macro- and mesoporosity for large water pressure ranges as well as practically small pressure ranges. In addition, tension infiltrometer measurements are usually taken at one or two water pressures with larger pressure intervals. Linearity between soil hydraulic conductivity and pore radius can not be guaranteed. Therefore, we recommend first to estimate soil hydraulic parameters and then to calculate soil water-conducting porosity using the new method.

For different hydraulic conductivity functions (i.e. Brooks and Corey's equation, Gardner's exponential and rational equations and van Genuchten-Mualem's equation), the water-conducting macroporosity for the pressure range between -0.06 and -0.3 kPa was nearly the same (Table 4.2). For the other pressure ranges, different models gave different water-conducting porosity values for the same set of field data. The Brooks

and Corey's (1966) equation under-estimated soil hydraulic conductivity at high water pressures (or large pore sizes) and over-estimated hydraulic conductivity at low pressures (or small pore sizes), leading to smaller porosity of large pore sizes (Figure 4.1). Conversely, the extensively used Gardner's (1958) single exponential equation under-estimated the initial decrease in hydraulic conductivity resulting from mesopore drainage when the water pressure decreases from -0.3 to -1 kPa. Similar observations have been made by Wilson and Luxmoore (1988), Ankeny *et al.* (1991) and Jarvis and Messing (1995). Consequently, the Gardner's (1958) single exponential function yielded the largest functional mesoporosity for the range of pressures over which data were collected. In contrast, both the Gardner rational (1965) and van Genuchten-Mualem (1980) models, which utilize an additional parameter compared to that of the Gardner (1958) exponential and Brooks and Corey (1966) model, fit the measured data very well resulting in nearly the same water-conducting porosity of surface soils over the entire range of water pressures studied.

Under the assumption of unit gradient and one dimensional flow, the infiltration rate can be used in Eq. [4.18] and consequently, in Eqs. [4.21], [4.24], [4.26], and [4.32] should Eqs. [4.19], [4.22], [4.25] and [4.31] be used to fit the infiltration rate as a function of soil water pressure. As a matter of fact, most of applications of tension infiltrometers in calculating water-conducting porosity in the literature used infiltration rate, rather than hydraulic conductivity.

The principal limitations of the proposed new approach are those associated with the simplifying assumptions of the analysis. Water-conducting porosity calculations assume macro- and mesopores to follow Poiseuille's law (laminar flow) and soil is viewed as a

bundle of smooth, cylindrical capillary tubes (capillary theory). Water flow in large macropores may not be laminar. The capillary equation does not apply to large macropores because they are not capillaries. The above mentioned assumptions, therefore, are not strictly valid, especially when the large macropores such as shrink-swell cracks are present. However, considering spatial and temporal variability, the calculations for field measurements are still satisfactory, especially for relative measurements.

Another limitation of the proposed method for calculation of soil water-conducting porosity is that a parametric model of $K(h)$ is required. However, most of the inverse procedures for estimation of soil hydraulic conductivity give hydraulic parameters for a certain hydraulic functions, not the actual measurement of hydraulic conductivity. Using the proposed new method, one can considerably reduce the number of hydraulic conductivity measurements for accurate estimation of water-conducting macro- and mesoporosity.

In this paper, comparison of new method with WL and DP approaches is based on one soil textural class (silt loam), and thus the demonstration is a preliminary assessment. Results from more experiments with soils having widely varying soil texture and macropores characteristics would be beneficial to refine, if necessary, the analytical solutions proposed. Moreover, the new analytical solutions could be further improved by incorporating two-domain approach, which considers water-conducting macro- and mesoporosity as made up of laminar and turbulent domains.

4.5 Conclusions

We derived a general equation for water-conducting porosity based on tension infiltrometer measurements. Further, for soils with their unsaturated hydraulic conductivity characterized by the Gardner's (1958) exponential, Brooks and Corey (1966), Gardner rational (1965), or van Genuchten-Mualem (1980) models, we obtained analytical solutions for the water-conducting macro- and mesoporosity in terms of relationships among the capillary water pressure and the parameters defining the hydraulic conductivity-water pressure relationships. In our derivation, no additional assumptions were made besides the well known capillary equation and Poiseuille's law. Field experiments demonstrated that our method could adequately and efficiently characterize the water-conducting porosity of surface soils *in situ*, regardless of the size of pressure ranges used in the calculation.

4.6 Appendix

A1: Gardner rational (1965) power model

We can rewrite Eq. [4.18] as follows:

$$\varepsilon(a, b) = \frac{2 \mu \rho g}{\gamma} (A - B) \quad [4.A1]$$

where

$$A = h^2 K(h) \Big|_{H(a)}^{H(b)} \quad [4.A2]$$

$$B = 2 \int_{H(a)}^{H(b)} h K(h) dh \quad [4.A3]$$

Substituting Eq. [4.16] and Eq. [4.25] into Eq. [4.A2], we get

$$A = K_s \left(\left(\frac{2\gamma}{\rho g b} \right)^2 \frac{1}{1 + \left(\frac{2\gamma \alpha_{GP}}{\rho g b} \right)^{\beta_{GP}}} - \left(\frac{2\gamma}{\rho g a} \right)^2 \frac{1}{1 + \left(\frac{2\gamma \alpha_{GP}}{\rho g a} \right)^{\beta_{GP}}} \right) \quad [4.A4]$$

Substitution of Eq. [4.25] into Eq. [4.A3] yields

$$B = 2 \int_{H(a)}^{H(b)} h \frac{K_s}{1 + (\alpha_{GP} h)^{\beta_{GP}}} dh \quad [4.A5]$$

Introducing a new variable, $V(r) = (\alpha_{GP} h(r))^{\beta_{GP}}$ we can rewrite the Eq. [4.A5] as

$$\begin{aligned} B &= \frac{2 K_s}{\alpha_{GP}^2 \beta_{GP}} \int_{V(a)}^{V(b)} \frac{V^{\frac{2}{\beta_{GP}} - 1}}{1 + V} dV \\ &= \frac{2 K_s}{\alpha_{GP}^2 \beta_{GP}} \left(\int_0^{v(b)} \frac{v^{\frac{2}{\beta_{GP}} - 1}}{1 + v} dv - \int_0^{v(a)} \frac{v^{\frac{2}{\beta_{GP}} - 1}}{1 + v} dv \right) \end{aligned} \quad [4.A6]$$

Following Gradshteyn and Ryzhik (2000, Eq. 3.194, p. 313), Eq. [4.A6] is integrated to give

$$B = \frac{2 K_s}{\alpha_{GP}^2 \beta_{GP}} \left(\frac{V(b)^{\frac{2}{\beta_{GP}}}}{\frac{2}{\beta_{GP}}} {}_2F_1 \left(1, \frac{2}{\beta_{GP}}; 1 + \frac{2}{\beta_{GP}}; -V(b) \right) - \frac{V(a)^{\frac{2}{\beta_{GP}}}}{\frac{2}{\beta_{GP}}} {}_2F_1 \left(1, \frac{2}{\beta_{GP}}; 1 + \frac{2}{\beta_{GP}}; -V(a) \right) \right) \quad [4.A7]$$

where ${}_2F_1$ is a hypergeometric function. Transformation of Eq. [4.A7] leads to (Oberhettinger, 1972, Eq. 15.3.4, p. 559)

$$B = \frac{2 K_s}{\alpha_{GP}^2 \beta_{GP}} \left(\frac{V(b)^{\frac{2}{\beta_{GP}}}}{\frac{2}{\beta_{GP}}} (V(b)+1)^{-1} {}_2F_1 \left(1, 1; 1 + \frac{2}{\beta_{GP}}; \frac{V(b)}{V(b)+1} \right) - \frac{V(a)^{\frac{2}{\beta_{GP}}}}{\frac{2}{\beta_{GP}}} (V(a)+1)^{-1} {}_2F_1 \left(1, 1; 1 + \frac{2}{\beta_{GP}}; \frac{V(a)}{V(a)+1} \right) \right) \quad [4.A8]$$

The function [4.A8] may be expressed in a series form

$$B = \frac{K_S}{\alpha_{GP}^2} \left(V(b)^{\frac{2}{\beta_{GP}}} (V(b)+1)^{-1} \sum_{j=0}^{\infty} f\left(j, 1, 1; 1 + \frac{2}{\beta_{GP}}; \frac{V(b)}{V(b)+1}\right) - V(a)^{\frac{2}{\beta_{GP}}} (V(a)+1)^{-1} \sum_{j=0}^{\infty} f\left(j, 1, 1; 1 + \frac{2}{\beta_{GP}}; \frac{V(a)}{V(a)+1}\right) \right) \quad [4.A9]$$

where the terms in the series can be calculated in the following recursive way (Seaborn, 1991):

$$f(j, c, d, e, z) = \begin{cases} 1 & j=0 \\ \left(\frac{(j+c-1)(j+d-1)}{j(j+e-1)} d f(j-1, c, d, e, z) \right) & \text{otherwise} \end{cases} \quad [4.A10]$$

A2: van Genuchten-Mualem (1980) Model

We can rewrite Eq. [4.18] as

$$\varepsilon(a, b) = \frac{2\mu\rho g}{\gamma^2} (C - D) \quad [4.A11]$$

where

$$C = h^2 K(h) \Big|_{H(a)}^{H(b)} \quad [4.A12]$$

$$D = 2 \int_{H(a)}^{H(b)} h K(h) dh \quad [4.A13]$$

substituting Eq. [4.16] and Eq. [4.31] into Eq. [4.A12], and substituting the limit we get

$$C = K_S \left(\left(\frac{2\gamma}{\rho g b} \right)^2 \frac{\left(1 - \left(\frac{2\gamma\alpha_{VG}}{\rho g b} \right)^m \left(1 + \frac{2\gamma\alpha_{VG}}{\rho g b} \right)^{-m} \right)^2}{1 + \left(\frac{2\gamma\alpha_{VG}}{\rho g b} \right)^{0.5m}} - \left(\frac{2\gamma}{\rho g a} \right)^2 \frac{\left(1 - \left(\frac{2\gamma\alpha_{VG}}{\rho g a} \right)^m \left(1 + \frac{2\gamma\alpha_{VG}}{\rho g a} \right)^{-m} \right)^2}{1 + \left(\frac{2\gamma\alpha_{VG}}{\rho g a} \right)^{0.5m}} \right) \quad [4.A14]$$

where $m = 1 - \frac{1}{n}$. After introduction of a new variable $w(r) = (\alpha_{VG} h(r))^n$, substitution of Eq.

[4.16] and Eq. [4.31] into Eq. [4.A13] leads to

$$D = \frac{2Ks}{n \alpha_{VG}^2} \int_{w(a)}^{w(b)} \left(\frac{V^{\frac{2}{n}-1}}{(1+V)^{0.5m}} - 2 \frac{V^{\frac{1}{n}}}{(1+V)^{1.5m}} + \frac{V}{(1+V)^{2.5m}} \right) dV \quad [4.A15]$$

where V is a dummy integration variable.

We can rewrite Eq. [4.A15] as

$$D = \frac{2Ks}{n \alpha_{VG}^2} (E - F + G) \quad [4.A16]$$

where

$$\begin{aligned} E &= \int_{w(a)}^{w(b)} \frac{V^{\frac{2}{n}-1}}{(1+V)^{0.5m}} dV \\ &= \int_0^{w(b)} \frac{V^{\frac{2}{n}-1}}{(1+V)^{0.5m}} dV - \int_0^{w(a)} \frac{V^{\frac{2}{n}-1}}{(1+V)^{0.5m}} dV \end{aligned} \quad [4.A17]$$

$$\begin{aligned} F &= \int_{w(a)}^{w(b)} 2 \frac{V^{\frac{1}{n}}}{(1+V)^{1.5m}} dV \\ &= 2 \left(\int_0^{w(b)} \frac{V^{\frac{1}{n}}}{(1+V)^{1.5m}} dV - \int_0^{w(a)} \frac{V^{\frac{1}{n}}}{(1+V)^{1.5m}} dV \right) \end{aligned} \quad [4.A18]$$

$$\begin{aligned} G &= \int_{w(a)}^{w(b)} \frac{V}{(1+V)^{2.5m}} dV \\ &= \int_0^{w(b)} \frac{V}{(1+V)^{2.5m}} dV - \int_0^{w(a)} \frac{V}{(1+V)^{2.5m}} dV \end{aligned} \quad [4.A19]$$

Following Gradshteyn and Ryzhik (2000, Eq. 3.194, p. 313), Eq. [4.A17] is integrated to give

$$E = \frac{w(b)^{\frac{2}{n}}}{\frac{2}{n}} {}_2F_1\left(\frac{m}{2}, \frac{2}{n}; 1 + \frac{2}{n}; -w(b)\right) - \frac{w(a)^{\frac{2}{n}}}{\frac{2}{n}} {}_2F_1\left(\frac{m}{2}, \frac{2}{n}; 1 + \frac{2}{n}; -w(a)\right) \quad [4.A20]$$

Transformation of Eq. [4.A20] leads to (Oberhettinger, 1972, Eq. 15.3.4, p. 559)

$$E = \left(\frac{w(b)^{\frac{2}{n}}}{\frac{2}{n}} (w(b)+1)^{-0.5m} {}_2F_1\left(0.5m, 1; 1 + \frac{2}{n}; \frac{w(b)}{w(b)+1}\right) - \frac{w(a)^{\frac{2}{n}}}{\frac{2}{n}} (w(a)+1)^{-0.5m} {}_2F_1\left(0.5m, 1; 1 + \frac{2}{n}; \frac{w(a)}{w(a)+1}\right) \right) \quad [4.A21]$$

The function [4.A21] may be expressed in a series form

$$E = \left(\frac{w(b)^{\frac{2}{n}}}{\frac{2}{n}} (w(b)+1)^{-0.5m} \sum_{j=0}^{\infty} f\left(j, 0.5m, 1; 1 + \frac{2}{n}; \frac{w(b)}{w(b)+1}\right) - \frac{w(a)^{\frac{2}{n}}}{\frac{2}{n}} (w(a)+1)^{-0.5m} \sum_{j=0}^{\infty} f\left(j, 0.5m, 1; 1 + \frac{2}{n}; \frac{w(a)}{w(a)+1}\right) \right) \quad [4.A22]$$

where the terms in the series can be calculated in the recursive way as shown in Eq. [4.A10].

Following Gradshteyn and Ryzhik (2000, Eq. 3.194, p. 313), Eq. [4.A18] is integrated to give

$$F = 2 \left(\frac{w(b)^{1+\frac{1}{n}}}{1+\frac{1}{n}} {}_2F_1\left(\frac{3m}{2}, 1 + \frac{1}{n}; 2 + \frac{1}{n}; -w(b)\right) - \frac{w(a)^{1+\frac{1}{n}}}{1+\frac{1}{n}} {}_2F_1\left(\frac{3m}{2}, 1 + \frac{1}{n}; 2 + \frac{1}{n}; -w(a)\right) \right) \quad [4.A23]$$

Transformation of Eq. [4.A23] leads to (Oberhettinger, 1972, Eq. 15.3.4, p. 559)

$$F = 2 \left(\frac{w(b)^{1+\frac{1}{n}}}{1+\frac{1}{n}} (w(b)+1)^{-1.5m} {}_2F_1 \left(1.5m, 1; 2 + \frac{1}{n}; \frac{w(b)}{w(b)+1} \right) - \frac{w(a)^{1+\frac{1}{n}}}{1+\frac{1}{n}} (w(a)+1)^{-1.5m} {}_2F_1 \left(1.5m, 1; 2 + \frac{1}{n}; \frac{w(a)}{w(a)+1} \right) \right) \quad [4.A24]$$

The function [4.A24] may be expressed in a series form

$$F = 2 \left(\frac{w(b)^{1+\frac{1}{n}}}{1+\frac{1}{n}} (w(b)+1)^{-1.5m} \sum_{j=0}^{\infty} f \left(j, 1.5m, 1; 2 + \frac{1}{n}; \frac{w(b)}{w(b)+1} \right) - \frac{w(a)^{1+\frac{1}{n}}}{1+\frac{1}{n}} (w(a)+1)^{-1.5m} \sum_{j=0}^{\infty} f \left(j, 1.5m, 1; 2 + \frac{1}{n}; \frac{w(a)}{w(a)+1} \right) \right) \quad [4.A25]$$

where the terms in the series can be calculated in the recursive way as shown in Eq. [4.A10]. Following Gradshteyn and Ryzhik (2000, Eq. 3.194, p. 313), Eq. [4.A19] is integrated to give

$$G = \left(\frac{w(b)^2}{2} {}_2F_1 \left(\frac{5m}{2}, 2; 3; -w(b) \right) - \frac{w(a)^2}{2} {}_2F_1 \left(\frac{5m}{2}, 2; 3; -w(a) \right) \right) \quad [4.A26]$$

Transformation of Eq. [4.A26] results (Oberhettinger, 1972, Eq. 15.3.4, p. 559)

$$G = \left(\frac{w(b)^2}{2} (w(b)+1)^{-2.5m} {}_2F_1 \left(2.5m, 1; 3; \frac{w(b)}{w(b)+1} \right) - \frac{w(a)^2}{2} (w(a)+1)^{-2.5m} {}_2F_1 \left(2.5m, 1; 3; \frac{w(a)}{w(a)+1} \right) \right) \quad [4.A27]$$

The function [4.A27] may be expressed in a series form

$$G = \left(\frac{w(b)^2}{2} (w(b)+1)^{-2.5m} \sum_{j=0}^{\infty} f \left(j, 2.5m, 1; 3; \frac{w(b)}{w(b)+1} \right) - \frac{w(a)^2}{2} (w(a)+1)^{-2.5m} \sum_{j=0}^{\infty} f \left(j, 2.5m, 1; 3; \frac{w(a)}{w(a)+1} \right) \right) \quad [4.A28]$$

where the terms in the series can be calculated in the recursive way as shown in Eq. [4.A10].

4.8 References

- Anderson, S.H., R.L. Peyton, and C.J. Gantzer. 1990. Evaluation of constructed and natural soil macropores using X-ray computed tomography. *Geoderma*. 46:13-29.
- Ankeny, M.D., M. Ahmed, T.C. Kaspar, and R. Horton. 1991. Simple field method for determining unsaturated hydraulic conductivity. *Soil Sci. Soc. Am. J.* 55:467-470.
- Ankeny, M.D., T.C. Kaspar, and R. Horton. 1990. Characterization of tillage and traffic effects on unconfined infiltration measurements. *Soil Sci. Soc. Am. J.* 54:837-840.
- Azevedo, A.S., R.S. Kanwar, and R. Horton. 1998. Effect of cultivation on hydraulic properties of an Iowa soil using tension infiltrometers. *Soil Sci.* 163:22-29.
- Bear, J. 1972. *Dynamics of fluids in porous media*. Elsevier Pub. Co. Inc, New York, NY.
- Beven, K. and P. Germann. 1982. Macropores and water flow in soils. *Water Resour. Res.* 18:1311-1325.
- Bouma, J. 1982. Measuring the hydraulic conductivity of soil horizons with continuous macropores. *Soil Sci. Soc. Am. J.* 46:438-441.
- Bouma, J.A., A. Jongerius, and D. Schoonderbeek. 1979. Calculation of saturated hydraulic conductivity of some pedal clay soils using micromorphometric data. *Soil Sci. Soc. Am. J.* 43:261-264.
- Bruckler, B., C. Ball, and P. Renault. 1989. Laboratory estimation of gas diffusion coefficient and effective porosity in soils. *Soil Sci.* 147:1-10.
- Buttle, J.M., and D.J. McDonald. 2000. Soil macroporosity and infiltration characteristics of a forest podzol. *Hydrol. Process.* 14:831-848.
- Delwiche, L.D., and S.J. Slaughter. 1998. *The little SAS book: A primer*. 2nd ed. Cary, NC: SAS Institute Inc.
- Dunn, G.H., and R.E. Phillips. 1991a. Macroporosity of a well-drained soil under no-till and conventional tillage. *Soil Sci. Soc. Am. J.* 55:817-823.
- Dunn, G.H., and R.E. Phillips. 1991b. Equivalent diameter of simulated macropore systems during saturated flow. *Soil Sci. Soc. Am. J.* 55:1244-1248.
- Flint, L.E., and A.L. Flint. 2002. The soil solution phase. Porosity. p. 241-254. *In* J. H. Dane and G. C. Topp (ed.) *Methods of soil analysis: Part 4. Physical methods*, SSSA, Madison, WI.

- Gardner, W.R. 1958. Some steady-state solutions of unsaturated moisture flow equations with application to evaporation from a water table. *Soil Sci.* 85:228-232.
- Gardner, W.R. 1965. Dynamics of soil-water availability to plants. *Annu. Rev. Plant Physiol.* 16:323-342.
- Ghodrati, M., and W.A. Jury. 1990. A field study using dyes to characterize preferential flow of water. *Soil Sci. Soc. Am. J.* 54:1558-1563.
- Gradshteyn, I.S., and I.M. Ryzhik. 2000. Table of integrals, series, and products. 6th ed. Academic Press, San Diego, CA, USA.
- Jarvis, N.J., and I. Messing. 1995. Near-saturated hydraulic conductivity in soils of contrasting texture measured by tension infiltrometers. *Soil Sci. Soc. Am. J.* 59:27-34.
- Logsdon, S.D., and D.B. Jaynes. 1993. Methodology for determining hydraulic conductivity with tension infiltrometers. *Soil Sci. Soc. Am. J.* 57:1426-1431.
- Luxmoore, R.J. 1981. Micro-, meso- and macroporosity of soil. *Soil Sci. Soc. Am. J.* 45:671-672.
- Luxmoore, R.J., P.M. Jardine, G.V. Wilson, J.R. Jones, and L.W. Zelazny. 1990. Physical and chemical controls of preferred path flow through a forested hillslope. *Geoderma.* 46:139-154.
- Messing, I., and N.J. Jarvis. 1993. Temporal variation in the hydraulic conductivity of a tilled clay soil as measured by tension infiltrometers. *J. Soil Sci.* 44:11-24.
- Oberhettinger, F. 1972. Hypergeometric functions. p. 556-566. *In* M. Abramowitz and I.A. Stegun (ed.) *Handbook of mathematical functions with formulas, graphs, and mathematical tables.* Dover Publications, Inc., New York.
- Rawls, W.J., and D.L. Brakensiek. 1989. Estimation of soil water retention and hydraulic properties. p. 275-300. *In* H.J. Morel-Seytoux (ed.) *Unsaturated flow in hydrologic modeling-Theory and practices,* NATO ASI Series, Vol. 9. Kluwer Academic Publishing, Dordrecht.
- Reynolds, W.D., D.E. Elrick, and E.G. Youngs. 2002. The soil solution phase. Single-ring and double- or concentric-ring infiltrometers. p. 821-826. *In* J. H. Dane and G. C. Topp (ed.) *Methods of soil analysis: Part 4. Physical methods,* SSSA, Madison, WI.
- Seaborn, J.B. 1991. *Hypergeometric functions and their applications.* Springer-Verlag, New York.

- Skopp, J. 1981. Comment on 'Micro- meso- and macroporosity of soil'. *Soil Sci. Soc. Am. J.* 45:1246.
- Timlin, D.J., L.R. Ahuja, and M.D. Ankney. 1994. Comparison of three field methods to characterize apparent macropore conductivity. *Soil Sci. Soc. Am. J.* 58:278-284.
- van Genuchten, M.Th. 1980. A closed-form equation for predicting the hydraulic conductivity of unsaturated soils. *Soil Sci. Soc. Am. J.* 44:892-898.
- Watson, K.W., and R.J. Luxmoore. 1986. Estimating macroporosity in a forest watershed by use of a tension infiltrometer. *Soil Sci. Soc. Am. J.* 50:578-582.
- Weiler, M., and F. Naef. 2003. An experimental tracer study of the role of macropores in infiltration in grassland soils. *Hydrol. Process.* 17:477-493.
- Wilson, G.V., and R.J. Luxmoore. 1988. Infiltration, macroporosity and mesoporosity distributions on two forested watersheds. *Soil Sci. Soc. Am. J.* 52:329-335.
- Wooding, R.A. 1968. Steady infiltration from a shallow circular pond. *Water Resour. Res.* 4:1259-1273.
- Yeh, Y.J., C.H. Lee, and S.T. Chen. 2000. A tracer method to determine hydraulic conductivity and effective porosity of saturated clays under low gradients. *Ground Water.* 38:522-529.

5. NEAR-SATURATED SURFACE SOIL HYDRAULIC PROPERTIES UNDER DIFFERENT LAND USE IN THE ST. DENIS NATIONAL WILDLIFE AREA, SASKATCHEWAN, CANADA

5.1 Abstract

Surface soil hydraulic properties are key factors controlling the partition of rainfall and snowmelt into runoff and soil water storage, and their knowledge is needed for sound land management. The objective of this study was to evaluate the effects of three land use (native grass, brome grass and cultivated) on surface soil hydraulic properties under near-saturated conditions at the St. Denis National Wildlife Area, Saskatchewan, Canada. For each land use, water infiltration rates were measured using double-ring and tension infiltrometers at -0.3, -0.7, -1.5, and -2.2 kPa water pressures. Macroporosity and unsaturated hydraulic properties of the surface soil were estimated. Mean field-saturated hydraulic conductivity (K_{fs}), unsaturated hydraulic conductivity at -0.3 kPa water pressure, inverse capillary length scale (α), and water-conducting macroporosity were compared for different land use. These parameters of the native grass and brome grass sites were significantly ($p < 0.1$) higher than that of the cultivated sites. At the -0.3 kPa water pressure, hydraulic conductivity of grasslands was two to three times greater than that of the cultivated lands. Values of α were about two times and values of K_{fs} about four times greater in grasslands than in cultivated fields. Water-conducting macroporosity of grasslands and cultivated fields were 0.04% and 0.01% of the total soil volume, respectively. Over 40% and 50% of the total water flux at -0.06 kPa water

pressure was transmitted through macropores (pores $> 1 \times 10^{-3}$ m in diameter) of the cultivated land and the grasslands, respectively. Land use modified near-saturated hydraulic properties of surface soil and consequently may alter the water balance of the area by changing the amount of surface runoff and soil water storage.

5.2 Introduction

Soil hydraulic properties include unsaturated hydraulic conductivity as a function of water content or matrix potential and soil water content as a function of matrix potential. These properties are important for understanding water balance, irrigation, and transport processes (Hillel, 1998). Hydraulic properties of surface soils also influence the partition of rainfall and snowmelt into runoff and soil water storage, and their knowledge is essential for efficient soil and water management.

Numerous studies have been conducted on soil hydraulic properties in relation to cultural practices such as tillage. Depending on cultivation history, climate zone, and the soil management, saturated and unsaturated hydraulic conductivity under no-till or minimum tillage can be either greater (Benjamin, 1993), or lower (Lindstrom and Onstad, 1984; Heard *et al.*, 1988; Miller *et al.*, 1998) than that under continuously tilled treatments, or not significantly different from that under continuously tilled treatments (Belvins *et al.*, 1983; Obi and Nnabude, 1988).

A few studies have been concentrated on macroporosity and hydraulic properties of forest soils and pasture lands. Watson and Luxmoore (1986) and Wilson and Luxmoore (1988) quantified water flow in forested watersheds with the use of a tension infiltrometer and a double-ring infiltrometer. Watson and Luxmoore (1986) observed that 73% of the ponded flux was conducted through macropores with diameter $> 1 \times 10^{-3}$

m while Wilson and Luxmoore (1988) found 85% of the ponded flux moved through macropores. Change in land use from natural forest to crop cultivation modified the hydraulic properties of the surface soil resulting in an increased runoff/infiltration ratio (Leduc *et al.*, 2001). Generally, permanent pasture plots had higher infiltration rates and saturated and unsaturated hydraulic conductivity than conventionally cultivated plots (Chan and Mead, 1989; McQueen and Shepherd, 2002; Sonneveld *et al.*, 2003). Hydraulic properties are highly correlated with structural stability and macroporosity. More stable soil structure and increased biological activity may be the reasons for improved hydraulic properties in forests, permanent pasture lands and no-till or minimum tillage systems.

Soil management or land use affects soil hydraulic properties, and thus the water balance and hydrology of the land. Several studies have been conducted on the hydrology of prairie sloughs (wetlands) (Meyboom, 1966; Winter, 1989; Woo and Rowsell, 1993; Hayashi *et al.*, 1998). Nevertheless, only a few investigations have concentrated on the effect of land use on soil water content and hydrology in the prairie soils. Studies carried out by Euliss and Mushet (1996) revealed that surface runoff due to precipitation is larger from cultivated catchments than that from grasslands. Christie *et al.* (1985) reported that the soils under cultivated lands have higher soil moisture content than that of undisturbed native grass lands. De Jong and Kachanoski (1987) documented that over-winter soil water recharge is about 0.05 to 0.1 m under tall stubble, buck-brush and native grass whereas it is virtually zero for fallow land. These findings suggest that infiltration of summer precipitation and snowmelt is likely to be greater and runoff is smaller in undisturbed grasslands than that in cultivated fields.

Van der Kamp *et al.* (1999) studied water levels of wetlands in St. Denis National Wildlife Area (SDNWA), Saskatchewan, Canada and concluded that conversion of croplands into permanent brome grass resulted in drying out of wetlands within the grassland area. Van der Kamp *et al.* (2003) showed that water level in the wetlands decreased drastically in the mid 1980s since the cultivated lands converted to permanent brome grasslands. They also studied the infiltration rate of soils using single-ring infiltrometers under ponded condition during summer and winter and concluded that infiltrability beneath brome grass was much higher than that of land under cultivation. They attribute the drying out of wetlands in the SDNWA to the better snow trapping and well-developed macropore network in brome grasslands. However, no measurement is available on macropore network (van der Kamp *et al.*, 2003).

Some of the pores in soils may be dead-ended and others may be continuous. The continuous macropores will contribute to fast water flow and we call these pores water-conducting (macro) pores and the ratio of the volume of these pores to the total soil volume the water-conducting (macro) porosity. Examination of water-conducting macropores allows characterization of pore connectivity and tortuosity and provides insight into effects of soil management on hydrological processes. Despite of its importance, there is a lack of systematic account of water-conducting macroporosity in different land use, particularly in the Canadian prairies, which has numerous wetlands. Further, previous studies on hydraulic properties under different land use were mainly focused on saturated hydraulic properties. However, soils in cold and semi-arid climate in the northern plains of North America remain mostly under unsaturated conditions. Effects of land use on unsaturated hydraulic properties, particularly in the near-saturated

region, have not been documented in the Canadian prairies to the best of our knowledge. This information is needed for improving our understanding of the effects of soil management/land use on runoff and infiltration, and thus on wetland hydrology. Therefore, the objectives of this study were to characterize and to compare the surface hydraulic properties of near-saturated soils and water-conducting porosity under native grassland, brome grassland and cultivated land, using *in situ*/laboratory measurements. *In situ* hydraulic property measurements are better-suited to represent the near-saturated flow and transport scenarios in the field than the unsaturated hydraulic properties derived from detached cores in the laboratory. The latter may destroy macropores, particularly for small cores.

5.3 Materials and Methods

5.3.1 Study site

This study was carried out during the summer 2002 at the St. Denis National Wildlife Area in Central Saskatchewan, Canada (106° 06' W, 52° 02' N; 545- to 560-m above sea level). Detailed description of the site is provided by Miller (1983), and van der Kamp *et al.* (2003). Briefly, the Saskatoon Airport, situated about 50 km west of the site, receives annual precipitation of 360 mm (20 year average), of which 84 mm occurs in winter mainly as snow. The annual mean air temperature is 2° C, with monthly means of -19° C in January and 18° C in July. The annual evaporation from large lakes in this area is 690- to 710-mm (van der Kamp *et al.*, 2003), based on data from Last Mountain Lake located 100 km southeast of the study site. The topography of the area is described as moderately rolling knob-and-kettle moraine with slopes varying from 10 to 15%. The soil of the area is dominantly Orthic Dark Brown Chernozems (fine-loamy, mixed,

frigid, Typic Haplustolls; Soil Survey Staff, 1999) developed from moderately to fine textured unsorted glacial till (Miller, 1983; van der Kamp *et al.*, 1999, 2003).

Three main land use exist at this site: native grasslands, brome grasslands (*Bromus inermis*) and cultivated lands. The dominant native grasses were spear grass (*Stipa spartea*), wheat grass (*Agropyron dasystachyum*) and fescue (*Festuca scabrella*) (Miller, 1983). The native grassland had never been disturbed and cultivated site has been in dry-land cultivation of wheat and canola in rotation with fallow since the 1950's. Between 1980 and 1983, a portion of the cultivated land was converted to a permanent cover of brome grass with the intention of providing improved nesting cover for waterfowl. This cover of brome grass has not been disturbed by grazing, mowing or burning.

5.3.2 Treatments and experimental design

Three land use, native grassland, brome grassland and land under crop cultivation, were chosen as treatments in a mensurative experimental design (Pennock, 2003). There were three replications. For each replicate, adjacent sites of the three land use with similar topography were selected for measurements of soil physical and hydraulic properties. All measurements were made between September and November, 2002. During the study period, the cultivated site was under canola cultivation and the measurements were carried out just after harvesting the crop

5.3.3 Measurements of bulk density, total porosity, organic carbon, and texture

Six undisturbed soil cores (0.05 m in diameter × 0.05 m in height) were taken from the surface soil (0- to 0.05-m) for each block and treatment (54 cores in total). These cores were used for determination of antecedent moisture content and bulk density by oven

drying at 105⁰ C. Total porosity was calculated from soil bulk density and particle density of 2.65 Mg m⁻³ (Danielson and Sutherland, 1986). A subset of composite samples for each plot was used to determine clay, sand, and silt content by hydrometer method (Gee and Bauder, 1986). Organic carbon content of another subset of the composite samples for each plot was determined by dry combustion using a Leco CR-12 carbon analyzer (Wang and Anderson, 1998). In total, there were nine measurements of soil textures and organic carbon content. A summary of the data is listed in Table 5.1.

5.3.4 Measurement of steady-state infiltration rate using double-ring infiltrometer

Six locations per plot were randomly selected for tension and double-ring infiltration measurements in order to account for spatial variability. To prepare for the infiltration measurement, surface litter was removed from an area of about 0.4 m in diameter. Any vegetation present was carefully trimmed to the soil surface using a pair of scissors and then removed. Surface litter removal will not affect infiltration rate because it is the soil properties and bio- and structural pores that control infiltration rate. The double-ring infiltrometer method (constant head) with inner and outer rings of 0.2 and 0.3 m in diameter, respectively, was used to determine steady infiltration rates (Bower, 1986). Steel rings were driven concentrically about 0.05 m deep into the soil with minimum soil disturbance. After the insertion of the rings the contact between the inside surface of the ring and the soil was tamped lightly using the blunt edge of a pencil to minimize the short-circuit flow along the inside wall of the ring. A steel pointer was positioned inside the inner cylinder with 0.03 m height above the soil surface. The inner cylinder was then filled with water equivalent to a 0.04 m water head initially. The time taken to drop the water level in the inner cylinder to the pointer was recorded. Thereafter, a

measured volume of water that is equivalent to 0.01 m in depth in the ring was filled successively and the time taken to infiltrate this amount was recorded. When the amount of water entered into the soil did not change with time for three consecutive measurements taken at 5-minute intervals, steady-state flow was assumed and steady-state infiltration rate was calculated based on the last three measurements. Generally, steady-state was achieved within 30- to 60-min. Water level in the outer ring was maintained at a level about the same as or slightly lower than the water level in the inner ring.

As illustrated by Reynolds *et al.* (2002), the steady-state infiltration rate measured using double-ring infiltrometer with a diameter of 20 cm, water level of 5 cm, and insertion depth of 5 cm, can be two times larger than the field-saturated hydraulic conductivity for a loam soil. Therefore, the field-saturated hydraulic conductivity, K_{fs} (LT^{-1}), was estimated for each location from the steady-state infiltration rates obtained from double-ring infiltrometer following the procedure outlined by Reynolds *et al.* (2002) for the single-head analysis of pressure infiltrometer. In the single-head approach, K_{fs} is given by (Reynolds *et al.*, 2002),

$$K_{fs} = \frac{\alpha G A R_1}{\left(a (\alpha H_1 + 1) + G \alpha \pi a^2 \right)} \quad [5.1]$$

where α (L^{-1}) is a soil texture-structure parameter, A (L^2) is the cross-sectional area of the inner ring of the infiltrometer, R_1 (LT^{-1}) is the quasi-steady infiltration rate, a (L) is the radius of the ring, H_1 (L) is the steady pressure head of water on the infiltration surface, and G is a dimensionless shape factor given by,

$$G = 0.316 \left(\frac{d}{a} \right) + 0.184 \quad [5.2]$$

where d (L) is the depth of ring insertion into the soil. There were six locations in each plot with a total of 54 double-ring infiltrometer measurements. A value of 12 m^{-1} was taken as the appropriate value for the α as it is the most common value for many agricultural soils (Elrick *et al.* 1989, in Reynolds *et al.* 2002). Water pressure head varied from 0.03 to 0.04 m during infiltration measurements. As an approximation, we treat the water level in the inner ring as 0.035 m on average (steady pressure head).

5.3.5 Measurement of infiltration rates using tension infiltrometer

Adjacent to the double-ring infiltrometer measurement, infiltration experiments were carried out using a tension infiltrometer with a 0.2 m diameter disk (Soil Measurement Systems, Tuscon, AZ). The infiltration disc was attached to the water supply reservoir and tension control tube via a flexible tube. Ensuring intimate contact between the soil surface and source of water (infiltrometer membrane) is crucial for the estimation of surface soil hydraulic properties from tension infiltrometer. Therefore, a thin layer (< 5 mm) of fine testing sand was added to the soil surface to ensure a level base and good contact between infiltrometer disk and the field soil. The testing sand is reported to have an air-entry value slightly higher than -3 kPa water pressure and saturated hydraulic conductivity of $5.3 \times 10^{-5} \text{ m s}^{-1}$. The nylon mesh attached to the tension infiltrometer disc had an air-entry value of about -3 to -3.2 kPa pressure. It should be noted that the testing sand layer may have a substantial impact on early-time hydraulic conductivity. However, as indicated by Clothier and Scotter (2002) and Vandervaere *et al.* (2000), the very thin (< 5 mm) layer of sand we added would not affect the steady-state

measurements of infiltration rate, and thus the estimated hydraulic properties of the surface soil.

The minimum water pressure used in our experiment, -2.2 kPa, was chosen because infiltration rate at -2.2 kPa is still large enough to have accurate measurement of infiltration rate and the pressure was also substantially higher than the air-entry values of testing sand and the nylon mesh in the tension infiltrometer disc. The infiltration rates were measured at -0.3, -0.7, -1.5 and -2.2 kPa water pressures. Measurements were performed from low to high pressures, i.e., beginning with the -2.2 kPa pressure. The tension infiltrometer, preset at -2.2 kPa water pressure (corresponding equivalent pore diameter 1.36×10^{-4} m), was gently placed on the sand layer and the amount of water infiltrating into soil, measured by the water level drop in the graduated reservoir tower, was recorded as a function of time. When the amount of water entered into the soil did not change with time for three consecutive measurements taken at 5-minute intervals, steady-state flow was assumed and steady-state infiltration was calculated based on the last three measurements. The water pressures were then set sequentially to -1.5, -0.7 and -0.3 kPa (corresponding to 2×10^{-4} , 4.29×10^{-4} and 1×10^{-3} m equivalent pore diameter, respectively) and the corresponding steady-state infiltration rates were obtained. Generally, steady-state was achieved within 20- to 30-min. Wetting depth was generally around 0.1 m. The experiments were repeated at six locations in each of nine plots.

5.3.6 Calculation of macroporosity

Immediately after the infiltration measurements at -0.3 kPa water pressure a soil core (0.05 m in diameter and 0.05 m in height) was taken from the surface soil layer and volumetric moisture content of the soil was determined by the gravimetric method.

Macroporosity (equivalent pore diameter $> 1 \times 10^{-3}$ m; Luxmoore, 1981) was determined as the difference between total porosity and volumetric moisture content held at the -0.3 kPa pressure. The sum of meso- and microporosity was estimated as volume of water retained at the -0.3 kPa water pressure.

5.3.7 Estimation of unsaturated hydraulic properties from tension infiltrometer measurements

Cumulative infiltration vs. elapsed time was plotted for each water pressure. The slope of the curve at steady-state was calculated and taken as steady-state infiltration rate. For Gardner's (1958) exponential hydraulic conductivity function

$$K(h) = K_{fs} \exp(\alpha h) \quad [5.3]$$

where $K(h)$ is the unsaturated hydraulic conductivity (LT^{-1}) for a given water pressure head, h (L), K_{fs} is the field-saturated hydraulic conductivity (LT^{-1}), and α is the inverse capillary length scale (L^{-1}), Wooding (1968) derived the following approximate solution for steady-state infiltration rate under a shallow circular disc,

$$q_{\infty}(h) = \left(1 + \frac{4}{\alpha \pi r_d}\right) K_{fs} \exp(\alpha h) \quad [5.4]$$

where $q_{\infty}(h)$ is the steady-state infiltration rate (LT^{-1}) corresponding to the applied water pressure h , and r_d is the radius of the disc (L). Equation [5.4] has two unknown parameters, K_{fs} and α . Following Logsdon and Jaynes (1993), these parameters were estimated through non-linear regression of q_{∞} as a function of h using MathCad 2000 (MathSoft, Cambridge).

5.3.8 Determination of water-conducting porosity

The maximum water-filled equivalent pore size at a specific water pressure can be calculated from the capillary rise equation (Bear, 1972)

$$r = \frac{2 \gamma \cos \beta}{\rho g h} \quad [5.5]$$

where r is the radius of the pore (L), γ is the surface tension of water ($M T^{-2}$), β is the contact angle between water and the pore wall, ρ is the density of water ($M L^{-3}$), g is the acceleration due to gravity ($L T^{-2}$), and h is the applied water pressure head (L). Assuming $\beta=0$ and rearranging Eq. [5.5], we get

$$h = \frac{2 \gamma}{\rho g r} \quad [5.6]$$

We assume that the equivalent pores with radii smaller than r calculated from Eq. [5.5] are full of water and are responsible for all the flux of water for a given water pressure, and that the equivalent pores with radii larger than the value calculated from Eq. [5.5] are not contributing to the water flux. According to Poiseuille's law and Eq. [5.5], the flow rate through a single macropore is given by,

$$Q(r) = \frac{\pi \rho g}{8 \mu} r^4 \quad [5.7]$$

where $Q(r)$ is the flow rate ($L^3 T^{-1}$) as a function of pore radius r and μ is the dynamic viscosity of water ($M L^{-1} T^{-1}$). We considered the number of pores per unit area (L^2) as a function of r . The total number of pores in a given pore size range, $n(r)$, is the cumulative pore number distribution and is given by

$$n(r) = \int_0^r P(r) dr \quad [5.8]$$

where $P(r)$ is the number of pores per unit soil surface area per unit pore radius. For unit hydraulic gradient, steady infiltration rate at a water pressure equals the hydraulic conductivity K (LT^{-1}). The hydraulic conductivity at a given pressure h or pore size r , $K(r)$ can be expressed by

$$K(r) = \int_0^r P(r) Q(r) dr \quad [5.9]$$

where r is the upper limit of the integrals determined by the water pressure. The expression for $P(r)$ can be obtained by taking derivatives of both sides of Eq. [5.9]

$$P(r) = \frac{dK(r)}{dr} \frac{1}{Q(r)} \quad [5.10]$$

The water-conducting porosity in given pressure range can be expressed as,

$$\varepsilon(a, b) = \int_a^b \pi r^2 P(r) dr \quad [5.11]$$

Substitution of Eq. [5.10] for $P(r)$ in Eq. [5.11] leads to

$$\varepsilon(a, b) = \int_a^b \frac{dK(r)}{dr} \frac{1}{Q(r)} \pi r^2 dr \quad [5.12]$$

Generally, soil hydraulic conductivity is expressed as a function of soil water content or water pressure. Since Eq. [5.12] involves hydraulic conductivity as a function of pore radius, in the following we revise Eq. [5.12] and express water-conducting porosity in terms of hydraulic conductivity as a function of water pressure, $K(h)$. For convenience, we use the following variable substitution

$$H(r) = \frac{2 \gamma}{\rho g r} \quad [5.13]$$

where $H(r)$ is the water pressure corresponding to the radius r .

Substituting Eq. [5.7] for $Q(r)$ and Eq. [5.13] for r into Eq. [5.12], leads to

$$\varepsilon(a,b) = \frac{2 \mu \rho g}{\gamma^2} \int_{H(a)}^{H(b)} \frac{dK(h)}{dh} h^2 dh \quad [5.14]$$

Integration of Eq. [5.14] by parts leads to

$$\varepsilon(a,b) = \frac{2 \mu \rho g}{\gamma^2} \left(h^2 K(h) \Big|_{H(a)}^{H(b)} - 2 \int_{H(a)}^{H(b)} K(h) h dh \right) \quad [5.15]$$

Substitution of Eq. [5.3] for $K(h)$ in Eq. [5.15] gives

$$\varepsilon(a,b) = \frac{2 \mu \rho g K_{fs}}{\gamma^2} \left(h^2 \exp(-\alpha h) \Big|_{H(a)}^{H(b)} - 2 \int_{H(a)}^{H(b)} h \exp(-\alpha h) dh \right) \quad [5.16]$$

Substituting Eq. [5.13] into Eq. [5.16] and following Gradshteyn and Ryzhik (2000) (Eq. 2.322, p.104), Eq. [5.16] is integrated to give

$$\varepsilon(a,b) = \frac{2 \mu \rho g K_{fs}}{\gamma^2} \left\{ \exp\left(\frac{-2 \gamma \alpha}{\rho g b}\right) \left(\frac{4 \gamma^2}{(\rho g b)^2} + \frac{4 \gamma}{\rho g b \alpha} + \frac{2}{\alpha^2} \right) - \exp\left(\frac{-2 \gamma \alpha}{\rho g a}\right) \left(\frac{4 \gamma^2}{(\rho g a)^2} + \frac{4 \gamma}{\rho g a \alpha} + \frac{2}{\alpha^2} \right) \right\} \quad [5.17]$$

From Eq. [5.13], it is evident that the value of 0 kPa water pressure can not be related to a pore size and hence the upper limit of the integral of Eq. [5.15] can not be defined. However, a small pressure can be related to a pore size. We assumed that the maximum pore diameter at the sites is 5×10^{-3} m. This is a reasonable assumption as no pores greater than 5×10^{-3} m in diameter existed at any of the infiltration measurement locations. Pores of this size and larger would have caused depressions in the infiltrometer sand bed we prepared to establish good contact between the disc and soil

surface, hence reducing contact between the sand and infiltrometer base. However, this was not observed at any infiltration measurement locations. The water pressure corresponding to the pore size of 5×10^{-3} m in diameter is -0.06 kPa. Combining the measurements of tension infiltrometer with double-ring infiltrometer, steady infiltration rates at +0.35, -0.3, -0.7, -1.5, and -2.2 kPa water pressures were plotted for each location, and the infiltration rate at -0.06 kPa pressure was estimated by spline interpolation. Equation [17] (with K_{fs} from double-ring infiltrometer and α from tension infiltrometer) was then used for the estimation of water-conducting porosity in -0.06 to -0.3, -0.3 to -0.7, -0.7 to -1.5, and -1.5 to -2.2 kPa water pressure ranges. The relative infiltration rate was determined as the infiltration rate difference in each water pressure range divided by the infiltration rate at -0.06 kPa pressure.

5.3.9 Statistical analysis

Natural log-transformed K_{fs} , $K(h)$ and α values were used for statistical analysis because their distributions are reported to be log normal (Nielsen *et al*, 1973; Sudicky, 1986). Analysis of variance was done using SAS (SAS Institute, Inc., 1990) with three replications. Treatments were compared by least significant difference (LSD) tests. Two treatment means were considered as significantly different whenever the absolute difference between the corresponding estimated means exceeds the LSD at a 10% significance level.

5.4 Results and Discussion

The soil texture did not show a significant difference among treatments, suggesting all the land use systems were uniform in soil texture (Table 5.1). Soil organic matter content is significantly different between grasslands and cultivated land. This is

expected because biomass removal through harvesting the crop and summer fallow, reduced biomass input to the soil in cultivated lands.

Table 5. 1 Grasslands had smaller bulk density and higher organic carbon content than cultivated land while soil separates contents in the surface 0.05 m of soil were not affected by land use.

Land use	Bulk density Mg m ⁻³	Organic carbon %	Soil separates		
			Clay	Silt	Sand
			%		
Native grassland	0.82 (0.05) ^{b^z}	5.9 (0.5) ^a	34(2.0)	38(4.9)	28 (3.5)
Brome grassland	0.81(0.09) ^b	5.2 (0.7) ^a	34(1.8)	39(1.4)	27(2.3)
Cultivated land	1.11(0.07) ^a	3.6 (0.3) ^b	37(2.1)	34(2.0)	29(3.7)

^zNumber in parentheses is the standard deviation calculated based on 18 observations for bulk density and 3 observations for others.

Means followed by different lower case letters in the same column are significantly different at $P < 0.1$.

The average total porosity (percent of soil volume occupied by pores) of cultivated land is 58%, which was substantially lower than that of native grassland (69%) and brome grassland (70%) (Figure 5.1). Total porosity was not significantly different between grasslands. These porosity values are consistent with the findings of van der Kamp *et al.* (2003) for the three land use and Naeth *et al.* (1990) for grasslands. Land use that had higher organic carbon contents resulted in higher total porosities (Table 5.1). Mean bulk density of cultivated site was significantly higher than that of the grasslands. The low bulk density in grasslands may be attributed to presence of higher amount of organic matter and roots as displayed in the soil cores from the two grasslands. Less organic matter in cultivated land may have reduced aggregate stability and percentage of stable aggregates (Elliott and Efetha, 1999). Consequently the soils become less porous (Mapa and Gunasene, 1995).

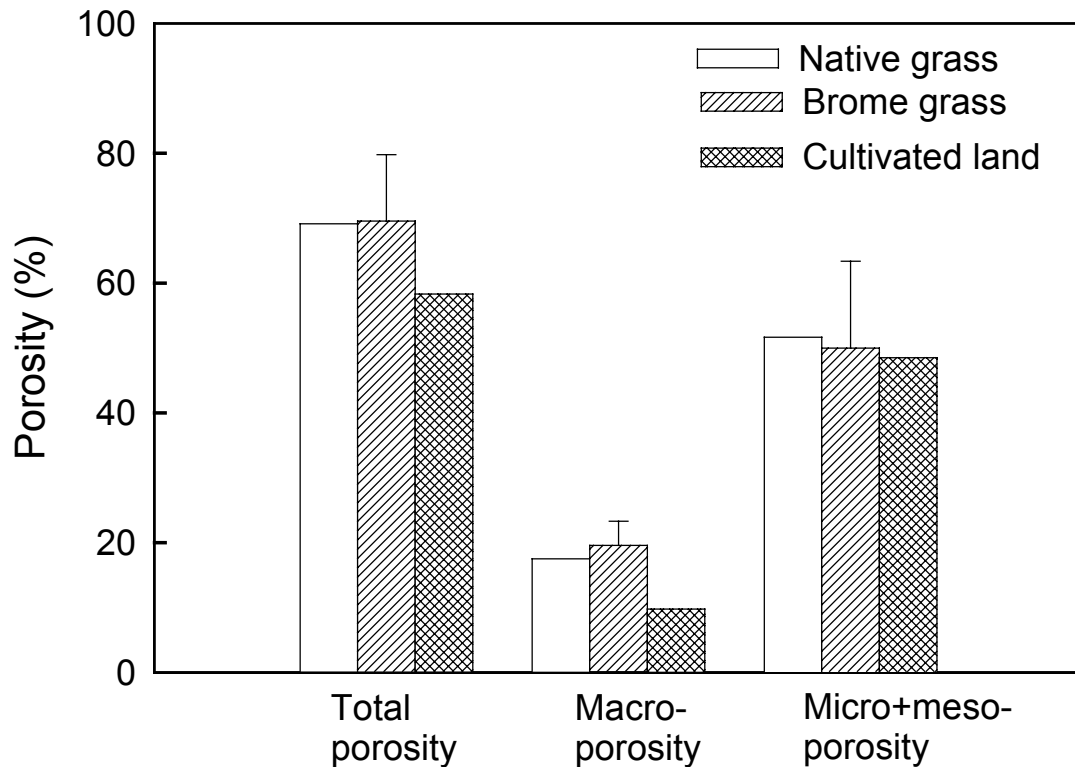


Figure 5. 1 Effect of land use on macro-, meso + micro-, and total porosity (% of soil volume). The vertical bars on the graph represent least significant difference at $p < 0.1$.

There was a significant difference in macroporosity between grasslands and cultivated land. The macroporosity is 10% for cultivated land, 17% for native grassland and 20% for brome grassland (Figure 5.1). Therefore, cultivation has appeared to reduce macroporosity while grasses tend to increase macroporosity. This is expected since grasslands had higher organic matter content and thus higher aggregate stability of soil, resulting in more macropores between aggregates (Mapa and Gunasena, 1995). Higher macro- and total porosities under grassland soils also arise due to the development of biopores such as root channels and animal burrows (Lepilin, 1989). This was reflected in the lower bulk density in grasslands than the cultivated lands (Table 5.1). The sum of

meso- and microporosity was higher than the macroporosity in all land use (Figure 5.1). However, the sum did not show a significant difference among land use suggesting meso- and microporosity is not affected by the land use tested.

The steady-state infiltration rates obtained from tension infiltrometer fitted very closely ($R^2 > 0.99$) to Eq. [5.4] that we employed for the estimation of K_{fs} and α (Figure 5.2). Hydraulic conductivity as a function of applied water pressure, $K(h)$, is shown in Figure 5.3. Decreases in water pressure resulted in decreases in hydraulic conductivity for all land use because decreases in pressure reduce the size and number of pores that participate in conducting water. Hydraulic conductivity decreased nearly by an order of magnitude across a small pressure range near saturation (zero to -2.2 kPa pressure). This finding is supported by Clothier and Smettem (1990) and Jarvis and Messing (1995). Soil hydraulic conductivity under grassland decreased more dramatically with the decrease in water pressure than that under cultivated lands. In other words, the removal of larger pores from the infiltration process had the greatest effect on hydraulic conductivity in grasslands. All the three land use had similar clay, silt and sand content (Table 5.1). Thus, the large differences in hydraulic conductivity between grasslands and cultivated soil suggest that grassland soils have a well-developed macropore structure and connectivity. Cultivation may have destroyed macropores and continuity of the macropore network and/or prevented from the formation of larger pores in the tilled layer that would conduct water at higher water pressures as reported by Maulé and Reed (1993). The $K(h)$ differed among land use treatments and the difference became larger as the soils approached saturation (Figure 5.3). The $K(h)$ among land use was not significantly different at -2.2, -1.5, and -0.7 kPa water pressures. At the -0.3 kPa

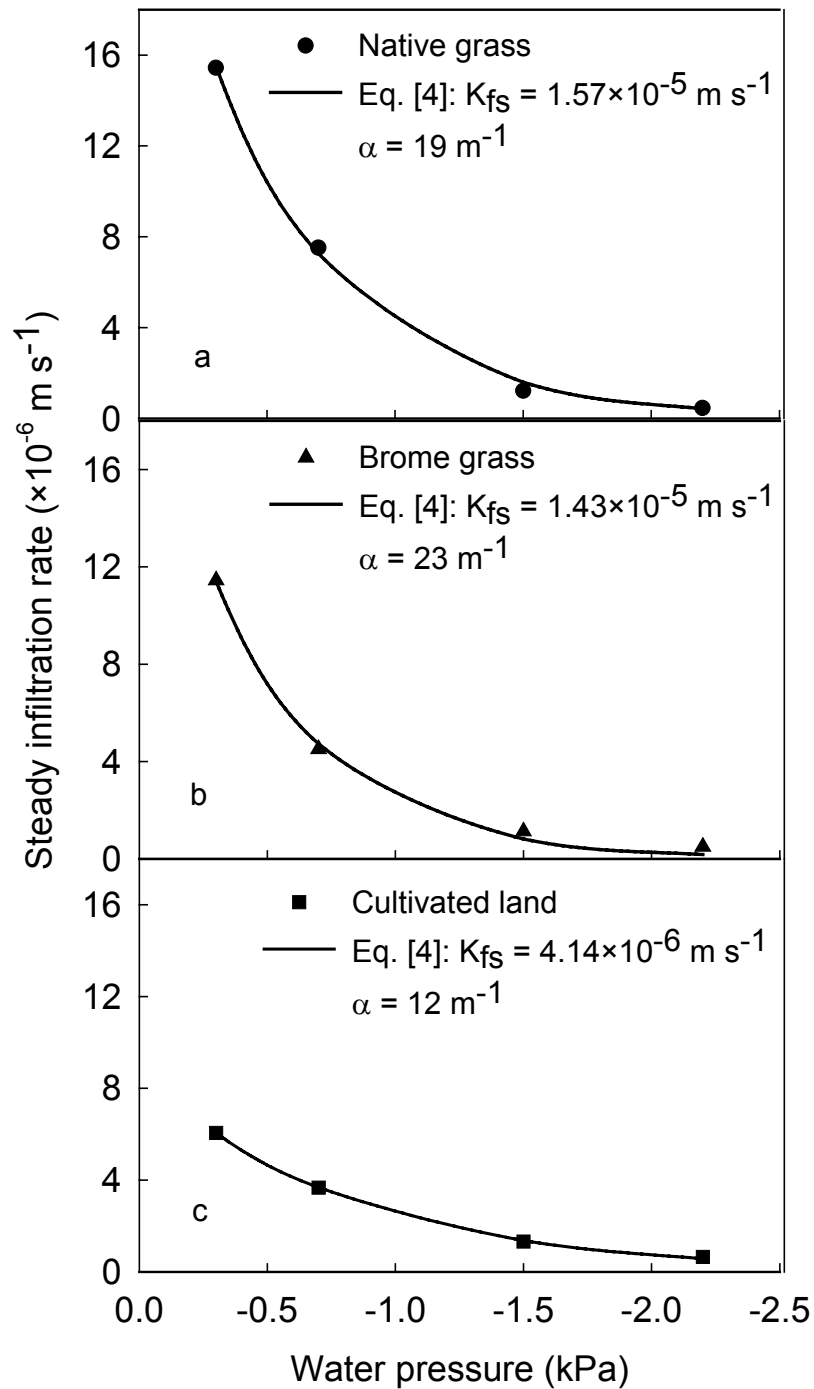


Figure 5. 2 Measured and fitted steady-state infiltration rates (mean) at different water pressures for the Wooding's (1968) function (Eq. [5.4]); a) Native grassland, b) Brome grassland, and c) Cultivated field.

pressure, there was no significant difference in $K(h)$ between the two grasslands. However, the two grasslands had significantly higher $K(h)$ than cultivated field. These results show that the grasslands are capable of transmitting more water than cultivated fields at near-saturated conditions.

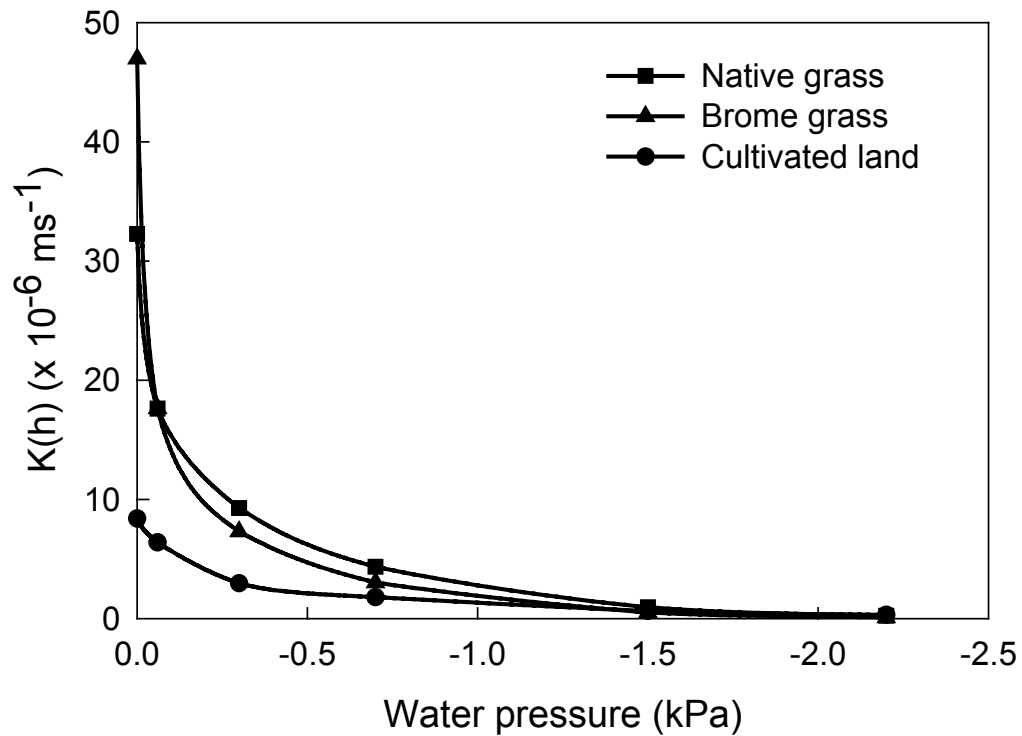


Figure 5. 3 Mean hydraulic conductivity ($K(h)$) of surface soils under three land use ($K(0)$ is from double-ring infiltrometer)

The inverse capillary length scale (α) is a shape parameter of hydraulic conductivity-water pressure relationship and is a measure of the relative importance of gravitational and capillary forces during water movement in unsaturated soils (Reynolds and Elrick, 1991). Grasslands had a significantly greater α value than the cultivated field (Table 5.2). Therefore, the contribution of gravitational force for the water flow near-saturated

condition in grasslands is larger than that of cultivated lands. Correlation analysis was carried out between the plot-averaged α values and plot-averaged organic carbon content or bulk density. As expected, there was a strong correlation between soil bulk density and α values ($R^2 = 0.45$) and between organic carbon content and α values ($R^2 = 0.53$). Organic matter increases aggregate sizes and enhances stability, and thus increases macroporosity. In addition to increased biological activity, long term undisturbed conditions prevailing in grasslands would have kept soil pore structure and continuity undisturbed, which consequently results in lower bulk density and higher α values.

Table 5. 2 Average and standard deviations of estimated surface soil hydraulic properties for the three land use

Land use	Parameter		
	K_{fs}^z (Tension infiltrometer) $\times 10^{-6} \text{ m s}^{-1}$	K_{fs} (Ring infiltrometer)	α^y m^{-1}
Native grassland	16 (1.5)a ^x	32 (2.0)a	19 (1.1)a
Brome grassland	14 (1.3)a	47 (1.6)a	23 (1.3)a
Cultivated land	4 (1.5)b	8 (1.1)b	12 (1.2)b

^z K_{fs} = field-saturated hydraulic conductivity.

^y α = inverse capillary length scale.

^xNumber in parentheses is the standard deviation calculated from 18 observations.

Means followed by different lower case letters in the same column are significantly different at $P < 0.1$.

The saturated hydraulic conductivity, K_{fs} determined by the tension infiltrometer was not significantly different between grasslands but the difference between cultivated land and the grasslands was significant (Table 5.2). The K_{fs} obtained from native grassland in

our study site is consistent with the values reported by Schwartz *et al.* (2000) for native grasslands in Texas High Plains. There was a significant correlation between saturated hydraulic conductivity and bulk density ($R^2 = 0.22$) based on all 54 measurements. Similar to α values, there was a significant correlation ($R^2 = 0.66$) between the plot-averages of saturated hydraulic conductivity and plot-averages of organic carbon content. Increases in organic carbon content that may have an indirect effect on soil aggregate formation and stability, can explain most of the variations in saturated hydraulic conductivity among plots.

The estimated K_{fs} and α values are highly correlated to soil macroporosity (Figure 5.4): the variation in macroporosity can explain more than 56 and 70 % of the variations in the plot-averaged K_{fs} and α , respectively. The high coefficients of determination suggest that macroporosity was a better indicator for K_{fs} and α than the bulk density and organic carbon content for this study. This is significant, because macroporosity is easy to obtain and may be able to improve significantly the pedotransfer functions for predicting soil hydraulic properties from readily-measured soil properties for different land uses (Rawls *et al.*, 1993).

Average K_{fs} values determined by the double-ring infiltrometer method was significantly greater in grasslands compared to the cultivated field. The K_{fs} values obtained by the double-ring infiltrometers were 2 to 3 times larger than that measured by tension infiltrometers for the same treatments. The differences in K_{fs} values measured by the two methods may be attributed to the different pore size ranges involved in the two methods. The K_{fs} values measured by double-ring infiltrometer (Table 5.2) are much larger, especially in grasslands, than the values given by Rawls *et*

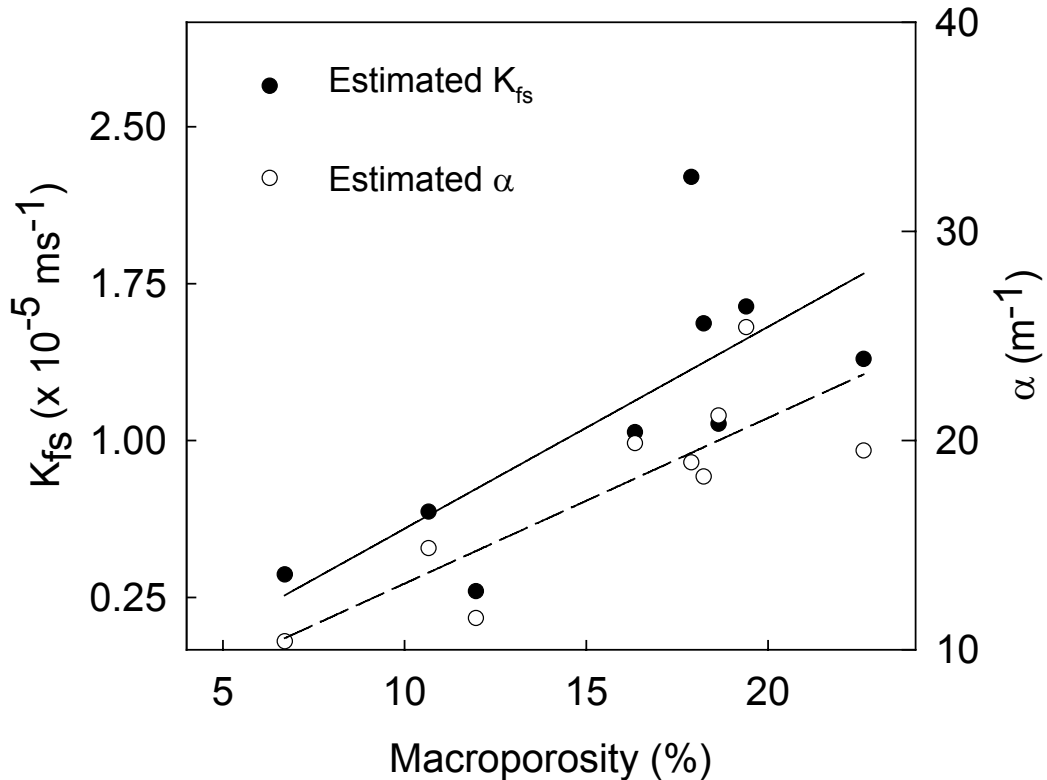


Figure 5. 4 Correlations between macroporosity and field-saturated hydraulic conductivity (K_{fs}) (solid line represents linear regression: $R^2=0.56$) and macroporosity and inverse capillary length scale, α (broken line represents linear regression: $R^2=0.70$). Each point was an average of six measurements.

al. (1993) for the USDA soil textural triangle for silt loam soils (i.e., $1.88 \times 10^{-6} \text{ m s}^{-1}$). In contrast, our K_{fs} values are consistent with the findings of Naeth *et al.* (1990) for the ungrazed grasslands in mixed prairie in Alberta, Canada. Our results are also comparable with that of van der Kamp *et al.* (2003) who found greater infiltration rates in brome grasslands than in cultivated fields. They reported that the infiltration rate of unfrozen soils measured by single-ring infiltrometers under brome grassland could vary from 2.7×10^{-5} to $2.8 \times 10^{-3} \text{ m s}^{-1}$.

The K_{fs} values measured by tension infiltrometers may be more representative in semi-arid zones, where soils are generally under unsaturated conditions. By excluding the effects of large pores, the use of near-saturated hydraulic conductivity should give more reliable predictions of unsaturated hydraulic conductivity in the dry range than the saturated hydraulic conductivity (Luckner *et al.*, 1989). For double-ring infiltrometer measurements, the saturated hydraulic conductivity is a measure of water flow rate under ponded conditions, and thus is more a reflection of macropore water flow. The combination of tension infiltrometer and double-ring infiltrometer measurements gives soil hydraulic properties at ponded and dry conditions.

The enhanced infiltrability and hydraulic conductivity in grasslands is likely due to gradual development of macropores such as root channels, animal burrows (biopores) and desiccation cracks, resulting in preferential flow (Lepilin, 1989; van der Kamp *et al.*, 2003). Our observations also indicated an abundance of animal burrows with varying sizes ($< 5 \times 10^{-3}$ m in diameter) and mole heaps in grasslands. Such animal activities were higher in brome grassland where there was a denser cover than in native grasslands. Animal activities were not noticeable in cultivated lands. These burrows could act as efficient water infiltration galleries, especially during infiltration under positive pressure, which in turn could increase infiltration rate and saturated hydraulic conductivity under grasslands.

When considering macropores, not only the total volume occupied by them, but also the amount of water they are capable of transmitting is important. Macropores consisted of over 10 to 20% of the total soil volume (Figure 5.1). However, the actual water-conducting macroporosity of the three land use varied from 0.01% in cultivated fields to

0.04% in grasslands (Table 5.3). While the range of values found for macroporosity in our study seem to be very small, they compare very well with the values reported by other researchers. Dunn and Phillips (1991) compared macroporosity (pores $> 7.5 \times 10^{-4}$ m in diameter) in silty loam soil with rye and vetch cover crops on conventional and no-till plots and the values varied from 0.006 to 0.013%. Macroporosity (pores $> 1 \times 10^{-3}$ m in diameter) quantified by Cameira *et al.* (2003) in silty loam soil on minimum tillage and conventional tillage plots planted with maize ranged from 0.01 to 0.05%. Buttle and McDonald (2000) characterized macroporosity (pores $> 1 \times 10^{-3}$ m in diameter) for a forest podzol and the values ranged between 0.001 and 0.021%. Watson and Luxmoore (1986) reported macroporosity (pores $> 1 \times 10^{-3}$ m in diameter) of 0.04% for a forest watershed.

Table 5. 3 Estimated water-conducting porosity \pm standard deviation (% of soil volume) in each pore diameter interval for the three land use

Land use	Pore diameter ($\times 10^{-3}$ m)				
	1 - 5	0.43 - 1	0.2 - 0.43	0.136 - 0.2	0.136 - 5
Water-conducting porosity					
Native grass	0.04 \pm 0.02	0.26 \pm 0.08	0.79 \pm 0.31	0.50 \pm 0.2	1.59 \pm 0.6
Brome grass	0.04 \pm 0.01	0.26 \pm 0.1	0.54 \pm 0.18	0.29 \pm 0.2	1.08 \pm 0.4
Cultivated land	0.01 \pm 0.01	0.06 \pm 0.03	0.28 \pm 0.1	0.28 \pm 0.1	0.63 \pm 0.2

The relative infiltration rate was determined as the infiltration rate difference for each water pressure range divided by the estimated infiltration rate at -0.06 kPa water

pressure. The results clearly showed the difference in the contribution of large pores (with a diameter $> 1 \times 10^{-3}$ m) to the total flow in the three land use (Figure 5.5).

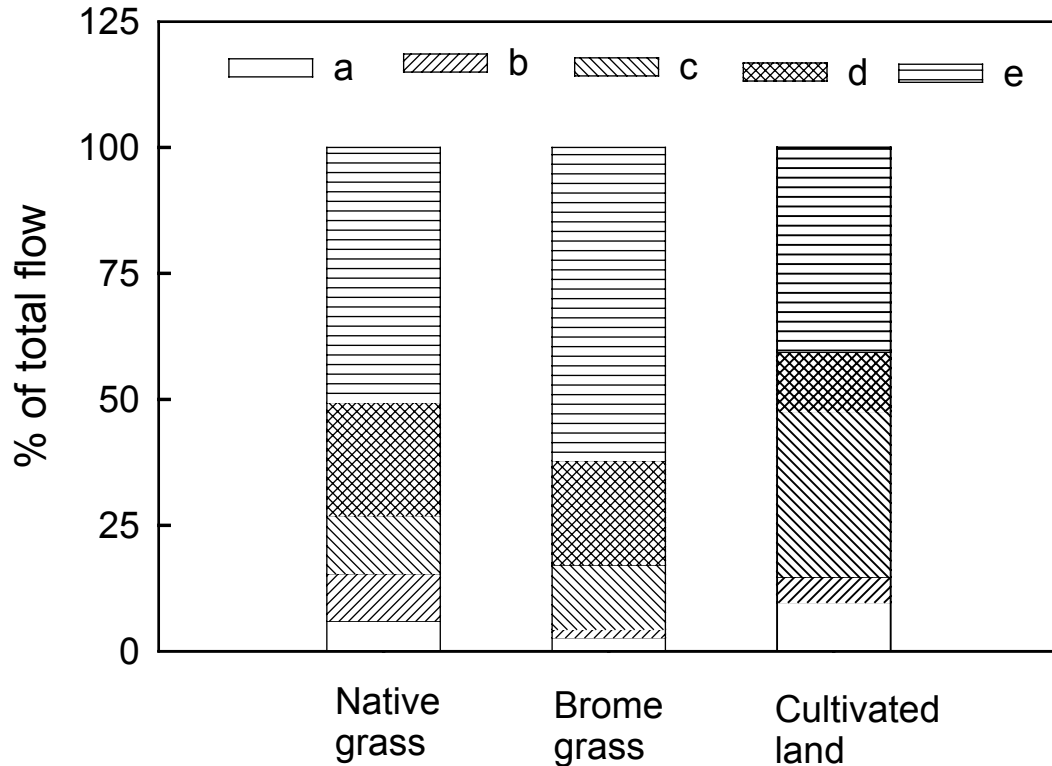


Figure 5. 5 Contribution to total flow at -0.06 kPa water pressure from the following pore diameter intervals: a: $< 1.4 \times 10^{-4}$ m; b: 1.4×10^{-4} - 2.0×10^{-4} m; c: 2.0×10^{-4} - 4.3×10^{-4} m; d: 4.3×10^{-4} - 1.0×10^{-3} m; e: $> 1.0 \times 10^{-3}$ m

Despite the fact that macropores comprised of the order of a ten-thousandth of the total soil volume, a very large percentage of water flow was conducted through them. Macropores (pores $> 1 \times 10^{-3}$ m in diameter) conducted on average as much as 51, 62 and 41% of the flow at -0.06 kPa water pressure in native grassland, brome grassland and cultivated land, respectively. Ninety two percent and 97% of the total water flow in native grassland and brome grassland, respectively, entered into the soils through pores

of an equivalent diameter of 1.36×10^{-4} m or larger (Figure 5.5), which accounted for only 1.6, and 1.1% of the total soil volume, respectively (Table 5.3). In cultivated lands, 90% of the total water flow is conducted through 0.63% of the total soil volume. Pores smaller than 1.36×10^{-4} m in diameter were responsible for only 10% of the total flow at -0.06 kPa water pressure in cultivated fields and it was less than 6% in grasslands. These estimates are comparable with relative flux obtained by other researchers who used tension infiltrometer for the estimation of water-conducting porosity. Watson and Luxmoore (1986) reported that 73% of the ponded flow was conducted through the pores with a diameter greater than 1×10^{-3} m in a forest watershed; 96% of the water flux was transmitted through only 0.32% of the total soil volume. Dunn and Phillips (1991) observed that 43% of the total flow was conducted through macropores while 77% of the total flow at -0.06 kPa water pressure was transmitted through the pores $> 2 \times 10^{-2}$ m in diameter in conventional tillage plots. Cameira *et al.* (2003) found about 55% of the flow moved through macropores and 90% of the flow transmitted through 0.005% of the total soil volume.

The pore connectivity was examined using the ratio of water-conducting porosity to macroporosity. The ratios of water-conducting porosity to macroporosity between -0.06 and -0.3 kPa water pressures were 0.0023 ± 0.0008 and 0.002 ± 0.0007 for native grasslands and brome grasslands, respectively, that were significantly different from cultivated fields (0.0008 ± 0.0005). These ratios suggest that grasslands have similar pore connectivity, which are more than twice as large as that of cultivated lands. Grasslands not only have higher macroporosity, but also have higher pore connectivity than cultivated lands (Schwartz *et al.* 2000). This is expected because grasslands had

more root channels and burrows of vertebrate and invertebrate organisms. The difference in water-conducting porosity and pore connectivity implies that during spring snowmelt, grasslands can transmit more snowmelt water into soil than cultivated lands. This is supported by van der Kamp *et al.* (2003), who indicated higher infiltration rate and less runoff during snowmelt in grasslands.

The storm event analysis was carried out to examine the difference in the area of ponding for different land use. In the experimental area, the amount of rain expected in a 1 h duration storm is $5.5 \times 10^{-6} \text{ m s}^{-1}$ for 2-year return period storm, and $1.4 \times 10^{-5} \text{ m s}^{-1}$ for a 25-year event (Gray, 1973). These values are compared with the saturated hydraulic conductivity values estimated from tension infiltrometer measurements for each location in each treatment. Infiltration rates early in the event would have exceeded these saturated hydraulic conductivity values. However, the comparison is still useful and may represent a situation where the soils were wet at the onset of storm. The cultivated field has a relatively small mean and variance of K_{fs} (Figure 5.6). Grasslands have much higher saturated hydraulic conductivity than the cultivated lands, with greater spatial variability. During a 2-year storm event, at most 83 and 6% of the land area under cultivation and native grass, respectively, would produce runoff while there would be no runoff from brome grasslands. As much as 94% of the land area of cultivated field would generate runoff during one in a 25-year storm compared with 44 and 61% of the land under native grasslands and brome grasslands, respectively. Land use alter the steady infiltration rate (saturated hydraulic conductivity). As a consequence, the potential runoff of summer precipitation varies among land use, which in turn may alter the water level of prairie wetlands.

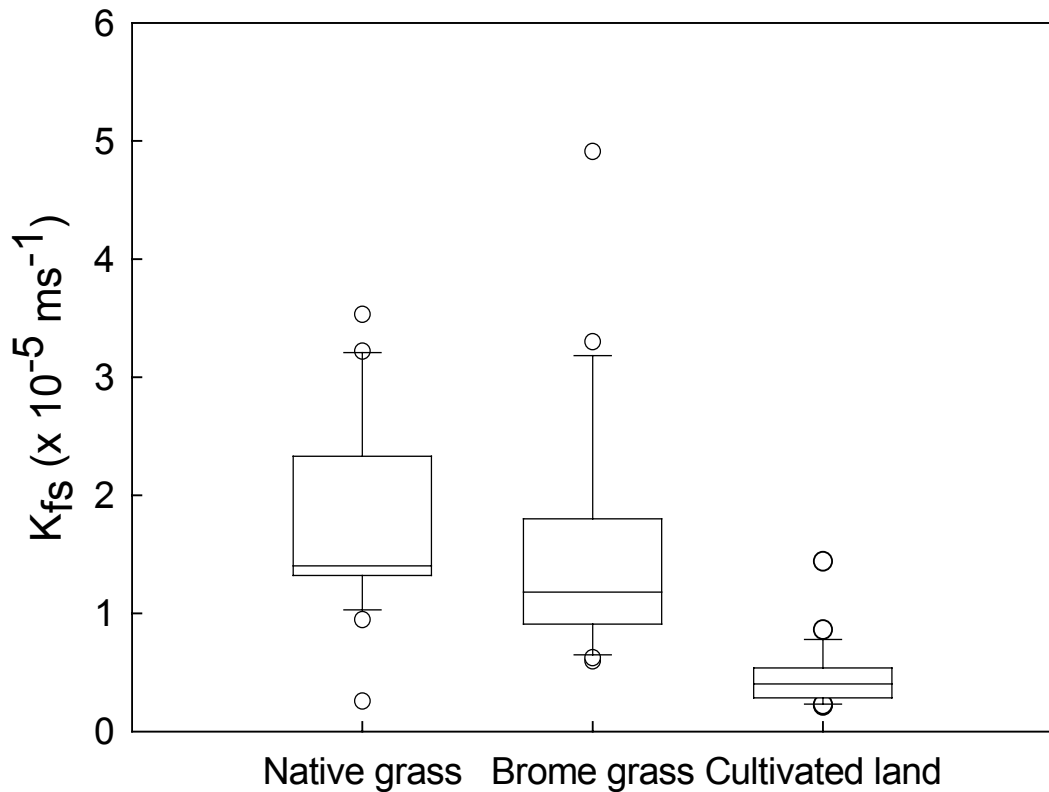


Figure 5. 6 Field-saturated hydraulic conductivities (K_{fs}) for the three land use (0 indicates values below and above 10th and 90th percentiles, respectively).

The results from this study have important implications for understanding drying-out of wetlands in the Canadian prairies. Van der Kamp *et al.* (2003) attributed the drying out of wetlands to efficient snow trapping due to tall brome grasses, and high infiltration rate in frozen and unfrozen soils in brome grass fields. We showed that there were significantly higher hydraulic properties and water-conducting macroporosity in grasslands than in cultivated lands, which could result in higher infiltration rates in both frozen and unfrozen soils, and thus less water runoff to depressions. In addition, storm events are more likely to create runoff in cultivated land than in grasslands because of the much higher hydraulic conductivity in the latter. All these suggest wetlands are

likely preserved in cultivated lands than in brome grasslands, which corroborates the claim by van der Kamp *et al.* (2003) that brome grass leads to drying-out of wetlands in the Canadian prairies.

Since there are no significant differences in hydraulic properties and macroporosity between brome grasslands and native grasslands, questions remain on whether native grass would also lead to drying out of wetlands. The difference between brome grasslands and native grasslands is that native grass is shorter and less efficient in trapping snow, enhancing snow transport from uplands to depressions. Therefore, native grassland is more likely to have wetlands than brome grassland. On the other hand, the high water-conducting macroporosity in native grassland makes it less likely to conserve wetlands than in cultivated lands. However, historical data indicated that there are fewer wetlands in the present than in the past when the native grasslands were the dominant land cover. Although climate change in the last century (Cutforth *et al.*, 1999) might play a role, further research is needed to identify the difference in hydrological processes between native grasslands and brome grasslands.

5.5 Conclusions

Results of this experiment revealed that the surface soil hydraulic properties vary considerably among land use. Field-saturated hydraulic conductivity determined by tension infiltrometers and double-ring infiltrometers were significantly higher in grasslands than in cultivated fields. At the -0.3 kPa water pressure, mean hydraulic conductivity of grasslands was significantly larger than that of cultivated fields. Macroporosity consisted of over 10-20% of the total soil volume while the actual water-conducting macroporosity of the three land use were less than 0.04%. Relative

importance of gravitational force in water movement under near-saturated condition is greater in grasslands than in cultivated fields. In the three land use, over 90% of the total water flow at -0.06 kPa water pressure was transmitted through pores $> 1.36 \times 10^{-4}$ m equivalent pore diameter, which accounts for $< 2\%$ of the total soil volume. Both tension infiltrometer and double-ring infiltrometer have to be used to evaluate the near-saturated hydraulic properties under different land use, especially when the development of large biopores is evident. Cultivated land had lower water-conducting macroporosity than grasslands and hence lowers infiltration of rain and snowmelt. As a result, cultivated land increases potential for runoff under saturated conditions. In prairies, the type of land use may alter the water balance of the area by changing the amount of surface runoff; therefore any changes in existing land use must be done cautiously.

5.6 References

- Bear, J. 1972. Dynamics of fluids in porous media. Elsevier Pub. Co. Inc, New York, NY.
- Belvins, R.L., G.W. Thomas, M.S. Smith, W.W. Frey, and P.L. Cornelius. 1983. Changes in soil properties after 10 years continuous no tilled and conventionally tilled corn. *Soil Tillage Res.* 3:135-146.
- Benjamin, J.G. 1993. Tillage effects on near surface soil hydraulic properties. *Soil Tillage Res.* 26:277-288.
- Bower, H. 1986. Intake rate. Cylinder infiltrometer. p. 825-843. *In* A. Klute (ed.) *Methods of soil analysis. Part 1. Physical and mineralogical properties.* 2nd ed. ASA, Madison, WI.
- Buttle, J.M., and D.J. McDonald. 2000. Soil macroporosity and infiltration characteristics of a forest podzol. *Hydrological Processes.* 14: 831-848.

- Cameira, M.R., R.M. Fernando, and L.S. Pereira. 2003. Soil macropore dynamics affected by tillage and irrigation for a silty loam alluvial soil in southern Portugal. *Soil Tillage Res.* 70:131-140.
- Chan, K.Y., and J.A. Mead. 1989. Water movement and macroporosity of an Australian Alfisol under different tillage and pasture conditions. *Soil Tillage Res.* 14:301-310.
- Christie, H.W., D.N. Graveland, and C.J. Palmer. 1985. Soil and subsoil moisture accumulation due to dry land agriculture in southern Alberta. *Can. J. Soil Sci.* 65:805-810.
- Clothier, B., and D. Scotter. 2002. Unsaturated water transmission parameters obtained from infiltration. p. 879-888. *In* G. C. Topp and J. H. Dane (ed.) *Methods of soil analysis. Part 4. Physical methods.* SSSA Book Ser. 5. SSSA. Madison, WI.
- Clothier, B.E., and K.R.J. Smettem. 1990. Combining laboratory and field measurements to define the hydraulic properties of soil. *Soil Sci. Soc. Am. J.* 54:299-304.
- Cutforth, H.W., B.G. McConkey, R.J. Woodvine, D.G. Smith, P.G. Jefferson, and O.O. Akinremi. 1999. Climate change in the semiarid prairie of southwestern Saskatchewan: late winter-early spring. *Canadian Journal of Plant Science.* 79:343-350.
- Danielson, R.E., and P.L. Sutherland. 1986. Porosity. p. 443-461. *In* A. Klute (ed.) *Methods of soil analysis. Part 1. Physical and mineralogical properties.* 2nd ed. ASA. Madison, WI.
- de Jong, E., and R.G. Kachanoski. 1987. The role of grasslands in hydrology. p. 213-215. *In* M. C. Healy and R. R. Wallace (ed.) *Canadian Aquatic Resources.* Can. Bull. of Fisheries and Aquatic Resources. No. 215. Can. Govt. Publishing Centre, Ottawa, Canada.
- Dunn, G.H., and R.E. Phillips. 1991. Macroporosity of a well-drained soil under no-till and conventional tillage. *Soil Sci. Soc. Am. J.* 55:817-823.
- Elliott, J.A., and A.A. Efetha. 1999. Influence of tillage and cropping system on soil organic matter, structure and infiltration in a rolling landscape. *Can. J. Soil Sci.* 79:457-463.
- Euliss, N.H., and D.M. Mushet. 1996. Water level fluctuations in wetlands as a function of landscape condition in the prairie pothole region. *Wetlands.* 16:587-593.
- Gardner, W.R. 1958. Some steady-state solutions of unsaturated moisture flow equations with application to evaporation from a water table. *Soil Sci.* 85:228-232.

- Gee, G.W., and J.W. Bauder. 1986. Particle size analysis. p. 389-409. *In* A. Klute (ed.) *Methods of soil analysis. Part 1. Physical and mineralogical properties.* 2nd ed. ASA. Madison, WI.
- Gradshteyn, I.S., and I.M. Ryzhik. 2000. *Table of integrals, series, and products.* 6th ed. Academic Press. San Diego, CA, USA.
- Gray, D.M. 1973. *Handbook on the principles of hydrology.* Water Information Center Inc., NY.
- Hayashi, M., G. van der Kamp, and D.L. Rudolph. 1998. Mass transfer processes between a prairie wetland and adjacent uplands. 1. Water balance. *J. Hydrol.* 207:42-55.
- Heard, J.R., E.J. Kladivko, and J.V. Mannering. 1988. Soil macroporosity, hydraulic conductivity and air permeability of silty soils under long-term conservation tillage in Indiana. *Soil Tillage Res.* 11:1-18.
- Hillel, D. 1998. *Environmental soil physics.* Academic Press. New York. Iowa State University Press. USA.
- Jarvis, N.J., and I. Messing. 1995. Near-saturated hydraulic conductivity in soils of contrasting texture as measured by tension infiltrometers. *Soil Sci. Soc. Am. J.* 59:27-34.
- Leduc, C., g. Favreau, and P. Schroeter. 2001. Long-term rise in a shahelian water-table: the continental terminal in south-west Niger. *J. Hydrol.* 243:43-54.
- Lepilin, A. 1989. Effect of the age of perennial grasses on the physical properties of Meadow-Chernozem soil. *Soviet Soil Sci.* 21:121-126.
- Lindstrom, M.J., and C.A. Onstad. 1984. Influence of tillage systems on soil physical parameters and infiltration after planting. *J. Soil Water Cons.* 39:149-152.
- Logsdon, S.D., and D.B. Jaynes. 1993. Methodology for determining hydraulic conductivity with tension infiltrometers. *Soil Sci. Soc. Am. J.* 57:1426-1431.
- Luckner, L., M.T. van Genuchten, and D.R. Nielsen. 1989. A consistent set of parametric models for the two-phase flow of immiscible fluids in the subsurface. *Water Resour. Res.* 25: 2187-2193.
- Luxmoore, R.J. 1981. Micro-, meso- and macroporosity of soil. *Soil Sci. Soc. Am. J.* 45:671-672.
- Mapa, R.B., and H.P.M. Gunasene. 1995. Effect of alley cropping on soil aggregate stability of a tropical Alfisol. *Agro Forestry Systems.* 32:237-245.

- Maulé, C.P., and W.B. Reed. 1993. Infiltration under no-till and conventional tillage systems in Saskatchewan. *Canadian Agricultural Engineering*. 35:165-173.
- McQueen, D.J., and T.G. Shepherd. 2002. Physical changes and compaction sensitivity of a fine-textured, poorly drained soil under varying durations of cropping, Manawatu region, New Zealand. *Soil Tillage Res.* 63:93-107.
- Meyboom, P. 1966. Unsteady ground water flow near a willow ring in hummocky moraine. *J. Hydrol.* 4:38-62.
- Miller, J.J. 1983. Hydrology of a morainic landscape near St. Denis, Saskatchewan, in relation to the genesis, classification and distribution of soils. M. S. Thesis. Univ. of Saskatchewan, Canada.
- Miller, J.J., N.J. Sweetland, F.J. Larney, and K.M. Volkmar. 1998. Unsaturated hydraulic conductivity of conventional and conservation tillage soils in southern Alberta. *Can. J. Soil Sci.* 78:643-648.
- Naeth, M.A., R.L. Rothwell, D.S. Chanasyk, and A.W. Bailey. 1990. Grazing impacts on infiltration in mixed prairie and fescue grassland ecosystems of Alberta. *Can. J. Soil Sci.* 70:593-605.
- Nielson, D.R., J.W. Biggar, and K.T. Erb. 1973. Spatial variability of field measured soil water properties. *Hilgardia*. 42:215-260.
- Obi, M.E., and P.C. Nnabude. 1988. The effect of different management practices on the physical properties of a sandy loam soil in southern Nigeria. *Soil Tillage Res.* 12:81-90.
- Pennock, D.J. 2003. Designing field studies in soil science. *Can. J. Soil Sci.* In press.
- Rawls, W.J., L.R. Ahuja, D.L. Brakensiek, and A. Shirmohammadi. 1993. Infiltration and soil water movement. p. 5.1-5.51. *In* D. R. Maidment. (ed.) *Handbook of hydrology*. McGraw Hill, Inc. NY.
- Reynolds, W.D., D.E. Elrick, and E.G. Youngs. 2002. Single-ring and double-or-concentric-ring infiltrometer. p. 821-826. *In* J. H. Dane and G. C. Topp (ed.) *Methods of Soil Analysis. Part 4. Physical methods*. SSSA. Book Ser. 5. SSSA. Madison, WI.
- Reynolds, W.D., and D.E. Elrick. 1991. Determination of hydraulic conductivity using a tension infiltrometer. *Soil Sci. Soc. Am. J.* 55:633-639.
- SAS Institute Inc. 1990. *SAS/STAT user's guide. Version 6*. SAS Institute Inc., Cary, NC.
- Schwartz, R.C., P.W. Unger, and S.R. Evett. 2000. Land use effects on soil hydraulic properties. http://www.cprl.ars.usda.gov/programs/land_use.pdf.

- Soil Survey Staff. 1999. Soil Taxonomy. A Basic System of Soil Classification for Making and Interpreting Soil Surveys. Agriculture Handbook number 436. 2nd ed. Natural Resources Conservation Service, US Department of Agriculture.
- Sonneveld, M.P.W., M.A.H.M. Backx, and J. Bouma. 2003. Simulation of soil water regimes including pedotransfer functions and land use related preferential flow. *Geoderma*. 112:97-110.
- Sudicky, E.A. 1986. A natural gradient experiment on solute transport in sand aquifer: Spatial variability of hydraulic conductivity and its role in the dispersion process. *Water Resour. Res.* 22:2069-2082.
- van der Kamp, G., M. Hayashi, and D. Gallen. 2003. Comparing the hydrology of grassland and cultivated catchments in the semi-arid Canadian Prairies. *Hydrological Processes*. 17:559-575.
- van der Kamp, G., W.J. Stolte, and R.G. Clark. 1999. Drying out of small prairie wetlands after conversion of their catchments from cultivation to permanent brome grass. *Hydrological Sciences J.* 44:387-397.
- Vandervaere, J.P., M. Vauclin, and D.E. Elrick. 2000. Transient flow from tension infiltrometers. I. The two-parameter equation. *Soil Sci. Soc. Am. J.* 64:1263-1272.
- Wang, D., and W. Anderson. 1998. Direct measurement of organic carbon content in soils by the Leco CR-12 carbon analyzer. *Commun. Soil Sci. Plant Anal.* 29(1&2):15-21.
- Watson, K.W., and R.J. Luxmoore. 1986. Estimating macroporosity in a forest watershed by use of a tension infiltrometer. *Soil Sci. Soc. Am. J.* 50:578-582.
- Wilson, G.V., and R.J. Luxmoore. 1988. Infiltration, macroporosity and mesoporosity distributions on two forested watersheds. *Soil Sci. Soc. Am. J.* 52:329-335.
- Winter, T.C. 1989. Hydrologic studies of wetlands in the northern prairie. p. 17-54. *In* A. van der Valk. (ed.) *Northern prairie wetlands*. Iowa State University Press.
- Woo, M.K., and R.D. Rowsell. 1993. Hydrology of a prairie slough. *J. Hydrol.* 146:175-207.
- Wooding, R.A. 1968. Steady infiltration from a shallow circular pond. *Water Resour. Res.* 4:1259-1273.

6. SUMMARY AND CONCLUSIONS

Near-saturated surface soil hydraulic properties are key factors controlling the partition of rainfall and snowmelt between runoff and soil water storage as well as chemical transport in soil. Slope gradient, water-conducting porosity and type of land use are among the main soil and management factors that influence surface soil hydraulic properties. Thus, information on surface soil hydraulic properties under these conditions is needed for efficient land and water management.

The majority of agricultural lands on the Canadian prairies are non-level. However, specifically designed instruments are not available for determining soil hydraulic properties in sloping landscapes. Conversely, extensively used equipment such as tension and double-ring infiltrometers have not been systematically evaluated for determining surface hydraulic properties in sloping landscapes. Knowledge of water-conducting porosity of soil is required in understanding water movement and chemical transport. The existing methods for quantifying water-conducting porosity *in situ*, however, have severe limitations. Land use systems may alter surface soil hydraulic properties and thereby water balance and wetland hydrology in the prairies. Nevertheless, information on surface soil hydraulic properties and water-conducting porosity in sloping lands with undisturbed grass cover and traditional crop cultivation is lacking, particularly on the Canadian prairies, which have numerous wetlands.

The goal of the study described in this thesis was to characterize saturated and near-saturated surface soil hydraulic properties and water-conducting porosity in sloping landscapes. The specific objectives included:

- 1 To evaluate the suitability of tension and double-ring infiltrometers for the estimation of surface soil hydraulic properties in sloping lands;
- 2 To develop an improved method for determining water-conducting porosity from tension infiltrometer measurements;
- 3 To apply these methods in characterizing surface soil hydraulic properties and water-conducting porosity in sloping lands under different land use systems in the St. Denis National Wildlife area (SDNWA), Saskatchewan (SK), Canada.

To achieve objective (1), water infiltration rates were measured in soil surfaces having 0 (level), 7, 15, and 20% slopes using a double-ring and a tension infiltrometer at -2.2, -1.7, -1.3, -1.0, -0.6, and -0.3 kPa water pressures in a field at Laura, SK, Canada. Hydraulic properties and water-conducting porosity were estimated and compared for different slope gradients. Level and sloping landscapes were not significantly different ($p < 0.05$) for field measured steady-state infiltration rates and estimated field-saturated hydraulic conductivity (K_{fs}), unsaturated hydraulic conductivity as a function of water pressure ($K(h)$), inverse capillary length parameter (α) and water-conducting macro- and mesoporosity. Three-dimensional computer simulation studies were also performed for tension infiltrometer with various disc diameters, water pressures applied at the soil surface and slope gradients. Simulated cumulative infiltration for 20-min period with 0.2 m diameter disc at different water pressures did not show marked differences among

slopes. The field experiment and the numerical results strongly indicated that both tension and double-ring infiltrometers are suitable for the measurement of surface soil hydraulic properties and water-conducting porosity in level as well as non-level lands of up to 20% slope. This innovation is significant because the instrument can be used for the characterization of surface soil hydraulic properties and water-conducting porosity in most of the agricultural fields including experimental plots, which generally lie below 20% slope. This also fulfills a long-standing requirement for characterizing hydraulic properties in non-level lands.

To meet objective (2), analytical solutions were developed for specific unsaturated hydraulic conductivity functions such as the Gardner's exponential and rational power models, the Brooks and Corey model, and the van Genuchten-Mualem model (new method). The analytical solutions were compared with numerical solutions and the existing methods for the calculation of water-conducting porosity using the double-ring and tension infiltration measurements taken at water pressures between -2.2 and -0.3 kPa in a level land at Laura, SK, Canada. Both analytical and numerical solutions of the new method can reliably estimate water-conducting porosity of surface soils from *in situ* tension infiltration measurements. Irrespective of the width of the water pressure range, the new method gave consistent water-conducting porosity values. In comparison with the new method, the existing methods overestimated water-conducting macroporosity by a factor of greater than two and water-conducting total porosity by a factor of greater than ten for measurements taken at large water pressure intervals. This novel approach allowed me not only to remove the unrealistic assumption of uniform pore-size distribution of the existing methods but also to characterize water-conducting

macro-and mesoporosity in a non-destructive and cost effective manner. It will also tremendously improve the performance of hydrological models, which use water-conducting porosity as a soil parameter.

To achieve objective (3), infiltration measurements were made using double-ring and tension infiltrometers at -2.2, -1.5, -0.7, and -0.3 kPa water pressures in native grasslands, brome grasslands, and cultivated fields at SDNWA, SK, Canada. Hydraulic properties and water-conducting porosity were estimated and compared for different land use. The K_{fs} , α , hydraulic conductivity at -0.3 kPa water pressure and water-conducting macroporosity under native and brome grasslands were significantly greater than in the cultivated fields. This suggests that soils under permanent grass cover have improved hydraulic properties and water-conducting porosity. These findings have important implications for understanding drying-out of wetlands in the SDNWA. Improved hydraulic properties and water-conducting macroporosity could result in higher infiltration rates in frozen as well as unfrozen soil conditions resulting in less snowmelt runoff to depressions (i.e., wetlands). Storm events are more likely to generate runoff in cultivated lands than grasslands. This information suggests that wetlands are more likely to be preserved in cultivated lands than in grasslands. Information gathered from this study will help for improving our understanding of the influence of land use on runoff and infiltration, and thus wetland hydrology. These rigorous quantitative data could also be useful for future sustainable land use planning in the Canadian prairies.

The major conclusions of this thesis are:

1. Both tension and double-ring infiltrometers are suitable for characterization of surface soil hydraulic properties in landscapes with slopes up to 20%;
2. In comparison to the existing methods, the new method developed can adequately and efficiently characterize water-conducting porosity of surface soils *in situ*, regardless of the size of the water pressure range used;
3. Land use modifies near-saturated surface soil hydraulic properties and water-conducting macroporosity. As a consequence, land use may alter the water balance of an area by affecting the partition between, and relative amount of infiltration and surface runoff.